Technical University of Denmark

Vertical-Cavity Surface-Emitting Lasers: Advanced Modulation Formats and Coherent Detection

Rodes Lopez, Roberto; Tafur Monroy, Idelfonso ; Jensen, Jesper Bevensee

Publication date:
2013

Document Version
Publisher's PDF, also known as Version of record

[Link back to DTU Orbit](#)

Citation (APA):
Rodes Lopez, R., Tafur Monroy, I., & Jensen, J. B. (2013). Vertical-Cavity Surface-Emitting Lasers: Advanced Modulation Formats and Coherent Detection. Kgs. Lyngby: Technical University of Denmark (DTU).

DTU Library
Technical Information Center of Denmark

Vertical-Cavity Surface-Emitting Lasers: Advanced Modulation Formats and Coherent Detection

Roberto Rodes Lopez

Supervisors:
Professor Idelfonso Tafur Monroy and
Assistant Professor Jesper Bevensee Jensen

Delivery Date: 15$^{\text{th}}$ January 2013

DTU Fotonik
Department of Photonics Engineering
Technical University of Denmark
Building 343
2800 Kgs. Lyngby
DENMARK

DTU Fotonik
Institut for Fotonik

Abstract

This thesis expands the state-of-the-art in coherent detection for optical fiber access networks employing vertical-cavity surface-emitting lasers (VC-SELs) as light sources. Bit rates up to 10 Gb/s over 25 km single-mode fibre (SMF) transmission distance have been achieved supporting a passive optical splitting ratio for 199 users. Extended transmission reach over 40 km SMF and a splitting ratio supporting up to 1024 users have been experimentally demonstrated for a bidirectional bit rate of 5 Gb/s. These novel proposed VCSEL-based transmission systems satisfy the requirements for next generation optical fiber access networks regarding long reach, high splitting ratio, no optical amplification, no external modulation, and use of a single fiber for upstream and downstream transmission.

An important contribution of this thesis is the novel concept of chirp-assisted coherent detection for direct current modulated VCSELs. A coherent receiver approach that exploits adiabatic frequency chirping of direct modulated VCSELs to improve the extinction ratio of received signals is introduced. This concept enables coherent detection systems to be fully based on VCSELs in contrast to conventional coherent detection approaches that require narrow linewidth light sources. Moreover, the proposed receiver configuration is based on envelope detection that simplifies its implementation. The results presented in this thesis include the first reported experimental demonstration of all-VCSEL-based coherent transmission link with real-time demodulation.

Furthermore, advanced modulation formats are considered in this thesis to expand the state-of-the-art in high-speed short-range data transmission system based on VCSELs. First, directly modulation of a VCSEL with a 4-level pulse amplitude modulation (PAM-4) signal at 50 Gb/s is achieved. This is the highest data rate ever transmitted with a single VCSEL at the time of this thesis work. The capacity of this system is increased to 100 Gb/s by using polarization multiplexing emulation and forward error correction

techniques. Compared to a non return-to-zero on-off keying (NRZ-OOK) system with the same bandwidth, this approach reduces by 2 the number of transceivers and by 4 the number of parallel lines needed to provide future standard capacity links. Secondly, carrierless amplitude phase (CAP) modulation and half-cycle quadrature amplitude modulation (HC-QAM) are experimentally demonstrated to increase the capacity for a given bandwidth and reduce the impact of optical fiber chromatic dispersion for a given capacity. Finally, 2 Gb/s bipolar impulse-radio ultra-wide band (IR-UWB) data communication over a combined distance of 25 km SMF optical fiber and 4 m air. These results show the suitability of VCSELs light sources for applications in hybrid optical fiber-wireless transmission links.

In conclusion, the results presented in this thesis have significantly extended the state-of-the-art in techniques for signal generation, transmission and detection for next-generation access networks and high- speed short-range systems employing vertical-cavity surface-emitting lasers as light sources.

Resumé

Denne afhandling udvider state-of-the-art indenfor optiske fibernetværk, der anvender kohærent detektion og "vertical cavity surface emitting lasers" (VCSEL) som lyskilder. Transmission af bit rater op til 10 Gb/s over 25 km single-mode fiber (SMF) er gennemført med understøttelse af passiv optisk signaldeling mellem 199 brugere. Udvidet transmissionsrækkevidde på 40 km med SMF og signaldeling mellen 1024 brugere er eksperimentielt demonstreret i et bi-direktionelt system med 5 Gb/s bit rate. Disse nye VC-SEl baserede transmissionssystemer lever op til næste generation fibernets krav om lang rækkevidde, høj delingsgrad, og anvendelsen af den samme fiber for upstream og downstream transmission.

Et vigtigt bidrag fra denne afhandling er det nye koncept chirp-assisteret kohærent detektion af signaler fra direkte modulerede VCSEL'er En tilgang til kohærente modtagere, der udnytter adiabatisk frekvenschirp af direkte modulerede VCSEL'er til at forbedre udslukningsgraden af det modtagne signal. Dette koncept muliggør kohærente systemer, der udelukkende betjener sig af VCSEL'er som lyskilder, i modsætning til konventionelle kohærente systemer, der baserer sig påsmal-spektrede lyskilder. Ydermere er den foreslåede modtagerkonfiguration baseret påenvelope-detektion, hvilket simplificer implemeteringen. Resultaterne præsenteret i denne afhandling inkluderer den første rapporterede demonmstration af et kohærent transmissionssystem, der udelukkende anvender VCSEL'er, og som benytter demodulering I realtid uden digital signalbehandling.

Avancerede modulationsformater er undersøgt i denne afhandling som metode til at udvide state-of-the-art indenfor VCSEL baserede højhastigheds-forbindelser med kort rækkevidde. For det første er direkte modulation af en VCSEL med et 4-niveau pulse-amplitude modulation signal ved en bit rate på 50 Gb/s demonstreret. Dette er den højeste bit rate, der er opnået med en enkelt VCSEL påtidspunktet for denne afhandling. Systements samlede kapacitet blev foroblet til 100 Gb/s ved hjælp af polarisationsmultipleksning

og fejlkorrigerende kodning (FEC). Sammenlignet med "non return-to-zero on-off keying" (NRZ-OOK) systemer med samme båndbredde er antallet af sendere og motagere halveret, og antallet af parallelle kommunikations-linjer reduceret med en faktor 4 for at tilfredsstille fremtidige krav om højhastighedsforbindelser. For det andet er bærebølgeløs amplitude- og fasemodulation (CAP) samt halv-cyklus quadratur amplitude modulation (HC-QAM) demonstreret eksperimentielt med henblik påat øge kapacitet og mindske følsomheden overfor kromatisk dispersion. Til sidst er 2 Gb/s bipolar impulsradio ultra-bredbånds (IR-UWB) datatransmission over en kombineret forbindelse bestående af en 25 km SMF optisk fiber og en 4 m trædløs forbindelse blevet demonstreret. Disse resultater viser VCSEL'er anvendelighed som lyskilder I hybride fiber/trådløse forbindelser.

Som konklusion kan anføres at de resultater, der er præsenteret i herværende afhandling, påsignifikant vis har udvidet state-of-the-art indenfor genera-tion, transmission og detektion af signaler til næste generation af access-net og højhastighedsforbindelser, der anvender VCSEL'er som lyskilder.

Acknowledgements

First, I would like to thank my supervisors, Assistant professor Jesper Bevensee Jensen and Professor Idelfonso Tafur Monroy. Jesper, for all the time we have spent together with interesting discussions, guidance and for always believing in me. Idelfonso, for all the opportunities you have opened to me, for your help when I was still a guest student applying for the M.Sc., for offering me a interesting topic for my M.Sc. thesis, for believing in me as a Ph.D. cadidate and finally for providing me with the best support and advices to develop my future carrier as an engineer. I also would like to thank Chris Kocot for the guidance during my successful internship in Finisar, and for all the support you gave me not only within Finisar, but also on personal issues whenever I needed it.

I would like to thank all my colleagues in the Metro-access group and in the Fotonik department. Thank you JJ and Xema for the interesting coffee-time discussion. Thank you Antonio for our friendship since the beginning of our Danish adventure as Erasmus students. Thank you Dani for all the fun we had in the department while researching in photonics. Thanks to the nice people I met during these years in Denmark, specially the Spanish invasion and rest of Erasmus students.

I would like to thank my friends in my home town Zaragoza from Teleco and from Miguel Catalan. It is always a great pleasure to meet you every time I come back to Zaragoza, and I am very grateful to see that our friendship stays as strong as always even though I have been far away from you during the last 5 years.

Special thanks to Diana for being a very important part in my life during my Ph.D. Thank you for all your support, for being so understanding when I could not spend as much time with you as I wanted, and for being such a brave woman.

Finally, I would like to thank all my family for giving me the support and energy to accomplish my goals; specially thanks to my parents and brother,

muchas gracias por todo el apoyo recibido y por la educación que me habéis inculcado. Os agradezco el enorme esfuerzo que habéis hecho para que yo pueda seguir alcanzando mis metas, y por estar siempre cuando os necesito. Gracias de corazón.

Summary of original work

This thesis is based on the following original publications:

PAPER 1 R. Rodes, J.B. Jensen, D. Zibar, C. Neumeyr, E. Ronneberg, J. Rosskopf, M. Ortsiefer, and I. Tafur Monroy, "Vertical-cavity surface-emitting laser based digital coherent detection for multigigabit long reach passive optical links," *Microwave and Optical Technology Letters* vol. 53, no. 11, pp. 2462-2464, 2011.

PAPER 2 J.B. Jensen, **R. Rodes**, D. Zibar, and I. Tafur Monroy, "Coherent Detection for 1550 nm, 5 Gbit/s VCSEL Based 40 km Bidirectional PON Transmission," in *Proc. of Optical Fiber Communication Conference and Exposition*, Paper OTuB2, 2011.

PAPER 3 R. Rodes, J.B. Jensen, D. Zibar, C. Neumeyr, E. Roenneberg, J. Rosskopf, M. Ortsiefer, and I. Tafur Monroy, "All-VCSEL based digital coherent detection link for multi Gbit/s WDM passive optical networks," *Optics Express* vol. 18, no. 24, pp. 24969-24974, 2010.

PAPER 4 R. Rodes, J.B. Jensen, A. Caballero, and I. Tafur Monroy, "1.3 um all-VCSEL low complexity coherent detection scheme for high bit rate and high splitting ratio PONs," in *Proc. of Optical Fiber Communication Conference and Exposition*, paper OThK7, 2011.

PAPER 5 R. Rodes, D. Parekh, J.B. Jensen, C.J. Chang-Hasnain, and I. Tafur Monroy, "Real Time 1.55 um VCSEL-based Coherent Detection Link," in *Proc. of IEEE Photonics Conference*, pp. 457-458, 2012.

PAPER 6 R. Rodes, N. Cheng, J.B. Jensen, and I. Tafur Monroy, "10 Gb/s Real-Time All-VCSEL Low Complexity Coherent scheme for PONs," in *Proc. of Optical Fiber Communication Conference and Exposition*, paper OTh4G, 2012.

PAPER 7 R. Rodes, J. Estaran, B. Li, M. Mueller, J.B. Jensen, T. Gruendl, M. Ortsiefer, C. Neumeyr, J. Rosskopf, K.J. Larsen, M.-C. Amann, and I. Tafur Monroy, "100 Gb/s single VCSEL data transmission link," in *Proc. of Optical Fiber Communication Conference and Exposition*, Post-deadline paper P5D.10, 2012.

PAPER 8 R. Rodes, M. Mueller, B. Li, J. Estaran, J.B. Jensen, T. Grundl, M. Ortsiefer, C. Neumeyr, J. Rosskopf, K.J. Larsen, M.-C. Amann, and I. Tafur Monroy, "High-speed 1550 nm VCSEL data transmission link employing 25 Gbaud 4-PAM modulation and Hard Decision Forward Error Correction," *Journal of Lightwave Technology*, accepted for publication.

PAPER 9 J. Estaran, **R. Rodes**, T.-T. Pham, M. Ortsiefer, C. Neumeyr, J. Rosskopf, and I. Tafur Monroy, "Quad 14Gbps L-Band VCSEL-based System for WDM Migration of 4-lanes 56 Gbps Optical Data Links," *Optics Express*, vol. 20, no. 27, pp. 28524-28531, 2012.

PAPER 10 R. Rodes, M. Wieckowski, T.-T. Pham, J.B. Jensen, and I. Tafur Monroy, "VCSEL-based DWDM PON with 4 bit/s/Hz spectral efficiency using carrierless amplitude phase modulation," in *Proc. of European Conference and Exhibition on Optical Communication*, paper Mo.2.C.2, 2011.

PAPER 11 R. Rodes, M. Wieckowski, T.-T. Pham, J.B. Jensen, J. Turkiewicz, J. Siuzdak, and I. Tafur Monroy, "Carrierless amplitude phase modulation of VCSEL with 4 bit/s/Hz spectral efficiency for use in WDM-PON," *Optics Express* vol. 19, no. 27, pp. 26551-26556, 2011.

PAPER 12 T.-T. Pham, **R. Rodes**, J.B. Jesper, C.J. Chang-Hasnain, and I. Tafur Monroy, "Half-cycle QAM modulation for VCSEL-based optical links," *Optics Express*, accepted for publication.

PAPER 13 R. Rodes, T.-T. Pham, J.B. Jensen, T.B. Gibbon, and I.Tafur
Monroy, "Energy-efficient VCSEL-based multiGigabit IR-UWB over
fiber with airlink transmission system," in *Proc. of IEEE Photonics
Society*, pp. 222-223, 2010.

Other scientific reports associated with the project:

[PAPER 14] J.B. Jensen, T.B. Gibbon, X. Yu, **R. Rodes** and I.Tafur Monroy, "Bidirectional 3.125 Gbps downstream / 2 Gbps upstream impulse radio ultrawide-band (UWB) over combined fiber and wireless link," in *Proc. of Optical Fiber Communication*, paper OThO5, 2010.

[PAPER 15] J.B. Jensen, **R. Rodes**, M. Beltran and I.Tafur Monroy, "Shared medium 2 Gbps baseband and 2 Gbps UWB in-building converged optical/wireless network with multimode fiber and wireless transmission," in *Proc. of European Conference and Exhibition on Optical Communication*, paper We.7.B.4, 2010.

[PAPER 16] K. Prince, T.B. Gibbon, **R. Rodes**, E. Hviid, C.I. Mikkelsen, C. Neumeyr, M. Ortsiefer, E. Ŕonneberg, J. Rosskopf, P. ́Ohlén, E. Betou, B. Stoltz, E. Goobar, J. Olsson, R. Fletcher, C. Abbott, M. Rask, N. Plappert, G. Vollrath and I. Tafur Monroy, "GigaWaM next-generation WDM-PON enabling gigabit per-user data bandwidth," *Journal of Lightwave Technology* vol. 30, no. 10, pp. 1444-1454, 2012.

[PAPER 17] A. Lebedev, **R. Rodes**, X. Yu, J.J. Vegas Olmos, I. Tafur Monroy and S Forchhammer, "Simplified fiber-wireless distribution of HD video in passive and active W-band close proximity terminals," in *Proc. of 3rd Fiber Optics in Access Network Conference*, 2012.

[PAPER 18] M. Beltran, J.B. Jensen, X. Yu, R. Llorente,**R. Rodes**, M. Ortsiefer, C. Neumeyr and I. Tafur Monroy, "Performance of a 60-GHz DCM-OFDM and BPSK-impulse ultra-wideband system with radio-over-fiber and wireless transmission employing a directly-modulated VCSEL," *IEEE Journal on Selected Areas in Communications* vol. 29, pp. 1295-1303, 2011.

[PAPER 19] Iglesias, M, **R. Rodes**, TT Pham and I.Tafur Monroy, "Real time algorithm temperature compensation in Tunable Laser / VCSEL based WDM-PON System," in *Proc. of International Congress on Ultra Modern Telecommunications and Control Systems*, 2012.

[PAPER 20] Gonzalez, NG, A Caballero, R Borkowski, V Arlunno, TT Pham, **R. Rodes**, X Zhang, MB Othman, K Prince, X Yu, J.B. Jensen, D Zibar and I. Tafur Monroy, "Reconfigurable digital coherent receiver for metro-access networks supporting mixed modulation

formats and bit-rates," in *Proc. of Optical Fiber Communication Conference and Exposition*, paper OMW7, 2011.

[PAPER 21] J. J. Vegas Olmos,**R. Rodes**, and I.Tafur Monroy, "Low power consumption O-band VCSEL sources for upstream channels in PON systems," in *Proc. of Opto-Electronics and Communications Conference*, pp. 130-131, 2012.

[PAPER 22] T.T. Pham, **R. Rodes**, J. Estaran, J.B. Jensen and I. Tafur Monroy, "Half-cycle modulation for VCSEL based 6-Gbaud 4-QAM transmission over 1 km multimode fibre link," *Electronics Letters* no. 17, pp. 1074-1076, 2012

[PAPER 23] **R. Rodes**, A. Caballero, X. Yu, T.B. Gibbon, J.B. Jensen and I. Tafur Monroy, "A comparison of electrical and photonic pulse generation for IR-UWB on fiber links," *IEEE Photonics Technology Letters* vol. 22, pp. 263-265, 2010.

[PAPER 24] **R. Rodes**, J.B. Jensen, A. Caballero, X. Yu, S. Pivnenko and I. Tafur Monroy, "Enhanced bit rate-distance product impulse radio ultra-wideband over fiber link," *Microwave and Optical Technology Letters* vol. 52, 2010.

[PAPER 25] **R. Rodes**, T.T. Pham, J.B. Jensen and I.Tafur Monroy, "Radio frequency over glass integrated into FTTx by using 1,3 um VCSELs: Experimental performance assessment," in *Proc. of IEEE Photonics Conference*, pp. 767-768, 2011.

[PAPER 26] **R. Rodes**, X. Yu, A. Caballero, J.B. Jensen, T.B. Gibbon, N.G. Gonzalez and I. Tafur Monroy, "Range extension and channel capacity increase in impulse-radio ultra-wideband communications," *Tsinghua Science and Technology*, 2010.

[PAPER 27] T.B. Gibbon, X. Yu, R. Gamatham, N.G. Gonzalez, **R. Rodes**, J.B. Jensen, A. Caballero and I.Tafur Monroy, "3.125 Gb/s impulse radio ultra-wideband photonic generation and distribution over a 50 km fiber with wireless transmission," *IEEE Microwave and Wireless Components Letters* vol. 20, pp. 127-129, 2010.

[PAPER 28] V.S.C. Teichmann, A.N. Barreto, T.T. Pham, **R. Rodes**, I. Tafur Monroy and D.A.A. Mello, "SC-FDE for MMF short reach optical interconnects using directly modulated 850 nm VCSELs, *Optics Express* vol. 20, no. 23, pp. 25369-25377, 2012.

[PAPER 29] X. Yu, T.B. Gibbon, **R. Rodes**, T.T. Pham and I. Tafur Monroy, "System wide implementation of photonically generated im-

pulse radio ultra-wideband for gigabit giber-wireless access," *Journal of Lightwave Technology* vol. 31, no. 2, pp. 264-275, 2012.

[PAPER 30]   J. Estaran, **R. Rodes**, T.T. Pham, M. Ortsiefer, C. Neumeyr, J. Rosskopf and I. Tafur Monroy, "Quad 14Gbps L-band VCSEL-based system for WDM migration of 4-lanes 56 Gbps optical data links," in *Proc. of European Conference and Exhibition on Optical Communication* paper Th.2.B.3, 2012.

[PAPER 31]   T.T. Pham, **R. Rodes**, J. B. Jensen, C. Chang-Hasnain and I. Tafur Monroy, "Half-cycle QAM modulation for VCSEL-based optical links," in *Proc. of European Conference and Exhibition on Optical Communication*, paper Mo.1.B.3, 2012.

Contents

Chapter 1

Introduction

1.1 Outline of the thesis

This thesis is structured in 3 chapters as follows: Chapter 1 provides an introduction to vertical-cavity surface-emitting lasers (VCSELs) describing their structure and operational characteristics. I review on the datacom and telecom application scenarios for VCSELs as light sources. Sections 1.4 and 1.5 introduce coherent detection and advanced modulation formats specially attractive for VCSEL-based systems. Section 1.6 analyzes the state-of the-art in VCSEL modulation bandwidth, coherent detection in access networks, and the latest work on advanced modulation formats with VCSEL light sources. Section 1.7 describes how the results during my Ph.D. has extended the state of the art. Section 1.8 presents the main contributions of this thesis. Chapter 2 describes the main contributions of each publication included in this thesis. To conclude, Chapter 3 summarizes the main achievements of this Ph.D. research and provides an outlook for future trends in coherent optical fiber access networks, and in high-speed short-range systems.

1.2 Vertical-cavity surface-emitting lasers (VCSELs)

VCSELs are one of the most important laser sources in optical communication systems. Vertical emission laser was first suggested by Professor Kenichi Iga at the Tokyo Institute of Technology. The main difference of VCSELs light sources in respect to conventional edge emitting lasers is the

1
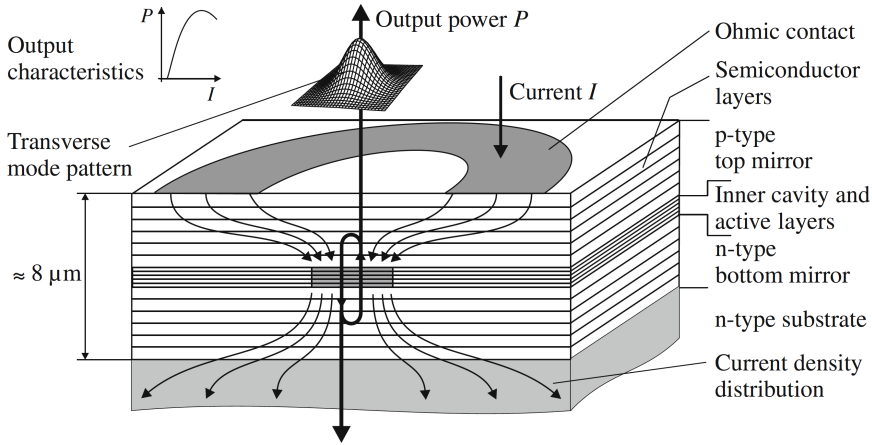
Figure 1.1: VCSEL structure [1].

emission being normal to the surface of the device. This unique characteristic makes VCSELs convenient for 2-D array integration, on wafer testing with potential low-cost manufacture, and circular emission with high fiber-coupling efficiency. Besides, the small cavity volume enables for low thresholds, and high-speed modulation at low currents. This combination of features has led to a high interest and rapid development of VCSELs for short reach high-capacity optical interconnects. In this section I describe the structure and principles of operation in VCSEL light sources.

1.2.1   Structure

The common structure to most VCSELs is shown in Figure 1.1. VCSEL structure includes a laser resonator consisting of two parallel reflectors which sandwich a thin active region. The reflectors are distributed Bragg reflectors (DBRs) with multiple pairs of layers. Each layer has a thickness of $1/4$ of the wavelength to obtain a strong reflexion of the light. The total reflexion of the DBR mirror has to be higher than 99.9% to reach lasing threshold [2]. The structure of the VCSEL provides multiple advantages. The small cavity volume enables for small threshold currents and high relaxation frequency even at low driving currents. Single-wavelength operation is obtained due to large mode separation resulting from the short cavity length. Therefore, it enables for wide and continuous wavelength tuning [3]. Different materials are used to grow VCSELs depending on the emission wavelength.

Wavelength (μm) 0.5   0.8   1.0   1.3   1.5

GaInAsP/InP   1.3 - 1.6
AlGaInAs/InP

GaInNAs/GaAs   1.2 - 1.3

GaInAs/GaAs   0.98 - 1.2

GaAlAs/GaAs   0.78 - 0.88

GaAlInP/GaAs   0.63 - 0.67
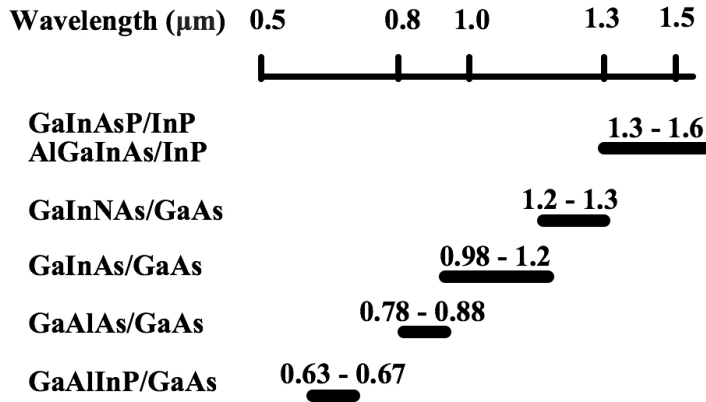
Figure 1.2: Materials of VCSEL light sources [2].

Figure 1.2 shows most common compounds and the wavelength range they provide. GaAs is used as a substrate for short-wavelength and up to 1.3 μm VCSELs, while for long-distance fiber optics systems, the most popular wavelength is around 1.5 μm with lasers grown on InP substrate. The most common technique for current confinement in GaAs-based VCSELs is oxide confinement, where a high aluminum content AlGaAs layer located in a null position of the standing wave above the active region is oxidized to form the oxide aperture with a typical diameter of 6 -10 μm [1], while InP-based VCSELs commonly employ a buried tunnel junction [4] [5].

1.2.2   DC operation

Fig.1.3 shows typical light-current-voltage (LIV) curves of a VCSEL light source. The abscissa represents the current injected into the laser, the right ordinate is the voltage across the VCSEL structure, and the left ordinate shows the optical power emitted. The small volume of the resonator allows for small current thresholds of approximately 1 mA. The rollover of the optical power of VCSEL light sources is typically 12-15 mA, reaching a maximum power out of approximately 0-5 dBm. The optical power out of the VCSEL can be calculated as [3].

$$P_{out} = \eta_i \eta_o \frac{h\nu}{q}(I - I_{th}) \qquad (1.1)$$

where η_i is the injection efficiency, η_o is the optical efficiency, h is Planck constant, ν is the frequency, q is the elementary charge, I is the injected current and I_{th} is the current threshold.
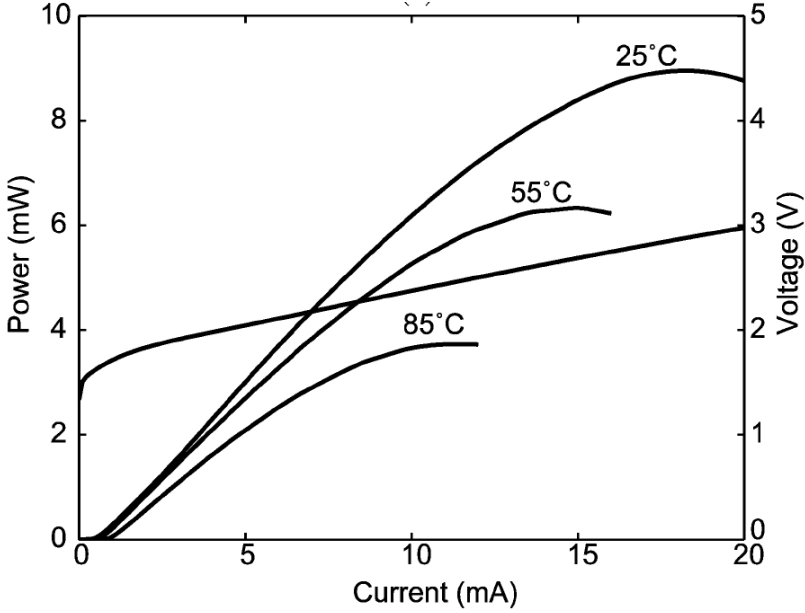
Figure 1.3: Output power versus current at $25°C$, $55°C$ and $85°C$ ambient temperature together with voltage versus current at $25°C$ for a GaAs VCSEL [6]

1.2.3 Dynamic operation

The non-linear electrical-to-optical conversion in a laser can be modeled by a set of differential equations called rate equations. The rate equation model determines the number of electrical carriers in the active region and photons in the laser cavity. There are multiple versions of the rate equation model with different explicit physical laser parameters. Dividing the number of carriers and photons by the volume of the active region and the cavity, respectively, the rate equations can be shown on their density form [3],

$$\frac{dN}{dt} = \frac{\eta_i I}{qV} - R_{sp}(N) - R_{nr}(N) - G(N, N_p)N_p \qquad (1.2)$$

$$\frac{dN_p}{dt} = -\frac{N_p}{\tau_p} + \Gamma\beta_{sp}R_{sp}(N) + \Gamma G(N, N_p)N_p \qquad (1.3)$$

where N is the carrier density, N_p is the photon density, I is the injection current, η_i is the current injection efficiency, q is the electron charge, V is the cavity volume of the laser, R_{sp} is the spontaneous recombination, R_{nr} is the non-radiative recombination, G is the laser gain, τ_p is the photon lifetime, Γ is the confinement factor and β_{sp} is the spontaneous emission
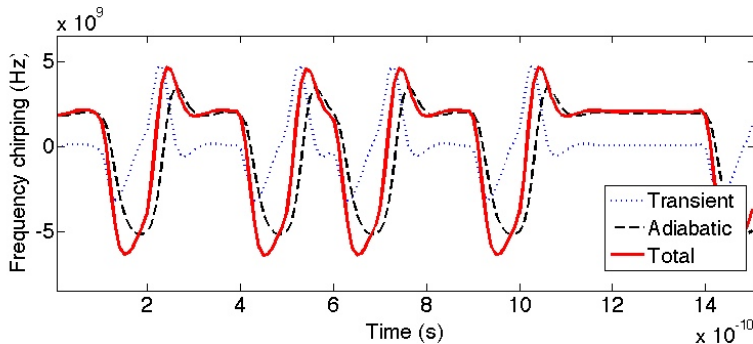
Figure 1.4: Transient, adiabatic and total modeled frequency chirping of a VCSEL light source

coupling coefficient.

We can calculate the power of the optical signal out of the laser from the photon density as [3],

$$P_{out}(t) = \eta_o h\nu \frac{N_p(t)V_p}{\tau_p} \qquad (1.4)$$

where V_p is the volume of the laser cavity.

The variation of the phase derivative over time of the optical signal is known as frequency chirping. Frequency chirping is specially important for coherent detection systems and for optical systems affected by chromatic dispersion. The derivative of the phase of the optical signal in direct current modulated VCSELs is modeled as

$$\frac{d\phi}{dt} = \frac{\alpha}{2}\Gamma G(N, N_p) - \frac{\alpha}{2\tau_p} + \frac{\alpha}{2}\frac{\varepsilon N_p}{\tau_p} \qquad (1.5)$$

where ϕ is the optical phase, α is linewidth enhancement factor and ε is the gain saturation factor. First and second terms of Eq.1.5 are associated with the transient chirp, while the third term is associated with the adiabatic chirp of the VCSEL. Fig.1.4 shows the modeled chirp of the VCSEL optical output with transient and adiabatic components.

1.2.4   Small signal modulation

Fig.1.5 shows a typical S21-parameter of a VCSEL light source for different bias current. Laser 3-dB bandwidth and frequency response damping increase as the bias current to the laser increases until a certain value. High
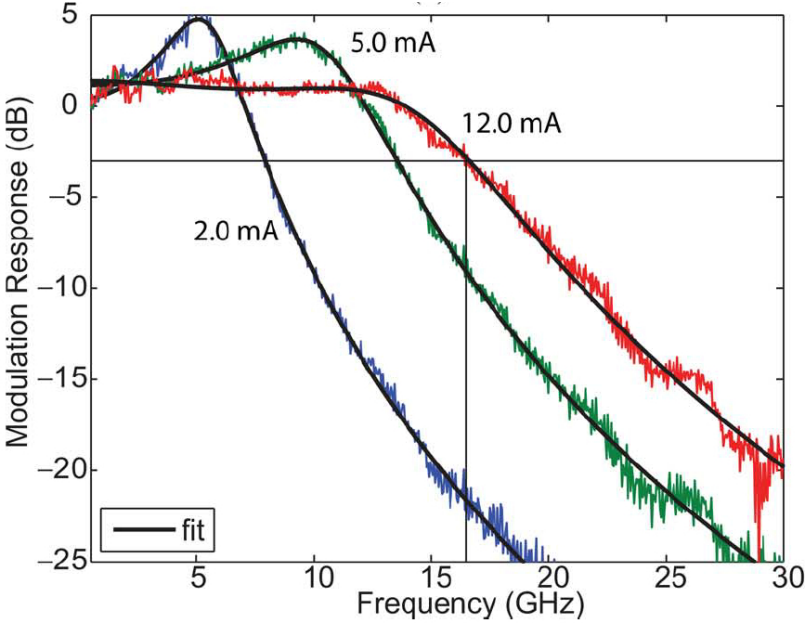
Figure 1.5: Small-signal modulation response at $25°C$ at different bias currents for a GaAs VCSEL [6]

values of bias current are desired for high speed modulation and flat frequency response, however it decreases the extinction ratio of your signal and produce optical power saturation on large signal modulation. The frequency response can be modeled as,

$$H(\omega) = \frac{\omega_R^2}{\omega_R^2 - \omega^2 + j\omega\gamma} \tag{1.6}$$

where ω is the relaxation resonance frequency and γ is the damping factor. The relaxation resonance frequency and the damping factor can be expanded as,

$$\omega_R^2 = \frac{\nu_g a}{qV_p}\eta_i(I - I_{th}) = \frac{\nu_g a N_p}{\tau_p} \tag{1.7}$$

$$\gamma = K f_R^2 + \gamma_0, \tag{1.8}$$

where ν_g is the group velocity and $a = \delta G/\delta N$ is the differential gain. K-factor and γ_0 describe the damping of the laser response,

$$K = 4\pi^2\tau_p\left(1 + \frac{\Gamma a_p}{a}\right) \tag{1.9}$$

$$\gamma_0 = \frac{1}{\tau_{\Delta N}} + \frac{\Gamma \beta_{sp} R_{sp}}{N_p} \qquad (1.10)$$

where $a_p = \delta G / \delta N_p$ and $\tau_{\Delta N}$ is the differential carrier lifetime.

An important design parameter for high-speed VCSELs is to increase the differential gain, because it increases the relaxation resonance frequency of the laser. Reducing the photon lifetime also increases the relaxation resonance frequency, however it decreases the damping factor leading to more peaking and less flat frequency response of the laser.

1.2.5   Thermal effects in VCSEL light sources

VCSEL light sources have a relatively high series resistance compared to edge emitting lasers. The DBR mirrors in the VCSEL structure are composed of multiple layers with small potential barrier. The addition of all DBR layers produces a significant voltage drop represented as a resistance in series with the diode [7]. The electrical power into the laser is expressed as [3],

$$P_{in} = I^2 R_s + I V_d + I V_s \qquad (1.11)$$

where I is the injected current into the laser, R_s is the series resistance, V_d is the current-independent series voltage, V_s is the ideal diode voltage. The power dissipated in the VCSEL is the difference between electrical power into the laser and the optical power out from the laser,

$$P_D = P_{in} - P_{out} \qquad (1.12)$$

The power dissipated in the laser induces to VCSEL self-heating. The internal temperature within the VCSEL can be described as,

$$T = T_o + P_D \cdot R_{th} - \tau_{th} \cdot \frac{dT}{dt} \qquad (1.13)$$

where T_o is the ambience temperature, R_{th} is the device thermal impedance, and τ_{th} is the thermal time constant. The device thermal impedance for a small-diameter VCSEL mounted on top of a relativelly thick substrate can be approximated as [3]

$$R_{th} = \frac{1}{2\xi s} \qquad (1.14)$$

which is obtained assuming a heat source with circular area, where s is the area diameter and ξ is the thermal conductivity of the material. The internal temperature raise caused by current self-heating has an impact on VCSEL

modulation performance. Increasing temperature contributes to a reduction of differential gain and internal quantum efficiency, and to an increase of the threshold current. These effects eventually cause the photon density, and therefore the output power and the resonance frequency, to saturate at a certain current level. This is called the thermal rollover current.

1.3   Application scenario

Immediately after the first room temperature demonstration of a continuous wave (CW) operation [8], Defense Advanced Research Projects Agency (DARPA) started the interest in VCSELs supporting programs to develop multigigabit optoelectronic interconnect technologies [9]. The exponential growth in computer performance and internet traffic, propitiated the interest in optics technologies to replace conventional electronics in data communication links. Optics technologies were able to out-perform electronics in terms of speed, power, and form factor [9]. VCSEL light sources were a key component to develop among several other optical components. Internet data traffic and computer performance have continue growing over the last decades and this trend is expected to continue in the future. Today, Internet data is routed through large datacenters made up of hundreds of thousand of servers operating in parallel. One of the main challenges in datacenter is to satisfy the increased capacity while keeping a moderate level of energy consumption, cost and space. To satisfy these requirements, VCSEL light sources offers better characteristics than edge emitting laser. VCSELs has become a main laser source for short-range high-speed optical links. Most of the Ethernet and Fiber Channel deployed links nowadays operate at 10 Gb/s or less in the 850 nm wavelength range. GaAs-based VCSELs are a mature technology at 10 Gb/s transmission rates, or even up to the latest Fiber Channel standard at 14 Gb/s [10]. Currently, the high volume of devices required by the market can be provided by companies such as Finisar and Oclaro. However, the challenge now facing the industry is to fulfill specifications of future data rates, while keeping a reduced power consumption, module cost and complexity. For instance, Google has stated in 2011 that 40 Gb/s would be the desired bandwidth for their new generation data centers [11]. IBM has planned 25 Gb/s optical interconnect speed in their roadmap for future Exaflop supercomputers in 2020 [12]. Different standard organizations are working on new recommendation. Table 1.1 shows the specifications already published by the different standard organizations. On the other hand, for the Telecom market operating at wavelengths be-

Standards	Speed	Year
IEEE 802.3ae	10 Gb/s	2003
Fiber Channel 10GFC	10 Gb/s	2008
Fiber Channel 16GFC	14 Gb/s	2011
IEEE 802.3ba	4,10x10 Gb/s	2010
Infiniband QDR	1,4,12 x 8 Gb/s	2008
Infiniband FDR	1,4,12 x 14 Gb/s	2011
Infiniband EDR	1,4,12x 25 Gb/s	2013
Fiber Channel 32GFC	28 Gb/s	2014

Table 1.1: Standards for optical systems [13] [14] [10]

yond 1.3 μm, the VCSEL design is based on InP. Historically, development of long-wavelength VCSELs has faced difficulties to design active materials with high optical gain compatible with high-reflexivity DBR mirrors [15]. Since 2000, new materials and design techniques have empowered long wavelength VCSEL development. InP-based VCSEL technology is not as mature as GaAs-based VCSEL, however, there is active research on long-wavelength VCSELs for the telecom market, for instance, in the European project GigaWaM [16]. GigaWaM aims to design, develop and manufacture all the components for a wavelength division multiplexing (WDM) passive optical network (PON) architecture providing a symmetric data rate of 1 Gb/s per-user over 20 km SMF [17]. The project employs long-wavelength VCSELs from Vertilas as the laser source for the downlink data transmission. Vertilas GmbH manufactures O-band, C-band and L-band VCSEL for telecom application. The Danish company Alight Technologies is currently manufacturing GaAs-based VCSELs operating at the low dispersion wavelength of 1.3 μm. BeamExpress SA and RayCan manufacture VCSELs in the O-band and C-band.

1.4   Coherent detection with VCSELs

Coherent detection has advantages compared to direct detection in terms of received optical power sensitivity. Therefore, coherent detection allows for higher power budget and it enables longer reach and higher splitting ratio in fiber-optic communication links. Passive optical networks (PONs) have become the preferable approach for current and future access networks.
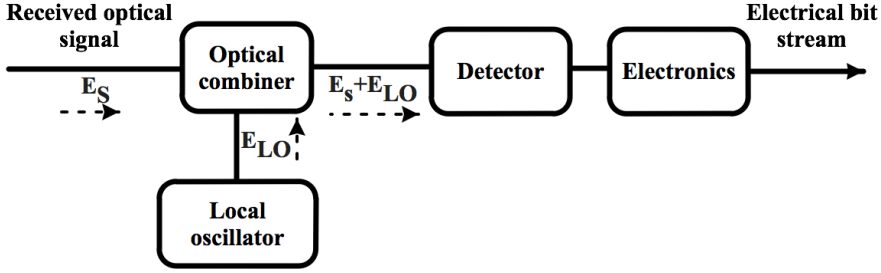
Figure 1.6: Schematic illustration of a coherent detection scheme

The optical unamplified transmission in PON links, together with the WDM architecture included in next generation PONs, have raised new interest in the advantages that coherent detection can offer. In this section, I describe the principles of coherent detection implementation, and it advantages in fiber optical access networks.

1.4.1 Principles

Fig. 1.6 shows a schematic of a coherent detection scheme. The basic idea of coherent detection is mixing in a photodiode the received optical signal with a continuous wave (CW) optical signal. The CW optical signal is generated by a laser called local oscillator (LO) which is normally part of the receiver. The received signal and the signal from the LO can be expressed as [18]

$$E_s = A_s exp[-i(\omega_s t + \phi_s)] \tag{1.15}$$
$$E_{LO} = A_{LO} exp[-i(\omega_{LO} t + \phi_{LO})], \tag{1.16}$$

where A_s, ω_s, ϕ_s and $A_{LO}, \omega_{LO}, \phi_{LO}$ represent the amplitude, frequency and phase of the received signal and LO respectively.
Assuming identical polarization on both signals, the optical power into the photodetector can be expresses as

$$P(t) = P_s + P_{LO} + 2\sqrt{P_s P_{LO}} \cos(\omega_{IF} t + \phi_s - \phi_{LO}), \tag{1.17}$$

where $P_s = KA_s^2$, $P_{LO} = KA_{LO}^2$ and $\omega_{IF} = \omega_s - \omega_{LO}$. P_s in the optical power of the received signal, P_{LO} is the optical power of the LO, K is a constant of proportionality and ω_{IF} is called intermediate frequency. The current out of the photodiode is proportional to its incident power and can be expressed as,

$$I(t) = RP_s + RP_{LO} + 2R\sqrt{P_s P_{LO}} \cos(\omega_{IF} t + \phi_s - \phi_{LO}), \tag{1.18}$$
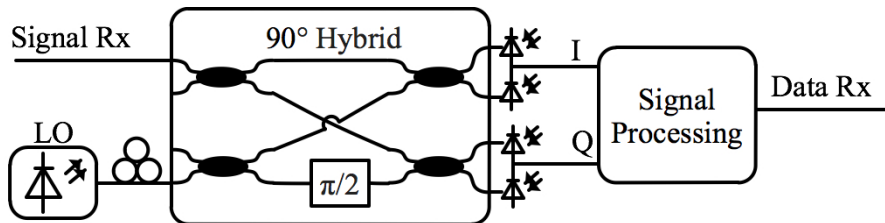
Figure 1.7: Schematic of general coherent receiver

where is R is the responsivity of the photodiode. Assuming AC-coupled output of the photodiode and $P_{LO} >> P_s$, the equation 1.18 can be simplified to

$$I(t) = 2R\sqrt{P_s P_{LO}} \cos(\omega_{IF} t + \phi_s - \phi_{LO}), \quad (1.19)$$

Eq. 1.19 shows that signal information can be received from the amplitude (P_s), frequency (ω_s) or phase (ϕ_s) of the optical signal. Since directly modulation is highly desired when using VCSEL light sources, we have considered amplitude modulation. In this case, received signal optical power in Eq. 1.19 is time-dependent, $P_s(t)$. Depending on the frequency offset between the received signal and optical signal from the LO (ω_{IF}), coherent detection can be divided into homodyne, heterodyne or intradyne. Homodyne coherent detection, $\omega_{IF} = 0$ is difficult to implement in practice because it requires an active control of the optical frequency of the LO to exactly match the carrier frequency. In heterodyne coherent detection, $\omega_{IF} > 2\pi R_s$ where R_s is the baud rate of the transmitted signal, the coherent receiver requires at least twice the bandwidth of the transmitted signal. Intradyne coherent detection is an intermediate case, where $0 < \omega_{IF} < 2\pi R_s$.

1.4.2   Coherent detection receivers

Fig. 1.7 shows a general coherent receiver schematic. The incoming signal is combined with the LO signal in a 90° optical hybrid which allows for detection of the in-phase (I) and quadrature (Q) components after mixing both optical signals in two pairs of balanced photodiodes. This scheme can be used for amplitude, frequency or phase demodulation since the whole optical field of the received signal is recovered. Phase information recovery of the optical signal enables chromatic dispersion compensation with digital signal processing. This scheme was used on **Papers 1-3**.

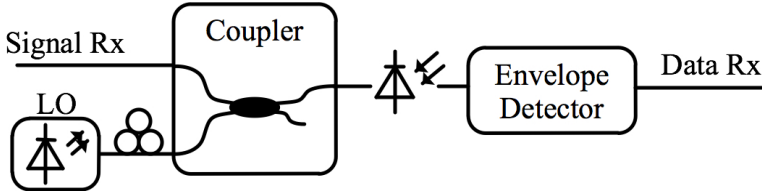In this thesis, coherent detection is intended for directly amplitude mod-

Figure 1.8: Schematic of ASK asyncronous coherent receiver

ulated VCSELs. Therefore, a simpler receiver scheme for amplitude modu-
lated signals can be used. Fig.1.8 shows a coherent receiver schematic used
in **Papers 4-6**. The receiver is composed of an optical coupler, a photodi-
ode branch and an envelope detection.This approach does not recover the
whole optical field of the incoming signal, and therefore, it can not compen-
sate for chromatic dispersion. However, it is very attractive for links where
chromatic dispersion is not dominant, such as systems in the low disper-
sion O-band region, or C-band systems with data-rates below 10 Gb/s and
distance of 20 km single-mode fibre (SMF).

1.4.3   Chirp-assisted coherent detection

Stable frequency relation between the transmitting laser and the LO has
been an important feature of coherent systems. External modulation and
narrow linewidth lasers have been usually employed for that purpose. Di-
rect current modulated VCSEL have not been previously used in coherent
systems due to higher frequency chirping compared to edge emitting lasers.
However, we can exploit adiabatic frequency chirping of the VCSEL to
improve the extinction ratio in amplitude modulated coherent detection
systems. Fig.1.9 shows the spectrum of a direct current modulated VCSEL
light source from a high resolution optical spectrum analyzer from Aragon
Photonics. Spectral power from $1's$ and $0's$ is separated due to frequency
chirping. The spectral separation increases as the peak-to-peak modulation
increases [19]. The LO is placed close to spectral frequency of the $1's$ and
opposite from the spectral frequency of the $0's$. Therefore, ω_{IF} after co-
herent detection is low for $1's$, and high for $0's$. The transfer function of
the photodiode, or an additional low pass filter, can be used to filter out
the high frequency signal from the $0's$ improving the extinction ratio of the
received signal. This technique has been used on **Papers 1-6**.
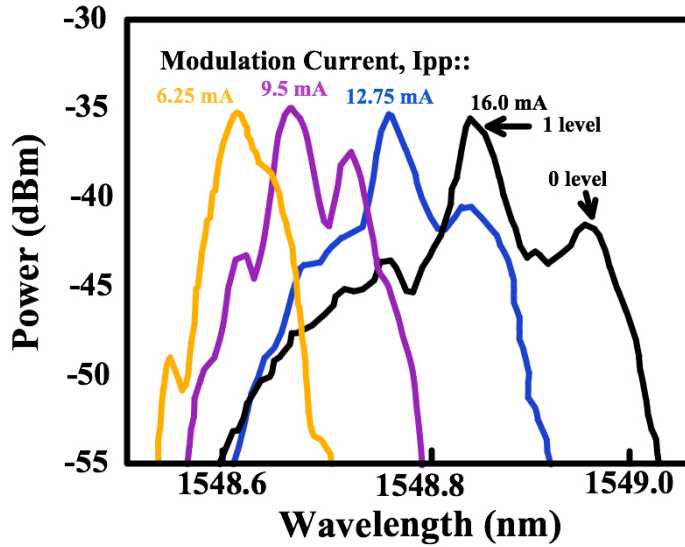
Figure 1.9: Optical spectrum of a directly modulated VCSEL [19]
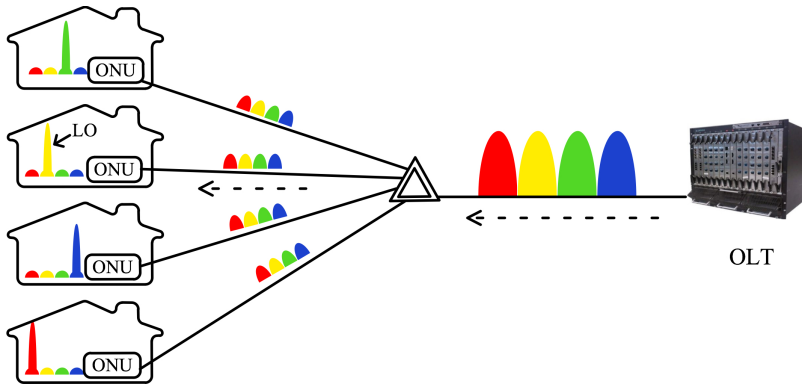
Figure 1.10: Coherent WDM-PON

1.4.4 Advantages on access networks

Passive optical networks (PONs) have become the predominant approach for next generation access networks. Coherent detection has two main advantages for fiber optical access networks on received optical power sensitivity and flexible wavelength allocation. Higher receiver optical power sensitivity of coherent systems provides wider power margins in the optical link, and therefore it allows for longer optical transmission distance and higher pas-

sive splitting ratio (more users). Extending transmission distance of the link and increasing the number of supported users reduce the number of required optical line terminations (OLTs), thereby reducing cost and network complexity. Installation of arrayed waveguide grating (AWG) to mux/demux WDM optical signals is one of the main concerns of internet operators for optical access networks based on wavelength division multiplexing passive optical network (WDM-PON) [20]. Besides the installation cost, the fixed frequency grid in AWG will not support future standards with closer frequency spaced channels. Wavelength tunability of coherent receivers, by tuning the local oscillator, provides flexibility in channel allocation and allows for closer frequency spaced channels increasing the overall capacity of WDM-PONs. Chromatic dispersion compensation enabled by coherent detection techniques allows for longer fiber transmission distance and higher bitrates on fiber links limited by chromatic dispersion. However, simplicity and cost reduction are two main challenges in order to make coherent attractive for next generation optical access networks.

1.5 Advanced modulation formats with VCSELs

Data communication systems based on VCSEL achieve higher capacities by applying high spectral efficient advanced modulation formats. Direct modulation of M-ary pulse amplitude modulation (PAM-M), single-carrier quadrature amplitude modulation (QAM), discrete multitone (DMT), and carrierless amplitude phase (CAP) modulation showed the potential to provide data transmission beyond 30 Gb/s with lower bandwidth requirements than NRZ-OOK. However, the higher spectral efficiency of these modulation formats comes together with higher requirements in terms of signal-to-noise ratio (SNR), and more complex transmitter and receiver architecture.
Ultra-wideband (UWB) modulation is intended for high-speed short-range wireless links with low power radiation. In this section, I review the advanced modulation formats used for direct modulation of VCSEL and their benefits.

1.5.1 M-ary pulse amplitude modulation

In non return-to-zero on-off keying (NRZ-OOK), the signal has two possible amplitude levels or symbols, "1" or "0", therefore, one symbol transmit one bit. In a M-ary PAM system, the signal has M possible amplitude levels, and $log_2(M)$ bits are transmitted per symbol, $R_b = R_{symb} \cdot log_2(M)$. M-
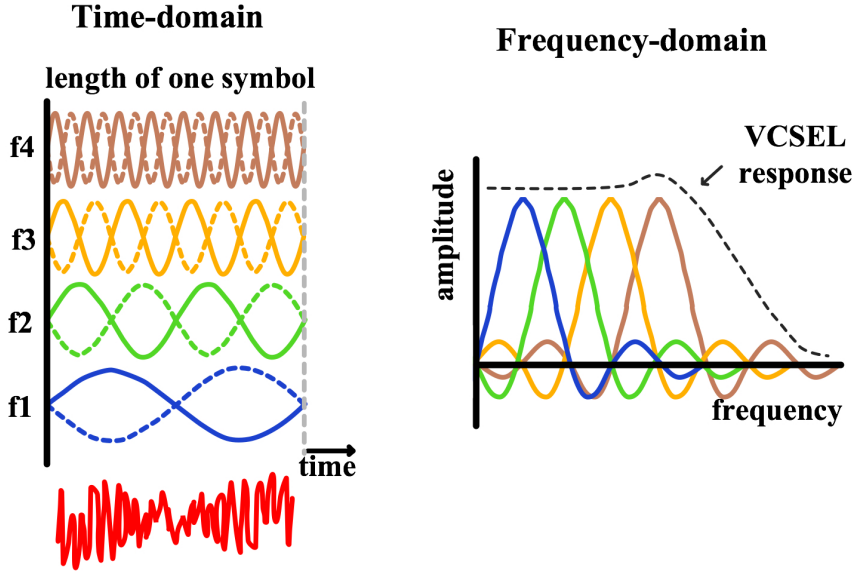
Figure 1.11: Single Cycle 16-QAM transmitter setup.

ary PAM modulation exhibits $log_2(M)$ higher spectral efficincy compared to NRZ-OOK. However, PAM-4 modulation multiplies by 3 the SNR requirements compared to NRZ-OOK. PAM-4 has lower system complexity compared to QAM or CAP modulations schemes, which makes it attractive for systems looking for doubling the spectral efficiency of NRZ-OOK modulation while maintaining a low complexity.

1.5.2   Quadrature amplitude modulation

Quadrature amplitude modulation (QAM) is a modulation scheme that uses two sinusoidal carriers with 90 degrees phase offset. The signal can be expressed as,

$$s(t) = I(t)cos(2\pi f_0 t) + Q(t)sin(2\pi f_0 t) \tag{1.20}$$

where $I(t)$ and $Q(t)$ are the components carrying the data stream, they are called in-phase and quadrature, respectively, f_0 is the carrier frequency. The two modulated orthogonal carriers are summed resulting in a signal with amplitude and phase modulation. QAM is a bandpass transmission with the spectrum centered on f_0. On direct modulation of VCSELs, low frequency carriers are desired in order to exploit the spectral bandwidth of the VCSEL.

Single-cycle & Half-cycle QAM

Single-Cycle and Half-Cycle QAM are particular cases of QAM where the carrier frequency is equal and half the symbol rate, respectively,

$$\text{Single-Cycle: } f_0 = R_b \qquad \text{Half-Cycle: } f_0 = R_b/2 \tag{1.21}$$

These particular cases are specially attractive for direct modulation of VCSELs as their spectrum is on the low frequency range. The first spectrum lobe occupies the spectral band from DC to $2 \cdot f_{sym}$ for single-cycle, and from

Figure 1.12: DMT representation of 4 subcarriers a) time domain b) frequency domain.

DC to $1.5 \cdot f_{sym}$ for half-cycle. Half-cycle quadrature amplitude modulation (HC-QAM) has 25% higher spectral efficiency than single-cycle quadrature amplitude modulation (SC-QAM). Both cases have been demonstrated with smart implementations with commercial available XOR-gates in [21] and **Paper 12**. Fig. 1.11 shows the structure of the SC-QAM transmitter setup for VCSEL modulation. A SC-4QAM signal is generated by XOR-gating a NRZ-OOK signal with the signal rate clock. Notice that, for research proposes, independent I and Q components are emulated by using both outputs of the XOR-gate and de-correlating the branches by delaying one of them. The multilevel block shown in Fig. 1.11 emulates two independent multilevel SC-QAM branches to generate a SC-16QAM. Several XOR-gates are required for independent data modulation of I and Q components and multilevel configuration. half-cycle quadrature amplitude modulation (HC-QAM) transmitter setup is similar to Fig. 1.11, but it uses a half signal rate clock to the XOR-gate.

1.5.3   Discrete multitone modulation

discrete multitone (DMT) is a baseband multicarrier modulation that is capable of high-speed transmission with VCSEL. Although DMT has not been part of the work included in this thesis, high speed modulation of
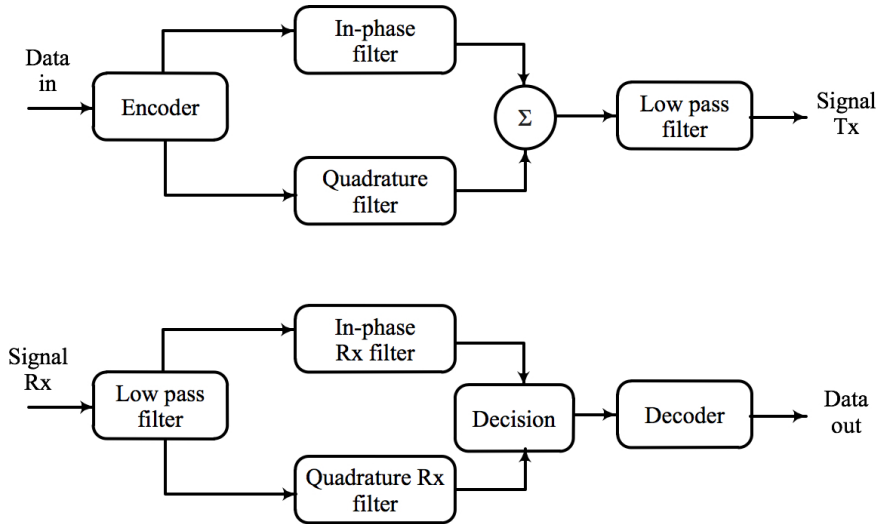
Figure 1.13: CAP transmitter and receiver setup

VCSELs with DMT has been reported [22]. DMT uses multiple orthogonal subcarriers to divide the available bandwidth in narrow bands and transmits the data from all bands in parallel. Fig.1.12 shows a representation in time and frequency domain of a DMT signal with 4 subcarriers. QAM is used as a modulation format for each subcarrier. The DMT transmitter employs an inverse fourier transform (IFT) to generate orthogonal subcarriers. At the receiver side, fast fourier transform (FFT) is used to demodulate the transmitted data from each subcarrier. Orthogonal subcarriers allow for independent subcarrier demodulation. DMT uses cyclic prefix to avoid inter-symbol interference (ISI) and inter-carrier interference (ICI) caused by dispersion, and training symbols to estimate and equalize the channel. An important feature of DMT is to offer flexible modulation order for each subcarrier, therefore it is possible to allocate the number of bits and power per subcarrier, depending on the SNR of each subcarrier (a technique known as bit loading). The main drawback of DMT is the high peak-to-average power ratio (PAPR). PAPR is proportional to the number of subcarriers, and it reduces the average power of the DMT signal driving the VCSEL. Amplitude clipping of the DMT signal reduce PAPR and increase the average electrical power of the DMT signal into the VCSEL light source [23], [24].
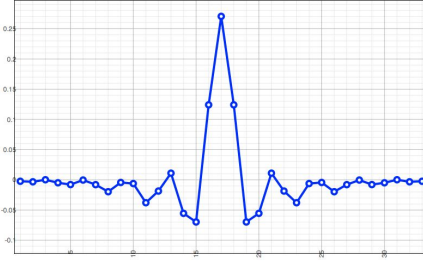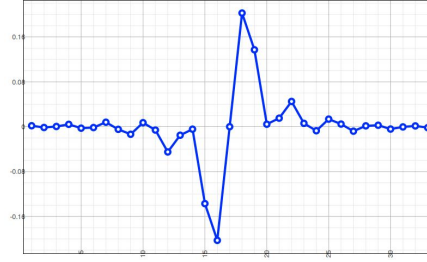
Figure 1.14: In-phase CAP filter

Figure 1.15: Quadrature CAP filter

1.5.4   Carrierless amplitude phase modulation

Carrierless amplitude phase (CAP) modulation was proposed in 1975 by
Bell Labs as a viable modulation technique for high-speed communication
links over copper wires [25]. It was derived from QAM and can be consid-
ered its variation, although there are fundamental differences in its gener-
ation and detection. Fig. 1.13 shows the general block diagram of a two-
dimensional CAP transmitter and receiver. The incoming data is encoded
into multilevel symbols. The multilevel symbols are shaped by orthogonal
filters, which represent different dimensions resulting in orthogonal wave-
forms. The orthogonal waveforms are combined and low pass filtered. For
two-dimensional CAP, an option for the shape of the orthogonal filters is
the product of a square-root raised cosine filter (SRRC) with a sine or cosine
waveform,

$$f_1(t) = h_{SRRC}(t) \cdot cos(2\pi f_c t) \tag{1.22}$$
$$f_2(t) = h_{SRRC}(t) \cdot sin(2\pi f_c t) \tag{1.23}$$

where $f_1(t)$ and $f_2(t)$ are the in-phase and quadrature filters. Fig.1.14 and
Fig. 1.15 show the filter shapes. At the receiver side, matched filtering is
used to recover each dimension. Higher order dimension CAP is achieved
by using more than two orthogonal filters. However, the filter design with
optimized orthogonality is challenging to obtain for higher orders [26]. The
number of bits per symbol with CAP modulation is $k = D \cdot log_2(L)$, where
D is the number of dimensions, and L is the number of levels in each
dimension. An important design parameter in a CAP system is the roll-off
parameter of the SRRC filter, with a design trade-off between bandwidth
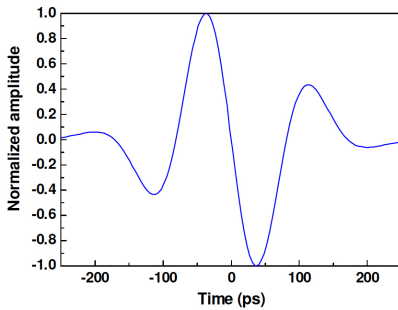occupation and inter-symbol interference (ISI).
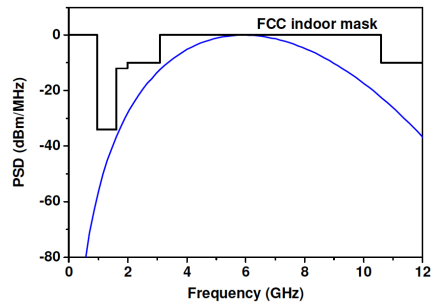
Figure 1.16: UWB pulse

Figure 1.17: Normalized UWB PSD and the FCC indoor mask

1.5.5   Ultra-wideband modulation

Ultra-wide band (UWB) is a short-range high-speed wireless communication technology with an extremely low power spectral density (PSD) radiation in order to co-exist with existing in-band wireless systems without interference. Compliance with the Federal Communications Commission (FCC) requires an equivalent isotropically radiated power (EIRP) power emission below -41.3 dBm/MHz on a wide spectral band from 3.1-10.6 GHz for ultra-wide band (UWB) systems [27]. Impulse-radio ultra-wideband pulse-shapes of high order derivate of a Gaussian function have been proposed for fulfillment of FCC regulation [28]. The 5th order derivative of the Gaussian pulse has the best fitting with the FCC mask. The function describing the pulse is,

$$y(t) = A\left(-\frac{t^5}{\sqrt{2\pi}\sigma^{11}} + \frac{10t^3}{\sqrt{2\pi}\sigma^9} - \frac{15t}{\sqrt{2\pi}\sigma^7}\right) exp\left(-\frac{t^2}{2\sigma^2}\right) \qquad (1.24)$$

where the optimum standard deviation, σ, is 60 ps and A is used to normalize the pulse amplitude. Fig.1.16 shows the 5th-order Gaussian pulse in the time domain and Fig.1.17 shows the corresponding power spectral density (PSD). The spectrum of a 5th-order derivative Gaussian pulse is effectively compliant with the FCC indoor mask. Current VCSEL can satisfy the bandwidth emission of UWB technology, with frequency occupation between 3 - 10 GHz. Moreover, the low driving current and power emission of the VCSEL agree with low consumption and power emission of UWB systems.

1.6   State-of-the-art analysis

1.6.1   VCSELs

Active efforts to improve VCSEL are currently taking place in both academia and industry. To analyze the state-of-the-art in VCSEL light sources for optical communications we should distinguish between different wavelength ranges, since they require different technologies and they face different challenges. At 850 nm, Chalmers University presented a VCSEL with a -3 dB bandwidth of 28 GHz at room temperature and has used it to demonstrate error-free direct modulation up to 44 Gb/s [29]. IBM and Finisar have experimentally demonstrated direct modulation up to 55 Gb/s with a VCSEL with -3 dB bandwidth of 23 GHz [30]. At 980 nm, University of California, Santa Barbara demonstrated 35 Gb/s direct VCSEL modulation in 2009 [31]. Recently, 44 Gb/s at $25°C$ [32] and 38 Gb/s at $85°C$ [33] have been demonstrated by the Technical University of Berlin. The same group has also reported a record transmission of 49 Gb/s at an operating temperature of $-14°C$. At a 1100 nm walength, 40 Gb/s has been demonstrated with a InGaAs-based VCSEL already in 2008 by NEC [34]. In the 1300 nm band, 30 Gb/s operation has recently been demonstrated on an InP-based VCSEL by the Technical University of Munich [35]. VCSEL transmission over 10 km SMF at 30 Gb/s was demonstrated, due to the low chromatic dispersion of the fiber on this wavelength range [35]. At 1550 nm, back in 2009, 22 Gb/s was demonstrated by University of California, Berkeley [36]. Recently, 35 Gb/s [37] and 40 Gb/s operation has been demonstrated with a 19 GHz 3-dB bandwidth VCSEL by the Technical University of Munich [38].

1.6.2   Coherent passive optical networks

During the last years, coherent detection has been gaining attention for next generation access networks. NEC Laboratories has shown multiple demonstrations on coherent detection with orthogonal frequency-division multiplexing access (OFDMA) transmission [39] [40] [41]. In [39], 108 Gb/s transmission over 20 km SMF on a single wavelenght is achieved by frequency multiplexing 18 Gb/s OFDMA signals, employing external modulated external cavity lasers (ECLs) and heterodyne coherent detection. In [41], a similar approach is combined in a WDM system with 25 channels to achieve a total capacity of 1.2 Tb/s. In 2010, NTT demonstrated 10 Gb/s quadrature phase shift keying (QPSK) transmission over 20 km SMF [42]. In [42], external modulation of a distributed feedback (DFB)

laser is used for the transmitter, and a VCSEL light source as LO [42], and a digital processing technique for phase noise cancellation. In 2011, Nokia Siemens Networks demonstrated a filterless ultradense-WDM-PON system with channels spacing of 2.8 GHz by using coherent detection and real time processing in a FPGA [43]. In [43], 64 channels at a bitrate up to 1.2 Gb/s per channel are demosntrated. Other approaches on coherent PONs use reflective semiconductor optical amplifiers (RSOAs) [44], [45]. In [44], 10 Gb/s QPSK over 80 km SMF in a RSOA-based WDM-PON has been demonstrated by KAIST, employing self-homodyne coherent detection and offline digital signal processing. In 2012, University Colleague of London presented a 10 Gb/s QPSK coherent PON based on a monolithically integrated C-band tunable digital supermode (DS) DBR [46]. In [46], externally modulated DBR laser, with polarization multiplexing emulation and parallel digital signal processing is employed.

1.6.3   Advanced modulation formats for VCSELs

4-level pulse amplitude modulation (PAM-4) of 850 nm VCSELs has been reported in [47] and [48]. In [47], Chalmers University of Technology demonstrated 30 Gb/s over 200 m multi-mode fibre (MMF) with real-time error measurement. In [48], 32 Gb/s was demonstrated by University of Cambridge with pre-distortion of the electrical signal to improve the VCSEL response. On discrete multitone (DMT), modulation up to 30 Gb/s was demonstrated over 500 m of MMF on a 850-nm VCSEL [22]. In [22], the spectral bandwidth occupation is 6 GHz, with bit loading implementation, achieving high spectral efficiency by modulating 150 subcarriers up to 128-QAM for the best SNR subcarriers. On carrierless amplitude phase (CAP), although not on a VCSEL, optical transmission with direct modulation up to 40 Gb/s was presented by University of Cambridge [49]. In [49], CAP-16 generation is done with two transversal filters. Recently, multidimensional CAP has been demonstrated on VCSELs by the Technical University of Denmark at low bitrates below 1 Gb/s [50]. On quadrature amplitude modulation (QAM), single cycle 16-QAM direct modulation of a 850 nm VCSEL at 37 Gb/s was presented by Chalmers University of Technology [21]. In [21], the inphase and quadrature signals are generated by a XOR gate, with the baseband data in one input and data clock in the other input. The advantage of this method comes from the simplicity of the high-speed transmitter, using a commercially available XOR gate. While both electrical and photonic generation of UWB signals have been researched [51], in particular for VCSELs, electrical generation and directly modulation has

mostly been employed. Direct current modulation of a 1.5 and 1.3 m VCSEL with multi-band orthogonal frequency-division multiplexing (MB-OFDM) UWB was presented by University of Essex on a bi-directonal system at 480 Mb/s [52]. In 2011, an experimental demonstration of impulse-radio ultra-wide band (IR-UWB) with a 850 nm VCSEL was presented by using a prototype notch filter cutting off the critical 3.1 GHz band [53]. VCSEL-based IR-UWB signal in the 60-GHz radio band has also been presented by the Technical University of Denmark [54].

1.7 Beyond state-of-the-art

The work presented in this thesis has significantly extended the state-of-the-art in the areas of coherent PONs by using non-conventional coherent techniques based on exploiting chirping on directly modulated VCSELs. **Paper 1** and **Paper 2** are, to the author knowledge, the first demonstration of a coherent detection system using a VCSEL as a transmitter optical light source. My work presented in **Paper 3** extends previous results on VCSEL-based coherent links [42], by replacing the low-linewidth LO laser used on **Paper 1** and **Paper 2**, therby showing, for the first time, a coherent PON link fully based on VCSEL light sources. **Paper 4** and **Paper 5** reduce complexity of the coherent detection receiver configuration and implement real time demodulation. These results represented a improvement of two times capacity and lower complexity compare to previous real time coherent demonstrations [43]. Finally, **Paper 6** combines previous work to experimentally demonstrate a PON link fully based on VCSELs, at 10 Gb/s transmission with a simplified coherent receiver scheme using realtime demodulation. The work in this thesis also extends the state-of-the-art in the area of advanced modulation formats and high-speed short range systems based on VCSELs. I have investigated multiple modulation formats on optical systems to increase capacity, efficiency, or to introduce novel modulation formats with advantages and new applications on optical systems. At publication date, **Paper 7** showed the highest capacity ever transmitted with a directly modulated VCSEL. In **Paper 7** and **Paper 8**, we extend the previous work done in PAM-4 modulation with VCSEL for high-speed optical short range links [47] [48]. We demonstrated 25 Gbaud PAM-4 modulation on a 1550 nm VCSEL achieving 50 Gb/s directly modulation on VCSEL. The capacity of the system is increased to 100 Gb/s by polarization multiplexing (PolMux) emulation system emulation and forward error correction techniques. **Paper 9** proposes a system based on

four PAM-4 modulated VCSELs to migrate 4-lanes 56 Gb/s optical data links to a compact WDM link. **Paper 10** and **Paper 11** presents a 50 GHz spaced WDM-PON link using CAP modulation for high spectral efficient optical network unit (ONU). **Paper 10** is the first demonstration of CAP modulation on VCSEL. **Paper 12** extend previous work done on QAM directly modulated VCSELs [21] introducing half cycle QAM modulation. Half-cycle QAM increases in 25% the spectral efficiency compared to previous approaches based on single-cycle QAM. **Paper 12** is the first demonstration of SC-QAM with VCSELs or any optical source. **Paper 13** introduce for the first time bipolar IR-UWB improving spectral occupation and increasing wireless distance and capacity of previous work [52], [51]. **Paper 13** presents a 2 Gb/s UWB system based on VCSEL light sources with optical fiber distribution over 25 km SMF and 4 meters air transmission for applications in hybrid optical fiber-wireless transmission links.

1.8 Main contributions of the thesis

The main contributions of this thesis are in the area of coherent detection using VCSEL sources for applications in next generation optical access networks, and on signal generation techniques using advanced modulation formats with VCSEL light sources for applications in high speed data communication links.

First, this thesis proposes and experimentally demonstrates a coherent demodulation approach for optical access networks with a simple receiver configuration exploiting frequency chirping of direct current modulated VCSELs. All-VCSEL-based coherent detection PON link at 10 Gb/s data transmission over 20 km SMF transmission distance is reported with real-time demodulation. Secondly, it contributes on exploring signal generation techniques with advanced modulation formats in VCSEL- based systems for high- speed data optical links. Directly modulation of a VCSEL light source at 50 Gb/s is reported with 4 levels pulse amplitude modulation. Link capacity is increased to 100 Gb/s by using polarization multiplexing emulation and forward error correction techniques.

Chapter 2

Description of papers

This thesis is based on a set of articles already published or accepted for publication in peer-reviewed journals and conference proceedings. These articles present the results obtained during the course of my doctoral studies, combining theoretical analysis, simulation and experimental results. The papers are grouped in two categories: coherent detection schemes based on VCSELs in PONs (**PAPER 1** to **PAPER 6**) and advance modulation formats with VCSEL light sources (**PAPER 7** to **PAPER 13**).

2.1 Coherent detection based on VCSELs for access networks

The papers presented on this first section summarize the research during my Ph.D. on coherent detection using VCSELs. The papers are organized in the same order the experiments were carried out. Publication dates do not completely follow the same order due to varying publication speeds of journals. Each individual paper has its own goal and advance respect to the previous one, however the constant goal while doing all of them was to investigate on the possibilities and advantages that coherent detection can offer on passive optical networks (PONs). We have focused on using VCSEL light source, and we removed the traditional idea that only low-linewidth lasers and complicated receivers are feasible for coherent detection. We started by using VCSELs as the transmitting light sources. Then, we implemented an all-VCSEL based optical system with conventional coherent detection receiver scheme including digital signal processing (DSP). Finally, we simplified the coherent detection receiver and implemented real-time de-

modulation.

PAPER 1 - *VCSEL transmission with a coherent receiver.*
In this paper, we reported on experimental demonstration of digital coherent detection based on a directly modulated VCSEL with bit rate up to 10 Gb/s. This system allows a cooler-less, free running, and optically unamplified transmission without optical dispersion compensation up to 105 km at 5 Gb/s long reach passive optical links. The system uses a conventional coherent receiver with a external cavity tunable laser as a local oscillator. The receiver optical power sensitivity and optical power margin are increased by 13 dB compare to direct detection. This is especially advantageous for scaling the uplink of PONs by placing the low cost VCSEL at the customer premises, whereas the more complex coherent receiver at the central office.

PAPER 2 - *Extending reach and going bidirectional.*
In this paper we present 5 Gb/s bidirectional 40 km SMF link transmission with coherent detection of directly modulated 1550nm VCSELs. Through the use of digital signal processing for demodulation and dispersion compensation, receiver sensitivities of -37.3 dBm downstream and -37.7 dBm upstream was achieved with no use of optical amplifiers or optical dispersion compensation. At a launch power of 0.6 dBm and 7.7 dB fiber loss, a system margin of 30 dB was achieved, corresponding to the loss of a record passive splitting ratio of 1024. This experiment uses conventional coherent receiver with a external cavity tunable laser as a local oscillator. The reported experiments demonstrate the potential for coherent detection in bidirectional access links employing directly modulated VCSEL transmitters.

PAPER 3 - *Fully VCSEL-based: Tx and LO VCSEL.*
We report on experimental demonstration of a digital coherent detection link fully based on VCSELs for the transmitter as well as for the local oscillator light source at the receiver side. We demonstrate operation at 5 Gb/s at a 1550 nm wavelength with record receiver sensitivity of -36 dBm after transmission over 40 km SMF. Signal processing algorithms were implemented to digitally compensate for the frequency offset between the transmitter and the local oscillator VCSELs, and for chromatic dispersion. This system allows for uncooled VCSEL operation and fully passive fiber transmission with no use of optical amplification or optical dispersion compensation.This is, to the best of our knowledge, the first demonstration of

coherent optical transmission systems using a VCSEL as the local oscillator as well as for the transmitter light source. The results show the potential for coherent systems to be implemented with low cost optical sources, thereby overcoming one of the main drawbacks of coherent systems for access networks.

PAPER 4 - *Simple coherent detection receiver with 1.3 um VCSEL.*
This papers present a full 1.3 μm VCSEL-based link with a simplified coherent detection receiver. We demonstrate up to 5 Gb/s. Received optical power sensitivity of -34 dBm at bit error rate (BER) below the forward error correction (FEC) limit correction of $2.2 \cdot 10^{-3}$ is achieved over 40 km SMF, resulting in a high splitting ratio of 95 with no optical amplification or dispersion compensation. Compared to previous work, this paper presents a simplified receiver scheme where we substitute the 90 degree hybrid and balanced photodiodes of conventional receiver, by a 3 dB coupler, a PIN photodiode and a envelope detector done on DSP. The simplicity of our proposed coherent approach is intended to overcome the complexity of conventional coherent systems for access networks.

PAPER 5 - *Getting to real-time implementation.*
This paper presents an experimental demonstration of a real-time implementation for the simplified coherent receiver presented previously in **PAPER 4**. VCSEL-based optical link with a simplified real time coherent detection receiver at 2.5 Gb/s is demonstrated. Receiver sensitivity of -37 dBm is achieved proving splitting ratio up to 2048 after 17 km fiber transmission. The real time implementation was done by using a simple XOR-gate and a filter at the receiver for envelope detection.

PAPER 6 - *Faster, longer and all-VCSEL based real time detection.*
In this paper, we use the real time receiver demonstrated in **PAPER 5** on a 10 Gb/s all-VCSEL based coherent PON link. Receiver sensitivity of -33 dBm is achieved after 25 km SMF, allowing for a passive splitting ratio of 199. The potential cost reduction and good performance of our proposed approach make VCSEL-based coherent PONs a strong candidate for application in future PONs. Future work on this approach will be adding more transmitting channels implementing a WDM system.

2.2   Advance modulation formats for VCSEL base optical networks

The second section is a compilation of experiments I have performed on advanced modulation formats during my Ph.D. All the papers investigate on modulation formats that have advantages in specific applications. Depending on the scenario, we want to asses total capacity, or high spectral efficiency or power consumption. **PAPER 7 - 9** pursue the highest capacity on a high-speed VCSEL and on a 4-lines L-band VCSEL system. **PAPER 10 - 12** focus on increase spectral efficiency since we are limited by the electrical modulator. **PAPER 13** investigates IR-UWB modulation for low power consumption and low interference approach for application in hybrid optical-wireless networks.

PAPER 7, **PAPER 8** - *PAM-4 to increase capacity per VCSEL.*
In this two papers we present an experimental demonstration of high-speed 4-level pulse amplitude modulation on a 1.5 μm VCSEL light source. We achieved 50 Gb/s per polarization by using PAM-4 modulation, and a total linerate of 100 Gb/s by polarization multiplexing emulation over 100 m SMF. **PAPER 8** includes longer explanation on the experimental setup, VCSEL characteristics and forward error correction used. Error free demodulation of $1.6 \cdot 10^8$ bits was achieved after forward error-correction with an effective bitrate of 86.5 Gb/s. The system reduces the number of channels needed to reach an aggregated capacity by increasing bandwidth efficiency and including error correction capability. Scaling by 4 the proposed system, by either spatial or wavelength multiplexing, is a candidate solution to provide future standards capacity of 400 Gb/s.

PAPER 9 - *4-lines WDM PAM-4 to increase total capacity.*
In this paper we report an experimental demonstration of 4x14 Gb/s L-band VCSEL-based WDM transmission over 10 km of SMF. We achieve successful transmission of four channels with 4-level pulse amplitude modulation at 7 Gbauds with post-FEC (7% overhead) error free operation. The crosstalk power penalty was measured to be 0.5 dB and the power budget margin ranges between 6 dB and 7 dB. Our results show the potential of the reported system to migrate 4-lanes 56 Gb/s data links into a compact WDM link.

PAPER 10 , **PAPER 11** - *CAP-16 on WDM-PON link.*

In this paper we propose and experimentally demonstrate directly modulation of CAP-16 in commercially available VCSELs for applications in next generation WDM-PON access networks. The system is evaluated with 4 close spaced WDM channels at 1.25 Gb/s each, with a spectral efficiency of 4 bit/s/Hz, for a total bitrate of 5 Gb/s over 26 km fiber transmission. All the channels achieved receiver power sensitivity below -24 dBm. In **PAPER 11** we have included simulation on the requirements of number of filter taps and amplitude level resolution for CAP signals generation. CAP allows for scalability in multilevel and multidimension. Therefore, CAP can potentially reach high spectral efficiency. For a given bit-rate, higher spectral efficiency results in lower bandwidth occupation allowing for close channel spacing without crosstalk. We believe direct CAP modulation of VCSEL light sources is a candidate for next generation PONs and short range systems.

In **PAPER 12** - *Half-cycle QAM modulation in VCSEL.*
In this paper we have investigated in QAM modulation utilizing sub-cycle subcarrier for VCSEL-based optical links to improve spectral efficiency. The transmission of 10-Gb/s 4-QAM data in 7.5- GHz electrical bandwidth over 20-km single mode fiber was demonstrated with BER below the FEC limit and only 2.5-dB power penalty. Half-cycle signals have superior dispersion tolerance compared to NRZ-OOK signals at the same data rate. Spectral efficiency can be improved by increasing the number of levels of the QAM signal. Both the transmitter and the receiver can be implemented using available electronics. Half-cycle subcarrier QAM modulation has potential for applications in high-speed PON networks as well as high-performance data centers.

In **PAPER 13** - *Wireless transmission with UWB modulation in VCSELs.*
This paper presents a system approach based on VCSEL light source for distributing high-speed IR-UWB signals in an energy efficient communication system.In this paper we demonstrate for the first time bipolarity on the UWB signal to eliminate spikes in the IR-UWB spectrum at the repetition rate frequency. By eliminating all amplifiers for the optical transmission part as well as for the wireless transmission part (apart from a single amplifier after the receiving antenna), system complexity and power consumption have been considerably reduced. With our proposed scheme, a 2 Gb/s IR-UWB signal was transmitted over 25 km SMF and a 2 meter in-home wireless link with no errors detected, and a BER of $4.99 \cdot 10^{-4}$ after 4 meters wireless transmission.

Chapter 3

Conclusions and future work

3.1 Conclusions

This PhD thesis addresses the design and performance evaluation of VCSEL-based coherent passive optical networks (PONs). It addresses as well as the utilization of advanced modulation formats with VCSEL light sources for local area networks (LANs) and wide area networks (WANs). The research results presented in this thesis are pioneering in the area of coherent detection PONs, high-speed interconnects and advanced modulation formats with VCSEL light sources. This thesis presents the first experimental demonstration of a coherent detection link fully based on VCSEL light sources with a simplified receiver configuration and real time demodulation at 10 Gb/s over 20 km SMF transmission distance. This thesis reports record transmission capacity on a direct current modulated VCSEL with 50 Gb/s on a VCSEL -3 dB bandwidth of > 20 GHz by using PAM-4 modulation. This thesis introduces first VCSEL-based PON links with HC-QAM and CAP modulations up to 10 Gb/s and 1.25 Gb/s, respectively. The work in this thesis shows for the first time bipolar IR-UWB signal generation with VCSELs light sources achieving 2 Gb/s data transmission over 25 km SMF and 4 meters air transmission.

3.1.1 VCSEL-based chirp-assisted ASK coherent access networks

Intensity-modulated with coherent detection links are shown in this thesis to be a prospective alternative to traditional intensity-modulated with direct detection systems for the longer transmission distance and higher

number of users required in next generation access networks [55]. **PAPER 1, PAPER 2** and **PAPER 3** provide an experimental demonstration of the capabilities of VCSEL light sources in coherent detection PON links. Better received power sensitivity is achieved by exploiting adiabatic frequency chirping to improve signal extinction ratio. Traditionally low-linewidth edge emitting lasers have been used for coherent detection. The results presented in this thesis experimentally shows that VCSELs can be used in coherent systems with ASK modulation. Although ASK coherent systems have theoretically lower sensitivity than PSK coherent systems [18] they allow for direct current modulation of VCSEL light sources, less complex receiver schemes, and higher robustness to phase noise as it is shown in **PAPER 4** and **PAPER 5**. **PAPER 6** presets a collaboration work with Huawei and shows the benefits in overall optical power budget of a system at 10 Gb/s compare to direct detection schemes. However, polarization matching of LO with the received signal and close wavelength emission are required to maximize the performance of the system on our experiments.

3.1.2   Advanced modulation formats on VCSELs

Advanced modulation formats such as PAM-4, HC-16QAM, and CAP-16 provide, 2, 3 and 4 times higher spectral efficiency, respectively, compare to NRZ-OOK modulation. Multilevel pulse amplitude modulation (PAM-M) represents a feasible solution to achieve high speed data transmission in short-range optical links with current technology. Direct modulation up to 50 Gb/s has been demonstrated in **PAPER 7** and **PAPER 8** using PAM-4 at 25 Gbaud. The capacity is increased to 100 Gb/s by using polarization multiplexing (PolMux) emulation and adaptive error correction. This system reduces by 4 the number of channels to reach future aggregated capacity of 400 Gb/s compare to non return-to-zero on-off keying (NRZ-OOK) with the same bandwidth. The results in **PAPER 9** show the potential to use four wavelength multiplexed channels at 7 Gbaud with PAM-4 signals over 10 km SMF transmission to migrate 4-lanes 56 Gbps data links into a compact WDM link. **PAPER 10** and **PAPER 11** demonstrated direct current modulation of 2-dimensional CAP-16 in VCSEL light sources, with a spectral efficiency of 4 bit/s/Hz in a WDM link. The system is evaluated with 4 channels 100 GHz spaced at 1.25 Gbps each, for a total bitrate of 5 Gbps over 26 km SMF transmission. CAP has lower transmitter and receiver complexity compared to modulation formats with carrier. Direct CAP modulation of VCSELs allows for very high spectral efficiency by increasing the number of levels and dimensions. **PAPER 12** demonstrate

10-Gbps data transmission over 20-km SMF with 4-QAM modulation with a VCSEL light source. HC-QAM improves the use of spectral bandwidth of the VCSEL with a 25% higher spectral efficiency than conventional QAM modulation formats. It has superior optical fiber chromatic dispersion tolerance than NRZ-OOK or SC-QAM modulated signals at the same data rate. From results in **PAPER 10**, **PAPER 11** and **PAPER 12** we conclude that HC-QAM and CAP modulation techniques with VCSEL light sources can provide high-speed data transmission with lower impact in the performance from optical fiber chromatic dispersion for application in high-speed optical access networks. However, advanced modulation formats increase the complexity of the transmitter and add a power penalty on receiver sensitivity [56]. **PAPER 13** demonstrated a 2 Gb/s IR-UWB signal transmitted over 25 km SMF and a 4 meters wireless link. IR-UWB modulation is shown to be a feasible solution to transport wireless signals over fiber providing transparent optical-to-wireless signal conversion. This approach is an attractive solution for hybrid optical-wireless access networks providing wireless connectivity to the end user with low power consumption.

3.2   Future work

In this section I would like to provide a view of future work that could be pursued in the area of coherent detection access networks and on high speed optical short range systems with VCSEL light sources.

3.2.1   Flexible coherent detection WDM acces networks

WDM-PON is the leading candidate technology for next generation access networks beyond 10 Gb/s [20]. Coherent demodulation has demonstrated to provide longer reach and higher passive splitting ratio, enabling reduction of network nodes and therefore simpler network architectures. However, it has to come together with more dense and flexible channel allocation on WDM-PON systems in order to provide service to the higher number of users per network node. Future work could cover implementation of coherent detection WDM-PON links based on tunable VCSEL light sources. High flexibility and close channel allocation can potentially be achieved. Minimum frequency spacing and crosstalk between channels, VCSEL light sources tunability range and maximum number of channels simultaneously transmitted should be investigated.

3.2.2   Towards 400 Gb/s systems

There is an unstoppable demand for higher data transmission capacity for optical interconnects and short-range optical systems. Higher spectral efficient systems have to be developed to satisfy future rates at 400 Gb/s and beyond. Future work could continue the investigation of this thesis increasing the modulation order and data transmission rate of CAP, HC-QAM and PAM-M modulations in VCSELs. Moreover, future work could explore new modulation techniques in VCSEL light source to increase capacity. Parallelization of several optical fiber channels and multicore fiber transmission with different core distribution patterns will also need to be considered and researched for future high-speed optical links based on VCSEL light sources.

Paper 1: Vertical-cavity surface-emitting laser based digital coherent detection for multigigabit long reach passive optical links

7. J.-U. Grabow, E.S. Palmer, M.C. McCarthy, and P. Thaddeus, Supersonic-jet cryogenic-resonator coaxially oriented beam-resonator arrangement Fourier transform microwave spectrometer, Rev Sci Instrum 76 (2005), 093106–093111.

8. P. Cerny, P. Piksa, T. Korinek, S. Zvanovec, and M. Mazanek, Broadband axial excitation of Fabry–Perot resonator, In: Antennas and propagation (EuCAP), 2010 proceedings of the fourth European conference, 2010, pp. 1–4.

9. P. Piksa, S. Zvanovec, and P. Cerny, Specific millimeter-wave features of Fabry–Perot resonator for spectroscopic measurements, In: I. Minin (Ed.), Microwave and millimeter wave technologies from photonic bandgap devices to antenna and applications, InTech, 2010, pp. 451–468.

10. H. Kogelnik and T. Li, Laser beams and resonators, Proc IEEE, 54 (1966), 1312–1329.

11. G. Goubau, Electromagnetic waveguides and cavities, Pergamon Press, New York, 1961.

12. D.M. Pozar, Microwave engineering, John Wiley & Sons, Inc., New York, NY, 1998.

13. P. Cerny, Optimization of UWB dipole feeding circuits, In: Antennas and propagation (EuCAP), 2010 proceedings of the fourth European conference, 2010, pp. 1–4.

VERTICAL-CAVITY SURFACE-EMITTING LASER BASED DIGITAL COHERENT DETECTION FOR MULTIGIGABIT LONG REACH PASSIVE OPTICAL LINKS

Roberto Rodes,[1] Jesper Bevensee Jensen,[1] Darko Zibar,[1] Christian Neumeyr,[2] Enno Rönneberg,[2] Juergen Rosskopf,[2] Markus Ortsiefer,[2] and Idelfonso Tafur Monroy[1]
[1] DTU Fotonik, Department of Photonics Engineering, Technical University of Denmark, DK-2800 Kgs. Lygnby, Denmark; Corresponding author: rrlo@fotonik.dtu.dk
[2] VERTILAS GmbH, Lichtenbergstr. 8, Garching D-85748, Germany

ABSTRACT: *We report on experimental demonstration of digital coherent detection based on a directly modulated vertical-cavity surface-emitting laser with bit rate up to 10 Gbps. This system allows a cooler-less, free running, and unamplified transmission without optical dispersion compensation up to 105 km at 5 Gbps long reach passive optical links.* © 2011 Wiley Periodicals, Inc. Microwave Opt Technol Lett 53:2462–2464, 2011; View this article online at wileyonlinelibrary.com. DOI 10.1002/mop.26331

1. INTRODUCTION

Emerging high bandwidth demanding services, such as high definition television (HDTV), are calling for capacity upgrade of existing and to be deployed fiber-to-the-customer (FTTC) networks [1]. Another challenge for FTTC networks is the need to support a growing number of end-users while keeping low the overall cost of delivered unit of bandwidth. Therefore, in FTTC architectures such as passive optical network (PON) architectures, it is important to reduce the cost of the optical network unit and concentrate complex signal processing at the central office, where complexity and cost can be shared among all users. Vertical-cavity surface-emitting lasers (VCSELs) are promising candidates for light sources at the customer premise because of their cost-effective production and capability for chip integration with low threshold and driving current operation.
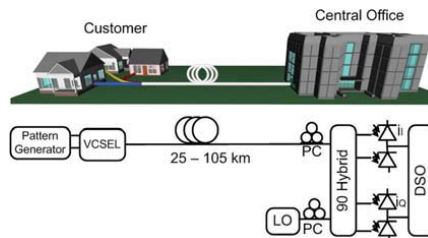

Figure 1 Experimental setup. Local oscillator (LO), polarization controller (PC), and digital sampling oscilloscope (DSO). [Color figure can be viewed in the online issue, which is available at wileyonlinelibrary.com]

Compared with DFB-lasers, the main challenge for VCSELs so far is the smaller optical power coupled into the optical fiber, which restricts the coverage range for application in PON links with a large splitting ratio and long transmission distance. A common solution for this power budget limitation would be to include optical amplifiers [2] that drastically would undermine the cost advantage of VCSELs. Until now, fiber transmission systems using VCSELs employ direct detection.

In this article, for the first time to our best knowledge, we experimentally demonstrate the use of digital coherent detection of a 10 Gbps amplitude shift keying system using a VCSEL as light source. Commonly, the typical large linewidth value of VCSELs has made them not suitable for coherent detection [3].
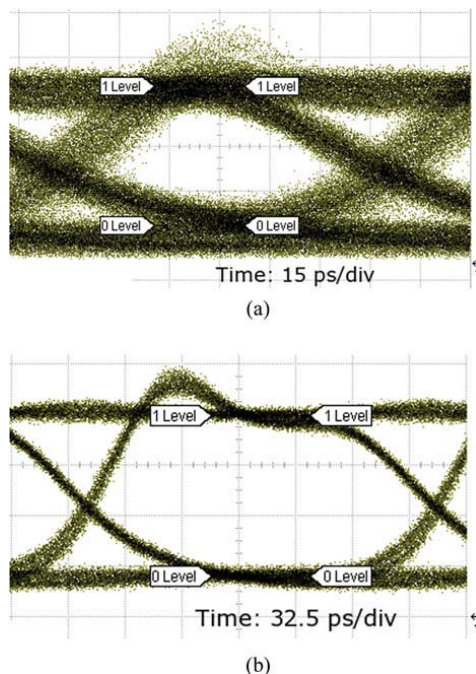

Figure 2 Optical back-to-back direct detected eye diagrams for (a) 10 Gbps and (b) 5 Gbps. [Color figure can be viewed in the online issue, which is available at wileyonlinelibrary.com]
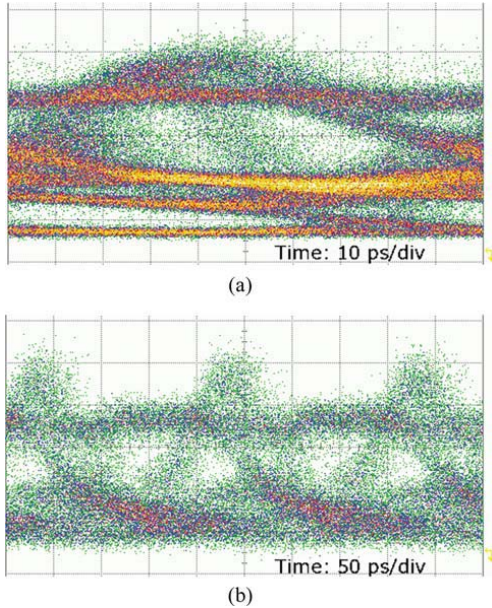
Figure 3 Optical direct detected eye diagrams for (a) 10 Gbps after 25 km SMF and (b) 5 Gbps after 60 km SMF. [Color figure can be viewed in the online issue, which is available at wileyonlinelibrary.com]

Using digital signal processing (DSP) algorithms, however, we demonstrate that these limitations can be overcome. Our experimental results show an increase of the receiver sensitivity up to -34 dBm after 105 km of fiber transmission with no optical amplification or optical dispersion compensation.

2. EXPERIMENTAL SETUP

Figure 1 shows a simplified scheme of our experimental setup and its relation to the application to a FTTC scenario. A signal
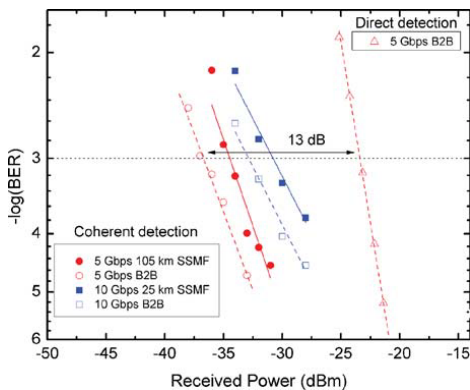
Figure 4 Bit-error rate curves for 10 and 5 Gbps. [Color figure can be viewed in the online issue, which is available at wileyonlinelibrary.com]

pattern generator directly modulates a 1550 nm VCSEL. The VCSEL has a measured linewidth of 350 MHz. A balance drive configuration is used for the VCSEL with a driving peak–peak voltage of 1.4 V. A pseudorandom binary sequence of length of 2^{15}–1 is used for this experiment. The output power of the VCSEL launched into the fiber is measured to be 0.6 dBm. The fiber lengths used for transmission experiments are 105 and 25 km of standard single mode fiber for 5 and 10 Gbps, respectively. The coherent receiver consists of a 90° optical hybrid and two pairs of balanced photodiodes. The local oscillator (LO) is generated by an external cavity laser set to 1550 nm and tuned to match the wavelength belonging to the transmitted ones. Phase and quadrature components are stored with a digital sampling oscilloscope (DSO). DSP is performed offline, consisting of a digital dispersion compensation and envelope detection; therefore, there is no carrier or phase estimation. The performance is assessed by bit-error rate counting as a function of optical received power, whose value is set using an optical variable attenuator placed before the coherent receiver; see Figure 1.

3. RESULTS

Figure 2 shows the optical eye diagram for a back-to-back (B2B) configuration. The bias point of the VCSEL was optimized for a maximum extinction ratio while the pulse overshooting is minimized. The extinction ratios were measured to 8.49 dB at 5 Gbps and 6.78 dB at 10 Gbps. For illustration purposes, Figure 3 shows the eye diagrams, using direct detection, after 25 and 60 km fiber transmission for 10 and 5 Gbps, respectively. We want to emphasize that for 5 Gbps, the coherent detection experiment was performed over 105 km SMF, though, for the illustration of the dispersion effect in Figure 3 and due to the sensitivity of the oscilloscope, we show it for 60 km SMF, where we already can see that the eyes diagrams were completely closed because of chromatic dispersion. However, after using DSP to compensate for chromatic dispersion and using adaptive decision thresholding, the signals can be successfully demodulated. Figure 4 shows the bit-error rate (BER) curves for 5 and 10 Gbps for B2B and fiber transmission with coherent detection. Considering as a reference the forward error correction limit of BER $< 10^{-3}$, the receiver sensitivity was measured to be -34 dBm for 5 Gbps after 105 km SMF and -31 dBm for 10 Gbps after 25 km SMF. Compared with the B2B case, there is a 2 dB penalty, whose attribution will be investigated in the future. Figure 4 also shows the BER curve for 5 Gbps B2B with direct detection, to compare in terms of sensitivity, coherent detection with direct detection performance with VCSELs. The receiver sensitivity with coherent detection was measured to be 13 dB higher than direct detection.

4. CONCLUSIONS

We present experimental results, for the first time, demonstrating the feasibility of using VCSELs up to 10 Gbps with coolerless and free running operation in combination with digital coherent detection as an advantageous solution for PONs with no need for optical dispersion compensation or optical amplification. BER curves are shown for fiber transmissions over 105 and 25 km SMF at 5 and 10 Gbps, respectively. The receiver sensitivity is increased by 13 dB, and therefore, the power budget margin is also increased. This is especially advantageous for scaling the uplink of PONs by placing the low cost VCSEL at the customer premises, whereas the more complex coherent receiver at the central office.

REFERENCES

1. P.E. Green, Fiber to the home: The next big broadband thing, Commun Mag IEEE 42 (2004),100–106.
2. K. Prince,Demonstration of 10.7-Gb/s transmission in 50-kmPON with uncooled free-running 1550-nm VCSEL, In: Conference on lasers and electro-optics (CLEO) and quantum electronics and laser science conference (QELS), 2010, pp.1–2.
3. M. Seimetz,Laser linewidth limitations for optical systems with high-order modulation employing feed forward digital carrier phase estimation, In: Conference on optical fiber communication (OFC), February 2008, pp.1–3.

COMPACT COPLANAR WAVEGUIDE-FED MONOPOLE ANTENNA WITH A FOLDED GROUND STRIP FOR 5-GHz WIRELESS APPLICATIONS

Chow-Yen-Desmond Sim, Chung-Hsien Ho, and Yu-Lun Chien
Department of Electrical Engineering, Feng Chia University, Taichung, Taiwan 40724, Republic of China; Corresponding author: cysim@fcu.edu.tw

ABSTRACT: *The design of a compact coplanar waveguide-fed monopole antenna partially surrounded and coupled by a folded ground strip is presented. By properly tuning the gap between the monopole antenna and the ground strip, it is able to operate in the 5-GHz band for wireless application. From the experimental results, a resonant mode excited at around 5.5 GHz is observed with 10-dB bandwidth measured from 4.88 to 6.3 GHz. Good radiation patterns with near omnidirectional pattern in the azimuth plane are also observed.* © 2011 Wiley Periodicals, Inc. Microwave Opt Technol Lett 53:2464–2466, 2011; View this article online at wileyonlinelibrary.com. DOI 10.1002/mop.26330

1. INTRODUCTION

Planar antenna with coplanar waveguide (CPW) feed line possesses several advantages over the microstrip feed line, such as lower radiation loss and ease in integration with monolithic microwave integrated circuit [1]. Furthermore, when the CPW-fed technique is applied to a slot or monopole antenna, a uniplanar structure and wide bandwidth characteristics can also be observed. Therefore, this feeding technique is widely used in small antenna designs for 5-GHz wireless application such as the 5.8-GHz RFID application [2–5]. Nevertheless, though the size of these antenna designs fabricated on a FR4 substrate can be downsized to as small as 14×8 mm^2 [3], they are incapable of covering the entire 5-GHz WLAN band. Hence, a compact CPW-fed monopole antenna for 5-GHz band application is proposed [6]; however, this design can only offer either the 5.2- or the 5.8-GHz operating band by tuning the length of its radiating element. To operate across the entire 5-GHz band, a folded-slot antenna is therefore studied [7], but the size of this antenna is twice of Ref. 6 at around 16.5×20 mm^2.

Hence, in this article, the design of a compact-size (17.68×11.2 mm^2) monopole antenna comprised a vertical monopole top loaded by an inverted L-shaped radiating element is studied. By extending a ground strips that fold around this monopole antenna, the coupling effects occurred between both the radiating and the ground strip elements would allow a broad 10-dB bandwidth of 25% that sufficiently covers the desired 5-GHz band for wireless application. Details of the proposed antenna designs are described, and typical experimental results are presented and discussed.

2. ANTENNA CONFIGURATION

Unlike the aforementioned designs [1–7] that built on a 1.6-mm FR4 substrate ($\varepsilon_r = 4.4$ and loss tangent 0.02), the proposed antenna geometry as depicted in Figure 1 is printed on a 0.8-mm-thick FR4 substrate. Here, a vertical monopole fed directly by a 50 Ω feed line is top loaded by an inverted L-shaped radiating element. As for the narrow ground strip (with 1-mm width) that extends from the far right side of the CPW ground plane and folds partially around the L-shaped element, the gaps (g_1 and g_2) that separates both elements will highly affect the impedance matching of the resonant mode excited at around 5.5 GHz. It is also note worthy that the total size of the proposed antenna is only 17.68×11.2 mm^2.

3. EXPERIMENTAL RESULTS AND DISCUSSION

The measured and simulated return losses of the proposed antenna are presented in Figure 2. Here, a good return loss of around 41.8 dB is measured at the resonant frequency (5.485 GHz) of the proposed antenna, whereas its 10-dB bandwidth is 25.4% centered at 5.59 GHz. Furthermore, good agreements are also demonstrated between both measured and simulated results, and the slight discrepancies are mainly attributed by the SMA connector and the unexpected tolerance during the process of fabricating the proposed antenna. In Figure 2, it is obvious that the good performances as aforementioned will be vanished
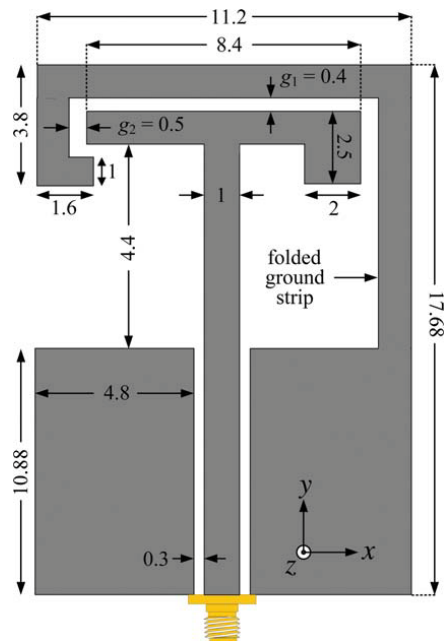

Figure 1 Geometry of the proposed CPW-fed monopole antenna (unit: mm). [Color figure can be viewed in the online issue, which is available at wileyonlinelibrary.com]

Paper 2: Coherent detection for 1550 nm, 5 Gbit/s VCSEL-based 40 km bidirectional PON transmission

Jensen, JB, **R. Rodes**, D. Zibar, and I.T. Monroy, "Coherent detection for 1550 nm, 5 Gbit/s VCSEL-based 40 km bidirectional PON transmission," *Optical Fiber Communication Conference and Exposition* 2011.

Coherent Detection for 1550 nm, 5 Gbit/s VCSEL Based 40 km Bidirectional PON Transmission

Jesper Bevensee Jensen, Roberto Rodes, Darko Zibar and Idelfonso Tafur Monroy

DTU Fotonik, Technical University of Denmark, Oersteds Plads Building 343, Kgs. Lyngby, DK-2800 Denmark
jebe@fotonik.dtu.dk

Abstract: Coherent detection of directly modulated 1550nm VCSELs in 5Gbit/s bidirectional 40km SSMF PON-links is presented. Receiver sensitivity of –37.3dBm after transmission is achieved with 30dB system margin, corresponding to 1:1024 passive power-splitting.

© 2010 Optical Society of America

OCIS codes: 060.4510, 140.7260, 060.1660.

1. Introduction

In next generation passive optical networks (PONs) for fiber to the home deployment (FTTH), bidirectional transmission of symmetric uplink/downlink data capacity will be increasingly important due to the growth of intrinsically bidirectional services such as on-line gaming and peer-to-peer networks. Moreover, for point-to-multipoint PONs, there is a desire to increase the reach as well as the amount of users serviceable from a single central office. Indeed, a passive splitting ratio of 1000 has been proposed for future PONs [1], a number unreachable by present PON technology without the introduction of e.g erbium doped fiber amplifiers (EDFAs) and dispersion compensating fiber (DCF) in the field; a solution which would be problematic in the access networks due to complexity and power consumption issues. Moreover, an EDFA/DCF based architecture does not lend itself well to single-fiber bidirectional transmission.

An alternative solution is to introduce coherent detection in access networks. By employing coherent detection, the receiver sensitivity can be significantly increased [2], dispersion compensation can be performed in the digital domain [3], and support for advanced modulation formats can be provided [4]. Moreover, as the current PON architecture based on passive optical transmission and splitting can be maintained, graceful migration can be performed by upgrading terminal equipment only with no changes in the optical fiber transmission path. Due to the cost sensitivity of optical access system, however, present day coherent technologies based on external modulation needs to be simplified.

In recent years, a number of breakthroughs within the area of long wavelength vertical cavity surface emitting lasers (VCSELs) have resulted in the emerge of 1550 nm VCSELs [5]. Due the cost-effectiveness and low drive voltage, these are attractive candidates for future PONs. Coherent detection of VCSEL based signals have been presented [6], albeit only with the employment external I/Q modulators; a solution which to some degree counteracts the cost and energy efficiency of VCSELs.

We present what is, to the best of our knowledge, the world's first demonstration of a bidirectional coherent detection PON link employing directly modulated (DM) VCSELs operating at 1550 nm wavelength as transmitters. Our system operates at 5 Gbit/s in both directions, and transmission is over a single, un-amplified 40 km standard single mode fiber (SSMF) link with no use of optical dispersion compensation. Receiver sensitivity at the 2×10^{-3} limit for forward error correction (FEC) was better than –37 dBm, corresponding to an improvement of more than 17 dB over direct detection using the same DM-VCSEL transmitter.

2. Experimental Setup

A block diagram of the bidirectional transmission system and optical spectra (a) and of the coherent/digital signal processing (DSP) reciver (b) is shown in Fig. 1.

A pulse pattern generator directly modulates two uncooled VCSELs (VCSEL$_1$ at 1550.8 nm center wavelength for downstream and VCSEL$_2$ at 1548.3 nm center wavelength for upstream) with a 5 Gbit/s pseudo random binary sequence (PRBS) with a word length of $2^{15} - 1$. Driving voltage is 1 V peak-peak, and bias current of the VCSELs is set to 12.4 mA for VCSEL$_1$ and 15.6 mA for VCSEL$_2$. Adjustment of bias current and drive voltage is optimized by maximizing the extinction ratio while minimizing the overshoot. The extinction ratio of the VCSELs at the transmitter
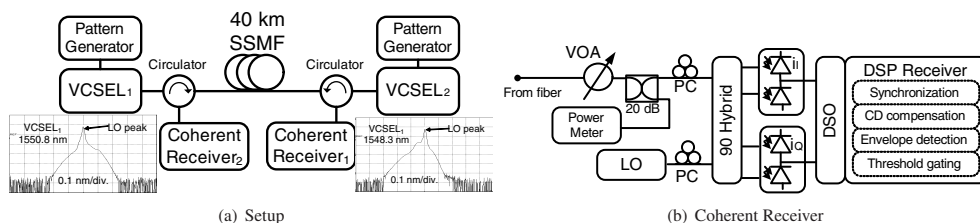
(a) Setup

(b) Coherent Receiver

Fig. 1. Experimental setup of the bidirectional system (a) and the coherent/DSP receiver (b). VOA is a variable optical attenuator, DSO is a digital storage oscilloscope with a samplig rate of 40 GSamples/s, LO is the local oscillator laser, and PC is polarization controllers.

is 6.8 dB measured with an oscilloscope. The different center wavelength of the two VCSELs is due to bias current dependence of a VCSELs emission wavelength. As the two VCSELs were not completely identical, and the bias current was optimized for identical extinction ration and overshoot for the two VCSELs, it was not possible to achieve exactly identical optical spectrum and center wavelength for the two VCSELs. The optical power spectra of the two VCSELs combined with the local oscillator (LO) laser are shown as inserts in Fig. 1 (a).

The two VCSELs are connected to opposite ends of a 40 km SSMF transmission span via optical circulators so that the received signal from $VCSEL_1$ can be received at the site of $VCSEL_2$ and vise versa, while the two signals are simultaneously counter-propagating in the fiber. Launch power into the fiber is 0.6 dBm in both directions; fiber attenuation is 7.7 dB; and total chromatic dispersion is 640 ps/nm.

At the receiver input, the signal is attenuated, and the receiver input power is measured with a calibrated optical power meter through a –20 dB directional coupler. After the coupler, the signal is mixed with light from a free running external cavity laser (ECL) local oscillator (LO) in a 90° optical hybrid, and detected by two sets of balanced photodetectors. The received I_I and I_Q components of the signal are stored by a digital storage oscilloscope with a sampling rate of 40 Gsamples/s.

The coherent detection is performed using intra-dyne detection, where the LO laser has a small frequency offset with respect to the transmitter laser center frequency. The narrow linewidth LO laser can be identified within the broader VCSEL spectra in Fig. 1 (a).

Demodulation of the data is performed by off-line digital signal processing (DSP), consisting of synchronization of the received bits, chromatic dispersion (CD) compensation, envelope detection by squaring and low pas filtering, and decision gating. Due to the chirp induced by the direct modulation of the VCSEL, optimum performance is achieved by over-compensating by 425 ps/nm. This residual chirp-compensation is independent of fiber length (the same value was used back to back and after transmission), and is therefore not expected to be a problem in system installations. The effect of random frequency offset between the VCSELs and LO laser does not effect the performance, as the DSP perform envelope detection of the in-phase and quadrature components of the received field.

3. Results

The measured BER of the coherently detected signals before (B2B) and after bidirectional transmission over 40 km SSMF is plotted in Fig. 2 (a) together with the measured BER after direct detection of $VCSEL_1$ with no counter propagating signal. Back to back receiver sensitivity at the FEC limit of 10^{-3} for the coherent detection case is −37.7 dBm for $VCSEL_1$ and −39.3 dBm $VCSEL_2$. After 40 km transmission with the counterpropagating signal, the receiver sensitivity is –37.3 dBm and –37.7 dB for $VCSEL_1$ and $VCSEL_2$ coreponding to transmission penalties of 0.4 dB and 1.6 dB. In order to benchmark these results against conventional direct detection unidirectional systems, the BER of $VCSEL_1$ is measured in this manner. The receiver sensitivities for $VCSEL_1$ employing direct detection are –23.6 dBm B2B and –19.8 dBm after transmission, corresponding to a transmission penalty of 3.8 dB. The increased transmission penalty using direct detection is due to chromatic dispersion, which for the coherent detection case was compensated by DSP. This is confirmed by inspection of the direct detection eye diagrams in Fig. 2 (b) which show severe waveform distortion after transmission. The low transmission penalty of the coherently detected signals shows that the chromatic dispersion has been successfully compensated in the DSP. The improvement in receiver sensitivity due to coherent detection for $VCSEL_1$ is 13.1 dB B2B and 17.5 dB after 40 km SSMF.
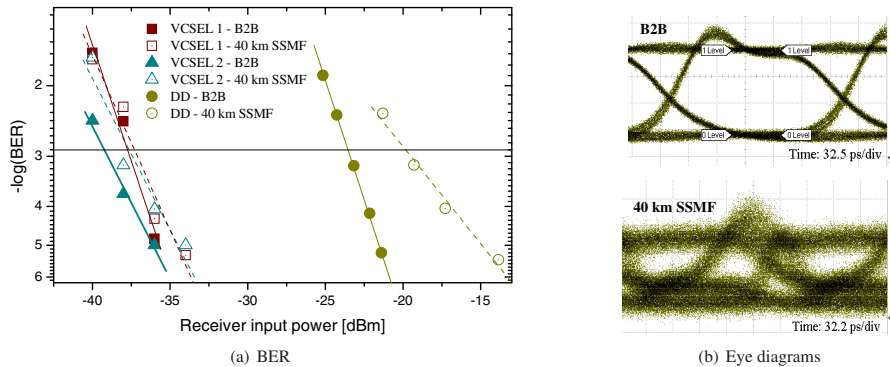
(a) BER

(b) Eye diagrams

Fig. 2. Measured BER back to back (B2B) and after 40 km SSMF bidirectional transmission. Direct detection (DD) direction, single transmission using VCSEL$_1$ is included for reference.

As the launch power is 0.6 dBm, and total fiber loss is 7.7 dB, the presented bidirectional coherent system provides a system margin above 30 dB, corresponding to a passive spitting ratio of 1024. This is a dramatic improvement over the direct detection margin of 12.7 dB corresponding to a passive splitting ratio of 18. Alternatively, as chromatic dispersion is compensated using DSP, the improved system margin could be utilized to extend the reach to e.g. 80 km. Assuming an 80 km link loss of 15.4 dB, the residual margin of 22.3 dB would be able to accommodate the loss of a 1:128 power splitter.

4.   Conclusion

We have presented experimental results from what we believe to be the worlds first demonstration of bidirectional 40 km SSMF link employing coherent detection with free running local oscillators and un-cooled directly modulated VCSEL transmitters. Through the use of digital signal processing for demodulation and dispersion compensation, receiver sensitivities of –37.3 dBm downstream and –37.7 dBm upstream was achieved with no use of optical amplifiers or optical dispersion compensation. At a launch power of 0.6 dBm and 7.7 dB fiber loss, a system margin of 30 dB was achieved, corresponding to the loss of a record passive splitting ratio of 1024.

The reported experiments demonstrate the potential for coherent detection in bidirectional access links employing directly modulated VCSEL transmitters. Future work include the investigation of the feasibility of using low-cost solutions for LO lasers, and upgrade to 10 Gbit/s bit rate.

References

1. S. Smolorz, H. Rohde, P. Ossieur, C. Antony, P. D. Townsend, T. De Ridder, B. Baekelandt, X. Z. Qiu, S. Appathurai, H.-G. Krimmel, D. Smith and A. Poustie, "Next generation access networks: PIEMAN and beyond", International Conference on Photonics in Switching (PS) (2009).
2. G. Lachs, S. M. Zaidi and A. K. Singh, "Sensitivity enhancement using coherent heterodyne detection", J. Lightw. Tech., Vol. 12, No. 6 (1994).
3. S. J. Savory, "Electronic signal processing in optical communications",in *Proceedings of SPIE* Vol. 7136 (2008).
4. X. Zhou and J. Yu,"Advanced coherent modulation formats and algorithms: higher-order multi-level coding for high-capacity system based on 100 Gbps channel", in *Optical Fiber Communication Conference* (OFC) (2010).
5. E. Kapon and A. Sirbu, "Long-wavelength VCSELs: Power-efficient answer", Nature Photonics 3, 27 - 29 (2009).
6. Sang-Yuep Kim, N. Sakurai, H. Kimura, H. Hadama, "VCSEL-based coherent detection of 10-Gbit/s QPSK signals using digital phase noise cancellation for future optical access systems", in *Conference on Optical Fiber Communication* (OFC) (2010).

Paper 3: All-VCSEL based digital coherent detection link for multi Gbit/s WDM passive optical networks

All-VCSEL based digital coherent detection link for multi Gbit/s WDM passive optical networks

Roberto Rodes,[1,*] Jesper Bevensee Jensen,[1] Darko Zibar,[1] Christian Neumeyr,[2] Enno Roenneberg,[2] Juergen Rosskopf,[2] Markus Ortsiefer,[2] and Idelfonso Tafur Monroy[1]

[1]DTU Fotonik, Department of Photonics Engineering, Technical University of Denmark
[2]Vertilas GmbH, Lichtenbergstr. 8, D-85748, Germany
*rrlo@fotonik.dtu.dk

Abstract: We report on experimental demonstration of a digital coherent detection link fully based on vertical cavity surface emitting lasers (VCSELs) for the transmitter as well as for the local oscillator light source at the receiver side. We demonstrate operation at 5 Gbps at a 1550 nm wavelength with record receiver sensitivity of −36 dBm after transmission over 40 km standard single mode fiber. Digital signal processing compensates for frequency offset between the transmitter and the local oscillator VCSELs, and for chromatic dispersion. This system allows for uncooled VCSEL operation and fully passive fiber transmission with no use of optical amplification or optical dispersion compensation. The proposed system demonstrates the potential of multi-gigabit coherent passive optical networks with extended reach and increased capacity. Moreover, this is, to the best of our knowledge, the first demonstration of coherent optical transmission systems using a low-cost VCSEL as the local oscillator as well as for the transmitter.

OCIS codes: (000.0000) General; (000.2700) General science.

References and links

1. P. E. Green, "Fiber to the home: the next big broadband thing," IEEE Commun. Mag. **42**, 100-106 (2004)
2. S. Smolorz, H. Rohde, P. Ossieur, C. Antony, P. D. Townsend, T. De Ridder, B. Baekelandt, X. Z. Qiu, S. Appathurai, H.-G. Krimmel, D. Smith, and A. Poustie, "Next generation access networks: PIEMAN and beyond," International Conference on Photonics in Switching (PS) (2009).
3. M. Alfani, J. M. Finochietto, and F. Neri, "Efficient multicast bandwidth allocation in TDM-WDM PONs," Conference on Optical Fiber Communication (OFC) (2009).
4. A. D. Ellis, and F. C. Garcia Gunning, "Spectral density enhancement using coherent WDM," IEEE Photonics Technology Letters (2005).
5. G. Lachs, S. M. Zaidi and A. K. Singh, "Sensitivity enhancement using coherent heterodyne detection," J. Lightwave Technol. **12**, 1036-1041 (1994).
6. X. Zhou, and J. Yu, "Advanced coherent modulation formats and algorithms: higher-order multi-level coding for high-capacity system based on 100 Gbps channel," Conference on Optical Fiber Communication (OFC) (2010).
7. S. J. Savory, "Electronic signal processing in optical communications," Proc. SPIE 7136, 71362C (2008).
8. S.-Y. Kim, N. Sakurai, H. Kimura, and H. Hadama, "VCSEL-based coherent detection of 10-Gbit/s QPSK signals using digital phase noise cancellation for future optical access systems," Conference on Optical Fiber Communication (OFC) (2010).
9. M. Seimetz, "Laser linewidth limitations for optical systems with high-order modulation employing feed forward digital carrier phase estimation," Conference on Optical Fiber Communication (OFC) (1998).
10. K. Prince, M. Ma, T. B. Gibbon, and I. Tafur Monroy, "Demonstration of 10.7-Gb/s transmission in 50-km PON with uncooled free-running 1550-nm VCSEL," Conference on Lasers and Electro-Optics (CLEO) and Quantum Electronics and Laser Science Conference (QELS) (2010).

1. Introduction

Next generation fiber-to-the-customer networks (FTTC) need to comply with a set of technical requirements, including support of a large number of end customers with emerging services, such as HDTV, demanding a high bandwidth surpassing 1 Gbit/s [1]. This requirement can be achieved e.g. by increasing the bit-rate of current time-domain

multiplexing (TDM) access systems and introducing a higher splitting ratio reaching the order of 1000 [2]. Another alternative is to employ wavelength division multiplexing (WDM), or to combine WDM and TDM approaches [3]. Conventional WDM approaches based on passive filtering by arrayed waveguide gratings (AWGs) are challenging for ultra-dense wavelength spacing, and the introduction of such architecture is therefore not straightforward in future access networks employing splitting ratios approaching 1000. Likewise, direct increase of passive splitting ratio in current TDM PONs is problematic due to the increased splitting loss. Other important challenges are the need for graceful migration and flexibility in order to support scalability as the network growths; a feature not straightforward compatible with a fixed AWG-based WDM architecture. These challenges motivate interest in optical fiber access solutions based on coherent detection due to its advantages of support of closely spectrally spaced channels with electrical narrow bandwidth selection [4], increased receiver sensitivity [5] and support for advanced modulation formats [6]. Moreover, with recent advancements in digital signal processing (DSP) [7] for optical digital receivers, the combination of DSP and coherent detection has the prospect to become the technology of choice for the next generation of optical access networks. It will, however, still be important to reduce the cost of the optical network unit (ONU) placed at the customer premises, and to concentrate complex signal processing at the central office where complexity and cost can be shared among a large number of users. The availability of suitable low complexity light sources in particular remains a challenge for such a coherent detection passive optical access network.

In this paper we propose the use of vertical-cavity surface-emitting lasers (VCSELs) as light sources and local oscillator for coherent detection in multi- Gbit/s access systems, due to their cost effective production and capability for chip integration with low threshold and driving current operation. We experimentally demonstrate that by employing a DSP supported coherent receiver to compensate for the transmitter and local oscillator frequency offset and fiber chromatic dispersion, an all-VCSEL, 5 Gbit/s amplitude shift-keying link can be achieved with transmission over 40 km of standard single mode fiber (SSMF) with no optical dispersion compensation with free running and un-cooled VCSEL operation.

2. All-VCSEL digital coherent receiver

Recently, the use of a VCSEL as local oscillator laser source for a coherent receiver has been demonstrated to be feasible [8]. In this case, however the transmitter light source used was a wavelength stabilized distributed feed-back (DFB) laser. The transmitter used a complex in-phase and quadrature (I&Q) optical modulator with external driver amplifiers, and required and extra auxiliary optical signal in an orthogonal polarization state to act as a phase reference at the coherent receiver side. It showed the potential of a VCSEL as a local oscillator although the complete system is rather complex. For applications in FTTC networks, a less complex configuration based on a single technology platform is desirable to reduce cost and overall system integration. Moreover, due to issues of power consumption, an approach based on direct laser modulation will be desirable for next generation access networks.

In this paper, we experimentally demonstrate the use of digital coherent detection using a directly modulated VCSEL as light source for the transmitter and another VCSEL for local oscillator. Traditionally, the broad linewidth of VCSELs has made them unsuitable for coherent detection [9]. By employing digital signal processing algorithms, however, we demonstrate that these limitations can be overcome. Additionally, coherent detection combined with digital signal processing facilitates the use of DSP based chromatic dispersion compensation, thereby eliminating the need for dispersion compensating fiber (DCF) [10]. In combination with the increased sensitivity of coherent detection systems, this makes coherent detection VCSEL based systems a strong candidate for future access networks, while also enabling graceful upgrade due to the ability to operate over the current PON architectures.

Our experimental results show receiver sensitivity up to −36 dBm after 40 km of fiber transmission with no optical amplification or optical dispersion compensation for a 5 Gbps amplitude shift keying (ASK) system. The same system was tested with direct detection, and

employing optical dispersion compensation in the form of 6 km of DCF to compensate 40 km SSMF. The measured sensitivity was −23 dBm and −19 dBm, with and without optical dispersion compensation, respectively. This represents an increase in receiver sensitivity of 13 dB for the coherent system when compared with direct detection system with optical dispersion compensation, and 17 dB compared with direct detection without optical dispersion compensation.
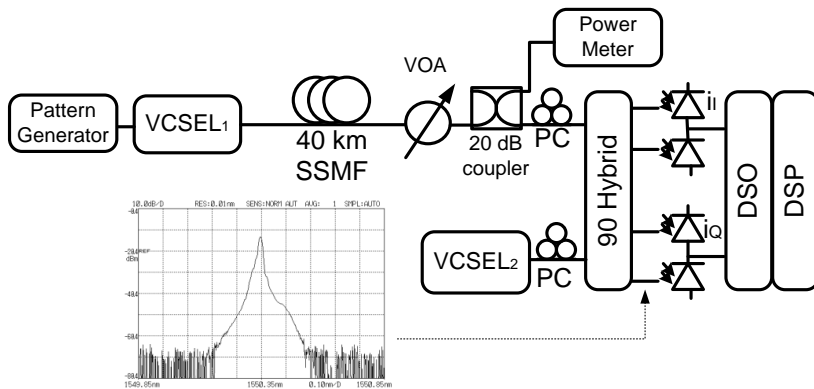
3. Experimental setup

Fig. 1. Experimental setup. Digital sampling scope (DSO), digital signal processing (DSP), polarization controller (PC), variable optical attenuator (VOA). The insertion shows the measured combined optical power spectrum of the signal and the LO.

Figure 1 shows a simplified scheme of our experimental setup. A pulse pattern generator directly modulates a 1550 nm VCSEL (VCSEL$_1$) at 5 Gbps. A balanced drive configuration is used for the VCSEL$_1$ with a driving peak-peak voltage of 1 V. The bias current of VCSEL$_1$ is set to 13.6 mA for optimum performance maximizing the extinction ratio while minimizing overshoot.

Figure 2 shows the optical spectrum of the transmitter VCSEL measured by heterodyne detection with a 100 kHz linewidth external cavity laser (ECL). The frequency offset between VCSEL$_1$ and the ECL is 5.8 GHz. The measured 3 dB linewidth of VCSEL$_1$ is 350 MHz.
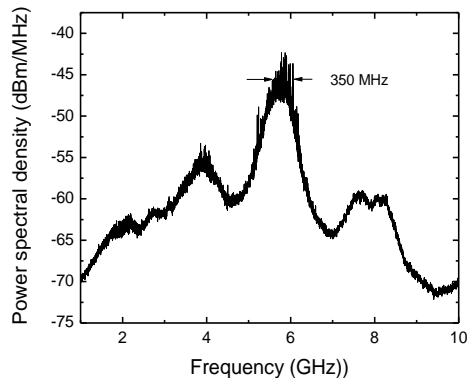
Fig. 2. Laser linewidth of the VCSEL measured by heterodyne detection with an ECL.

The data pattern used for the full VCSEL coherent detection transmission experiment is a pseudo random binary sequence (PRBS) of length of 2^{15}-1. The average output power of the $VCSEL_1$ launched into the fiber is 0.6 dBm. The transmission experiment is over 40 km of SSMF with a total attenuation of 7.7 dB, and a total dispersion of 640 ps/nm. In order to measure the optical power going into the coherent receiver, a variable optical attenuator (VOA), a 20 dB coupler and an optical power meter is placed after the transmission fiber. The coherent receiver consists of a 90° optical hybrid and two pairs of balanced photodiodes. The local oscillator (LO) signal is generated by a free running, continuous wave, 1550 nm VCSEL ($VCSEL_2$). The LO $VCSEL_2$ has been wavelength tuned to match the wavelength of the transmitting $VCSEL_1$ at 1550.34 nm by adjusting the bias level to 16.7 mA for intradyne detection. The insertion in Fig. 1 shows the measured optical power spectrum of the signal and the LO. Due to the intradyne detection scheme, the spectrum of the LO is masked by the signal spectrum.

The wavelength tuning range of $VCSEL_2$ was measured to be 5 nm from 1547 nm to 1552 nm by varying the bias current from 5 mA to 19 mA. This demonstrates the feasibility of bias current wavelength tuning of VCSELs employed as local oscillators in coherent networks. The optical output power of the LO varies from 0.3 mW at 1547 nm to 1.3 mW at 1552 nm.

The in-phase and quadrature components from the coherent receiver are stored with a digital sampling oscilloscope (DSO) with a sampling rate of 40 Gsamples/s. Digital signal processing, consisting of a digital dispersion compensation, synchronization, envelope detection and decision gating, is performed off-line. The detected signals have a random frequency offset. This frequency offset does not affect the demodulation, as the DSP performs envelope detection of the absolute value of in-phase and quadrature components.

4. Results

Figure 3 (a) shows the optical eye diagram at the output of the transmitter. At the bias current of 13.6 mA, beginning overshooting of the VCSEL is observed. The extinction ratio at the transmitter is 6.8 dB measured with an oscilloscope. Figure 3(b) shows the eye diagram after 40 km SSMF transmission. The fiber attenuation has decreased the signal to noise ratio (SNR), and the fiber dispersion has severely distorted the waveform, resulting in significant reduction of eye opening in amplitude as well as time domain.
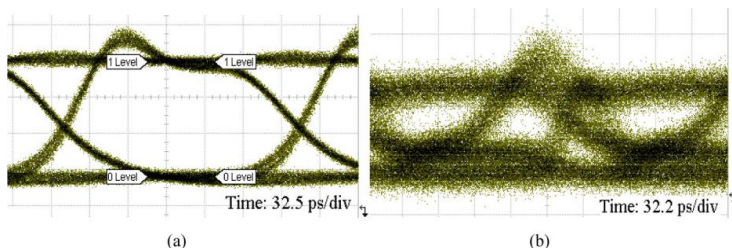

Fig. 3. Optical eye diagrams. 5 Gbps, I_{bias} = 13.6 mA, V_{pp} = 1 V. (a) Back-to-back. (b) After 40 km SSMF

The bit error ratio (BER) of the 5 Gbps signal back-to-back (B2B) and after 40 km SSMF transmission is plotted in Fig. 4. The plot shows the measured BER with direct detection with and without optical dispersion compensation. The plot also shows the BER after coherent detection where the dispersion compensation was performed using DSP.

For direct detection, back to back (B2B) receiver sensitivity at the forward error correction limit of BER<10^{-3}, was measured to be −23. After 40 km of SSMF transmission, the measured sensitivity was −19 dBm, corresponding to 4 dB receiver sensitivity penalty. After

DCF for optical dispersion compensation, the measured sensitivity was −23 dBm, and no observable penalty is measured compare to the B2B configuration.

For the coherent detection with DSP based dispersion compensation $2 \cdot 10^5$ bits were stored. DSP dispersion compensation was used to compensate for the chromatic dispersion of the 40 km of SMF transmission link. Best performance after demodulation was achieved by overcompensation so that the total compensated dispersion was 765 ps/nm. This is attributed to the chirp caused by the direct modulation of the VCSEL at the transmitter. Receiver sensitivity was measured to be −36 dBm B2B as well as after transmission, showing that the DSP effectively compensates dispersion. Comparing to the direct detection cases with and without optical dispersion compensation, sensitivity has been improved by 13 dB and 17 dB, respectively.

In order to estimate the number of users that can be reached with this system, a simple power budget calculation has been performed. Considering the launch power of 0.6 dBm, for direct detection without optical dispersion compensation, the total power budget is 19.6 dB with a power margin of 11.9 dB when the 7.7 dB fiber attenuation is taken into account. This corresponds to a passive slitting ratio of 15. By using optical dispersion compensation on direct detection, the total power budget increases to 23.6 dB, but not the power margin which is reduced to 11.5 dB due to the added attenuation of 4.4 dB by the DCF. Therefore, the corresponding passive splitting ratio is reduced to 14 users. For coherent detection the total power budget is 36.6 dB with a margin of 28.9 dB after fiber attenuation. This corresponds to a passive splitting ratio of 776. For the calculation, a total length of 40 km is assumed for the combined metro-access link before the passive splitting point and the distribution fiber link after the passive splitter.
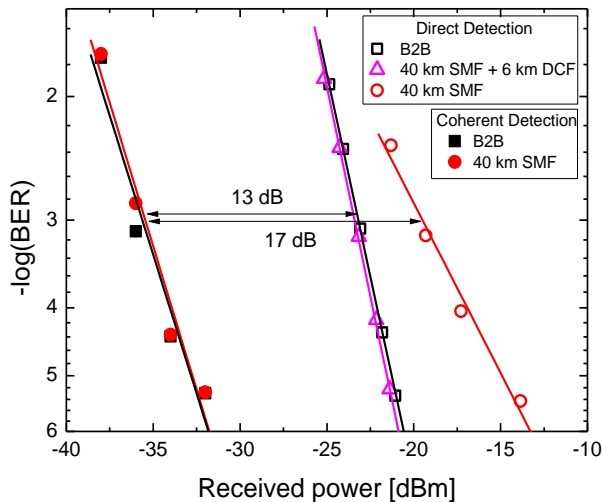

Fig. 4. BER curves after 40 km SSMF and for B2B configuration. Bit-rate: 5 Gbps, ER: 6.82 dB, LO power: 0 dBm.

5. Conclusions

We present experimental results, for the first time, demonstrating the feasibility of using VCSELs with uncooled and free running operation as transmitter as well as local oscillator laser in a digital coherent receiver.

The transmitter VCSEL was directly modulated at 5 Gbps, and after 40 km SSMF the signal was received using a coherent receiver with a VCSEL as local oscillator. Sensitivity of −36 dBm has been achieved with 28.9 dB power margin and no need for optical dispersion compensation or optical amplification.

A comparison between coherent detection and direct detection approach has been presented. Coherent detection resulted in a sensitivity improvement of 13 dB and 17 dB, comparing with direct detection with and without optical dispersion compensation, respectively. Moreover, in terms of power budget, power margin for direct detection correspond to a passive splitting ratio of 15, while for coherent detection the achievable splitting ratio is 776.

We have presented what is to the best of the authors knowledge, the first full VCSEL coherent PON link demonstration. The results show the potential for coherent systems to be implemented with low cost optical sources, thereby overcoming one of the main drawbacks of coherent systems for access networks. Therefore, VCSEL-based coherent PONs can be considered as strong candidate for future PONs.

Acknowledgments

Paper 4: 1.3 um all-VCSEL low complexity coherent detection scheme for high bit rate and high splitting ratio PONs

R. Rodes, J.B. Jensen, A. Caballero, and I.T. Monroy, "1.3 um all-VCSEL low complexity coherent detection scheme for high bit rate and high splitting ratio PONs," *Optical Fiber Communication Conference and Exposition*, pp. 1-3, 2011.

1.3 µm all-VCSEL low complexity coherent detection scheme for high bit rate and high splitting ratio PONs

Roberto Rodes, Jesper Bevensee Jensen, Antonio Caballero and Idelfonso Tafur Monroy
DTU Fotonik, Department of Photonics Engineering, Technical University of Denmark, Ørsteds Plads, B. 343, DK 2800 Kgs. Lyngby
email:rrlo@fotonik.dtu.dk

Abstract: Full 1.3 µm VCSEL-based simplified coherent detection receiver is demonstrated at 5 Gbps. Receiver sensitivity of -34 dBm is achieved providing link reach and splitting ratio extension for future passive optical access networks.

OCIS codes: 060.2330 Fiber optics communications, 140.7260 Vertical cavity surface emitting lasers, 060.1660 Coherent communications

1. Introduction

Passive optical networks (PONs) have become a dominant approach for fiber-to-the-customer (FTTC) network deployments. However, the demand for increasing bandwidth has raised the question of extending the reach, bit-rate and splitting ratio of conventional PON solutions designed for 20 km, 1.25-2.5 Gbps and splitting ratios up to 64 [1]. An interesting approach for extending the reach of PON networks is to consider optical coherent detection. This is motivated by the fact that coherent detection offers advantages on supporting closely spectrally spaced channels with electrical narrow bandwidth selection [2], increased receiver sensitivity [3] and support for advanced modulation formats [4]. However, it will still be important to reduce the cost of coherent networks and put them at the same level with traditional direct detection approaches in order to make them attractive for a real implementation in future wavelength division multiplexing (WDM) PONs.

Vertical cavity surface emitting lasers (VCSELs) are gaining attention for application in access networks due to lower manufacturing cost and lower power consumption than edge-emitter laser [5].

In this paper we propose an all-VCSEL low complexity transmitter and coherent receiver operating close to the zero dispersion wavelength of standards single mode fiber (SSMF) of 1.3 µm, chosen for its compatibility with the up-stream wavelength of PONs architectures. The optical transmitter is a directly modulated photonic bandgap GaInNAs VCSEL TOSA from Alight Technologies ApS. The coherent receiver is realized in a simple configuration using only a 3-dB coupler, local oscillator VCSEL of same type as the transmitter, and a single ended photodiode with the aim of maintaining the overall systems complexity reduced. We experimentally demonstrate the feasibility of our proposed approach in a 5 Gbps amplitude shift-keying (ASK) coherent link with transmission over 40 km of SSMF with no optical dispersion compensation, employing free running and un-cooled VCSEL operation for transmitter as well as local oscillator.

2. Experimental setup

Fig. 1 shows our experimental setup. A pulse pattern generator directly modulates a 1.3 µm VCSEL ($VCSEL_1$) at 5 Gbps. A balanced drive configuration is used for $VCSEL_1$ with a driving peak-peak voltage of 0.9 V. The bias current of $VCSEL_1$ is set to 11.7 mA for optimum performance maximizing the extinction ratio while minimizing pulse amplitude overshoot. The data pattern used for the experiment is a pseudo random binary sequence (PRBS) of length of 2^9-1. The average output power of the $VCSEL_1$ launched into the fiber is -0.7 dBm. The transmission experiment is over 40 km of SSMF with a total attenuation of 13.5 dB at 1.3 µm, and a total dispersion of -45 ps/nm. In order to measure the optical power going into the coherent receiver, a variable optical attenuator (VOA), a 20 dB coupler and an optical power meter are placed after the transmission fiber. Due to the low chromatic dispersion in the spectral region of 1.3 µm, dispersion compensation can be omitted, and the in-phase and quadrature components of the signal are not required in the coherent demodulator. Therefore, the coherent scheme can be simplified from a conventional 90° hybrid scheme to a simpler one composed of a light source as local oscillator (LO), a 3 dB coupler to do the beating between the received signal and the LO, a photodiode and a subsequent envelope detector. The LO signal is generated by another free running, continuous wave, 1.3 µm VCSEL ($VCSEL_2$). The LO $VCSEL_2$ has been wavelength tuned to match the wavelength of the transmitting $VCSEL_1$ at 1274 nm by adjusting the bias level to 13 mA for intradyne detection. The insertion in Fig. 1 shows the measured optical power spectrum of the signal and the LO. Due to the intradyne detection scheme, the signal spectrum is partially masked by the spectrum of the LO.
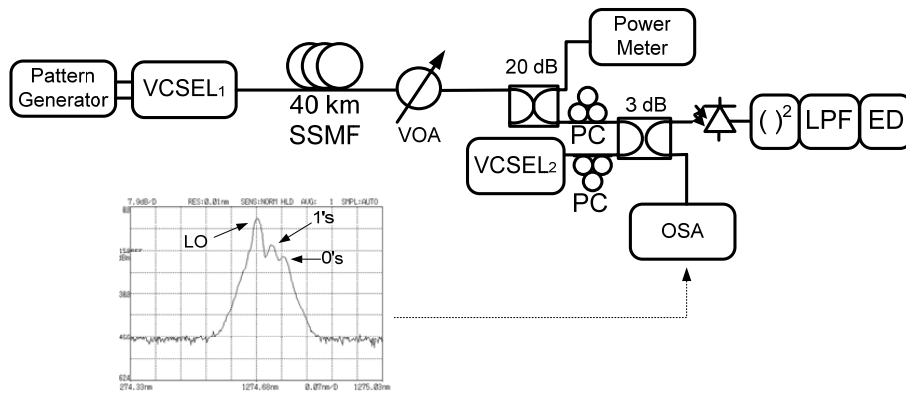
Figure 1: Experimental setup. Local oscillator (LO), optical spectrum analyzer (OSA), polarization controller (PC), variable optical attenuator (VOA), low pass filter (LPF), error detector (ED). The insertion shows the measured combined optical power spectrum of the signal and the LO.

The wavelength tuning range of VCSEL$_2$ was measured to be 5 nm from 1271.1 nm to 1275.8 nm by varying the bias current from 5 mA to 16 mA. This demonstrates the feasibility of bias current wavelength tuning of VCSELs employed as local oscillators in coherent networks. The optical output power of the LO varies from 0.32 mW to 0.85 mW.

The coherent receiver used electronic envelope detection for the ASK signal which removes the frequency offset between the signal and the LO. The envelope detector is emulated digitally in off-line processing by squaring and low pass filtering the signal stored in a digital sampling scope (DSO) with a sample rate of 40 Gsample/s. The signal is compared offline with the PRBS sequence by the error detector (ED) for BER measurements. No extra digital signal processing has been done offline; therefore the digital envelope and ED could be directly substituted by a commercial envelope detector and a 5 Gbps ED for real time measurements.

3. Results

Fig. 2(a) shows the optical eye diagram at the output of the transmitter. At the bias current of 11.7 mA, beginning overshooting of the VCSEL is observed. The extinction ratio (ER) at the transmitter is 4.62 dB measured with an oscilloscope. Fig. 2(b) shows the eye diagram after 40 km SSMF transmission. The fiber attenuation has decreased the signal to noise ratio (SNR), but no pulse broadening is observed due to the negligible chromatic dispersion at 1.3 µm.
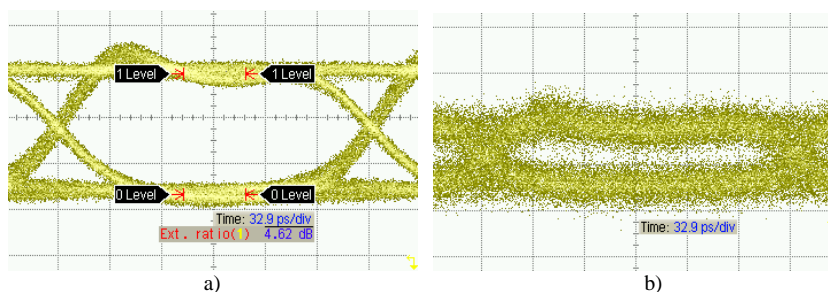

Figure 2. Direct detected optical eye diagrams. 5 Gbps, Ibias= 11.7 mA, Vpp= 0.9 V. (a) Back-to-back. (b) After 40 km SSMF

The measured bit error ratio (BER) of the 5 Gbps signal back-to-back (B2B) and after 40 km SSMF transmission is plotted in Fig. 3. The plot shows the measured BER with coherent and with direct detection.

For direct detection, a back to back (B2B) receiver sensitivity at the forward error correction limit of BER< $2.23 \cdot 10^{-3}$, was measured to be –26 dBm for B2B configuration and after 40 km of SSMF. SSMF thus negligible power penalty was observed. For the coherent detection case, $2 \cdot 10^5$ bits were stored for further offline analysis. Receiver sensitivity was measured to be -34 dBm for B2B as well as after transmission. Comparing to the direct detection case, the receiver sensitivity has been improved by 8 dB. This corresponds to a passive splitting ratio 6.3 times higher, or an extension of the unamplified transmission reach by 23 km.

In order to estimate the potential maximum transmission that can be reached with this system a simple power budget calculation has been performed considering 0.34 dB/km attenuation and negligible dispersion of the fiber at 1,3 µm. The launch power is -0.7 dBm and the receiver sensitivity of -34 dBm, result in a power margin of 33.3 dB, corresponding to almost 100 km of SSMF. In terms of splitting ratio, after 40 km, the achieved power margin of 19.8 dB correspond to and splitting ratio of 95.
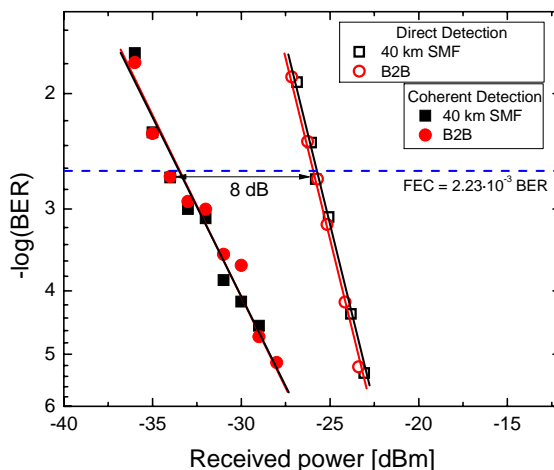
Figure 3: BER curves after 40 km SSMF and for B2B configuration. Bit-rate: 5 Gbps, ER: 4.62 dB, LO power: -0.8 dBm.

4. Conclusion

We have proposed and experimentally demonstrate for the first time, the feasibility of a full VCSELs based coherent detection system with un-cooled and free running operation of the transmitter as well as the local oscillator VCSEL light source. Our experimental demonstration successfully shows 5 Gbps operation at 1.3 µm with increased sensitivity of -34 dBm. Extended link reach over 40 km SSMF and high splitting ratio of 95 have been achieved with a low complexity coherent receiver and with no need of optical amplification or dispersion compensation. The simplicity of our proposed coherent approach is intended to overcome the complexity of conventional coherent systems for access networks. The potential cost reduction and good performance of our proposed approach make VCSEL-based coherent PONs a strong candidate for application in future PONs. We believe that future work on this approach will result in upgrade to 10 Gbps systems.

References

[1]   P.E. Green et al., "Fiber to the home: the next big broadband thing," IEEE Communications Magazine, vol.42, no.9, pp. 100- 106, Sept. 2004.
[2]   A.D. Ellis et al., "Spectral density enhancement using coherent WDM," IEEE Photon. Technol. Letters, vol.17, no.2, pp.504-506, Feb. 2005.
[3]   G. Lachs et al., "Sensitivity enhancement using coherent heterodyne detection," IEEE J. Lightwave Technol., vol.12, no.6, pp.1036-1041, Jun 1994.
[4]   X. Zhou et al., "Advanced coherent modulation formats and algorithms: Higher-order multi-level coding for high-capacity system based on 100Gbps channel," OFC, 21-25 March 2010.
[5]   E. Kapon et al., "Long-wavelength VCSELs: Power-efficient answer, " Nature Photonics 3, 27 - 29 (2009).

Paper 5: Real time 1.55 um VCSEL-based coherent detection link

R. Rodes, D. Parekh, J.B. Jensen, C.J. Chang-Hasnain, and I.T. Monroy, "Real time 1.55 um VCSEL-based coherent detection link," *IEEE Photonics Conference*, 2012.

Real time 1.55 μm VCSEL-based coherent detection link

R. Rodes[1], D. Parekh[2], J. B. Jensen[1], C. J. Chang-Hasnain[2] and I. Tafur Monroy[1]

[1] DTU Fotonik, Technical University of Denmark, Denmark, rrlo@fotonik.dtu.dk
[2] Department of Electrical Engineering and Computer Sciences, University of California, Berkeley, USA

Abstract This paper presents an experimental demonstration of VCSEL-based PON with simplified real-time coherent receiver at 2.5 Gbps. Receiver sensitivity of -37 dBm is achieved proving splitting ratio up to 2048 after 17 km fiber transmission.

Introduction

Passive optical networks (PONs) have become the dominant approach for fiber-to-the-customer (FTTC) network deployments. However, the demand for increasing bandwidth has raised the question of extending the reach, bit-rate and splitting ratio of conventional PONs [1]. An interesting approach for extending the reach and increasing the capacity of PON networks is to consider optical coherent detection. This is motivated by the fact that coherent detection offers advantages on supporting closely spectrally spaced channels [2] and increased receiver sensitivity [3]. Coherent PONs approaches have been presented with distributed Bragg reflector (DBR) lasers [4], distributed feedback lasers (DFBs) [5] and reflective semiconductor optical amplifiers (RSOAs) [6]. Different receivers have been proposed using offline digital signal processing (DSP) [4,5], or in real time using FPGAs [7]. However, cost of coherent networks needs to be put at the same level as traditional direct detection approaches to make them attractive for deployment in future wavelength division multiplexing (WDM) PONs. Previously, we presented results on vertical cavity surface emitting lasers (VCSEL) based coherent detection link for PONs using DSP [8].

In this paper we propose a real time and low complexity coherent receiver. The optical transmitter is a directly modulated 1550 nm VCSEL and the coherent receiver is realized in a simple configuration using a 3-dB coupler, local oscillator, single ended photodiode, XOR gate and low pass filter.

We experimentally demonstrate the feasibility of our approach in a 2.5 Gbps amplitude shift-keying (ASK) coherent link with transmission over 17 km.

Experimental Setup

Fig. 1 shows the experimental setup. A pulse pattern generator (PPG) directly modulates a VCSEL with non-return-to-zero (NRZ) on-off keying (OOK) signal at 2.5 Gbps. The PPG uses a pseudorandom binary sequence (PRBS) with pattern length of 2^9-1. The driving peak-to-peak voltage into the VCSEL is 500 mV at a bias current of 7 mA. The VCSEL wavelength is 1535 nm and the output power coupled into the fiber is 0 dBm. The signal is launched into 17 km single mode fiber (SMF) with a measured attenuation of 3.8 dB. An optical attenuator is placed after transmission for bit error rate (BER) measurements. An optical 3 dB coupler combines the received signal and the local oscillator (LO). An external cavity laser (ECL) is used as LO. A polarization controller is used to match the polarization of the LO with the received signal. A 10 GHz PIN+TIA photoreceiver receives the optical signal and it is split by an electrical 6 dB. Length matched cables are used for both inputs of the XOR gate. A low pass filter with a cut off frequency of 2.5 GHz is used before the error detector for BER measurements.

Real time coherent receiver

The LO was placed at 1534.96 nm for heterodyne coherent detection, with a 0.04 nm offset. Figure 2.a shows the coherently detected signal after the photodiode. There is an oscillation of 5 GHz due to the 0.04 nm
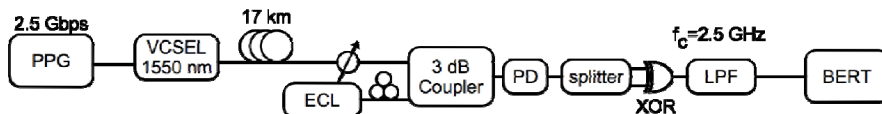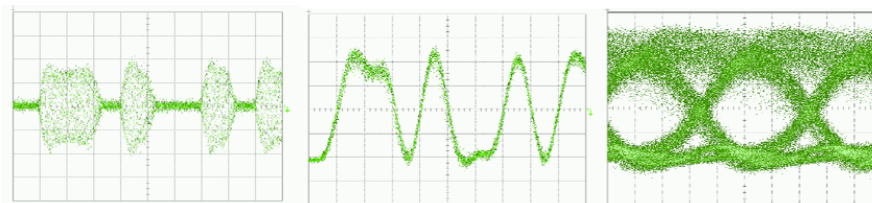

Fig. 1 Experimental setup

457

Fig 2. a) Signal after the photodiode. b) signal after LPF. c) eyediagram at -33dBm received power

offset between the LO and the received signal. After 6 dB power splitter, 2 identical copies of the received signal are connected from the photodiode to the XOR gate with phase matching cables. As both signals inputs are identical, the inverted output of the XOR gate is always digital value '1' (+170 mV) when the input level exceeds the sensitivity of the gate. When the amplitude of the input signal of the XOR gate is lower than the sensitivity of the gate, the output of the gate is 0 mV. The integrated DC block removes the DC offset. The XOR gate acts as a rectifier. The low pass filter at 2.5 GHz is used to filter out the oscillation due to the frequency offset. The Fig. 2.b and 2.c show the output of the low pass filter and eyediagram, respectively.

Results

The performance of the system is evaluated for back-to-back (B2B), and after 17 km SMF. Fig. 3 shows the BER for the optimum LO power of 1 dBm. Receiver sensitivity of -37 dBm was measured at the forward error correction (FEC) limit of $2\bullet10^{-3}$. No receiver power penalty sensitivity is observed after transmission compare to B2B. In order to estimate the potential maximum splitting ratio that can be reached with this system, a simple power budget calculation has been
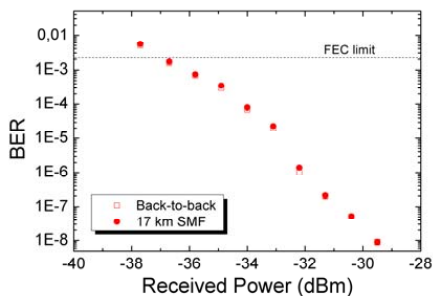

Fig. 3 Bit error rate curve at 2.5 Gbps with real time coherent detection.

performed. The measured optical power of -3.8 dBm after 17 km SMF and the receiver sensitivity of -37 dBm, result in a power margin of 33.2 dB. The power margin corresponds to a splitting ratio of 2048

Conclusion

We have demonstrated a real time implementation of a VCSEL-based coherent PON by using a simple XOR gate at the receiver. Our experimental demonstration successfully shows 2.5 Gbps operation at 1.5 μm with increased sensitivity of -37 dBm. High splitting ratio of 2048 have been achieved after 17 km transmission. The simplicity of our proposed coherent approach is intended to overcome the complexity of conventional digital coherent systems for access networks. The potential cost reduction and good performance of our proposed approach make VCSEL-based coherent PONs a strong candidate for application in future PONs. We believe that future work on this approach will result in upgrade to 10 Gbps systems, and full VCSEL-based system for the local oscillator as for the transmitter.

Acknowledgements

References

[1] Green, P.E., IEEE Comm. Magazine, vol.42, no.9, pp. 100- 106, 2004.
[2] Ellis A.D. et al., PTL, vol.17, no.2, pp.504-506, 2005.
[3] Lachs, G. et al., JLT, vol.12, no.6, pp.1036-1041, 1994.
[4] Lavery, D. et al., OFC 2012, PDP5B.
[5] Kim, S-Y. et al., OFC 2009, OMN6.
[6] Cho, K.Y. et al., OFC 2008, OtuH4.
[7] Smolorz, S. et al., OFC 2011, PDPD4.
[8] Rodes, R. et al., Optics Express, vol. 18, no.24, pp. 24969-24974, 2010.

Paper 6: 10 Gb/s real-time All-VCSEL low complexity coherent scheme for PONs

R. Rodes, N. Cheng, J.B. Jensen, and I.T. Monroy, "10 Gb/s real-time All-VCSEL low complexity coherent scheme for PONs," *Optical Fiber Communication Conference and Exposition*, 2012.

10 Gb/s Real-Time All-VCSEL Low Complexity Coherent scheme for PONs

Roberto Rodes[1], Ning Cheng[2], Jesper Bevensee Jensen[1] and Idelfonso Tafur Monroy[1]

1.DTU Fotonik, Department of Photonics Engineering, Technical University of Denmark, DK2800 Kgs. Lyngby, Denmark.
2.Advanced Technology Department, Huawei Technologies, 2330 Central Expressway, Santa Clara, CA 95050, USA.
rrlo@fotonik.dtu.dk

Abstract: Real time demodulation of a 10 Gb/s all-VCSEL based coherent PON link with a simplified coherent receiver scheme is demonstrated. Receiver sensitivity of -33 dBm is achieved providing high splitting ratio and link reach.
OCIS codes: (060.2330) Fiber optics communications; (140.7260) Vertical cavity surface emitting lasers; (060.1660) Coherent communications

1. Introduction

The demand for high-speed access networks is continuously growing. This demand is driven by new applications that require higher bandwidth. Applications such us youtube, Netflix etc. are becoming the preferable form of video entertainment offering [1]. Typically, fiber-to-the-home (FTTH) networks are based on passive optical networks (PONs). WDM-PON is the leading candidate technology for next generation access networks beyond 10 Gb/s [2]. The main for WDM-PON is cost efficiency. Therefore, several assumptions have to be taken: colorless ONUs, single fiber operation for upstream and downstream, no use of external modulators and no use of optical amplifiers [3].

It is well known that coherent detection has many advantages such us increasing sensitivity, extending reach, increasing network capacity by close wavelength allocation, allowing for dispersion compensation or demodulation of advances modulation formats. Although, the main remaining challenge of coherent PONs is cost reduction in order to make it comparable with typical direct detection systems. Coherent detection has been typically associated with high quality lasers and complex receivers with digital signal processing not suitable for cost effective PON.

Vertical cavity surface emitting lasers (VCSELs) are gaining attention in access networks due to lower manufacturing cost and lower power consumption than edge-emitter lasers [4].

Previously, in [5] we have demonstrated coherent detection using VCSELs for signals as well as LO. In this case, however, the system only operated at 5 Gb/s and digital sampling at 20 GSa/s was required for the demodulation. The latter is problematic in PON scenarios due to cost issues. In this paper we present, for the first time to our knowledge, an all VCSEL coherent PON system employing real-time detection with no use of digital signal processing. Additionally, the bit rate of the system has been doubled to 10 Gb/s. This demonstration of a real-time 10 Gb/s all VCSEL, no DSP coherent PON represents the lowest cost and complexity coherent system ever reported for PON scenarios. The only added equipment when compared with conventional direct detection is a VCSEL, 3 dB fiber coupler, 6 dB electrical splitter and an XOR gate.

The optical transmitters and the LO are photonic bandgap GaInNAs VCSEL TOSAs from Alight Technologies Aps. Direct modulation at 10 Gb/s amplitude shift-keying (ASK) over 25 km SMF was performed. Free running and un-cooled VCSEL operation were used for the transmitters as well as for the local oscillator.
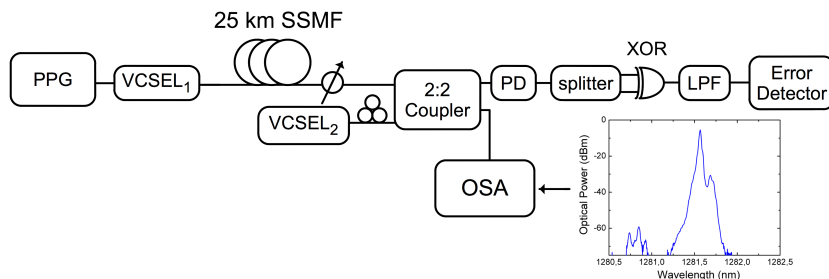
2. Experimental Setup

Figure 1. Setup. Pulse pattern generator (PPG), Photodetector (PD), Variable optical attenuator (VOA), Low pass filter (LPF)

Figure 1 shows the experimental setup. A pulse pattern generators directly modulate a 1.3 µm VCSEL. Single drive configuration is used for the VCSEL. The measured wavelength of the VCSEL is 1281.68 nm. The VCSEL is free-running with no cooling or temperature control. The signal is transmitted through 25 km of standard single mode fiber (SSMF) with no optical amplification. Fiber launch power of the VCSEL into the fiber is -1 dBm. At the coherent receiver input, a variable optical attenuator (VOA) is used to assess BER vs. receiver input power and to emulate the loss of a passive PON splitter.

Coherent Receiver:

Due to the low chromatic dispersion in the spectral region of 1.3 µm, dispersion compensation can be omitted, and the in-phase and quadrature components of the signal are not required for signal demodulation. Therefore, for amplitude modulation, the coherent receiver scheme can be simplified from a conventional 90 degree hybrid scheme with two photodiodes and digital signal processing [6], to a simpler one composed of a 3 dB coupler, a single photodiode and an analogue envelope detector [5]. The LO is a free running, un-cooled and continues-wave VCSEL with a polarization controller to maximize the output at the photodiode. Bias of the LO VCSEL is used for wavelength for intradyne coherent detection. Embedded graph in Fig.1 shows the combined spectrum of the received signal and the LO.

The envelope detector is composed of a 6 dB electrical splitter, an XOR gate and a low pass filter. The outputs of the 6 dB electrical splitter are connected to the inputs of the XOR gate with phase-matched RF cables. The XOR gate is not used for its typical digital behavior but for its analogue behavior instead to rectify the signal. Figure 2 shows the signals in each step of the envelope detection. The sensitivity of the XOR is approximately 20 mV. When a logical '0' is transmitted, the amplitude level at the output of the photodiode is lower than the XOR sensitivity, and the output of the XOR gate is 0 mV. This is observed from Fig. 2.a. When a logical '1' is transmitted, the amplitude level of the signal out of the photodiode is higher than the XOR sensitivity. As matched RF cables are used between the 6 dB splitter and the XOR gate, the two input signals are equal, and the XOR gate will produce a positive signal (200 mV) at its inverted output irrespective of the sign of the signals at the input. In this way, the XOR gate is able to rectify the signal from the photodiode. This is illustrated in Fig. 2.b, where the signal after the XOR gate and a DC block is shown. The bandwidth limitation of the XOR gate removes most of the oscillation in the signal due to the frequency offset of the transmitted signal and local oscillator. Fig. 2.c shows the signal after additional low pass filtering. As can be observed, the signal now has properties similar to an NRZ-OOK signal, and can therefore be detected in real time using a standard error detector.
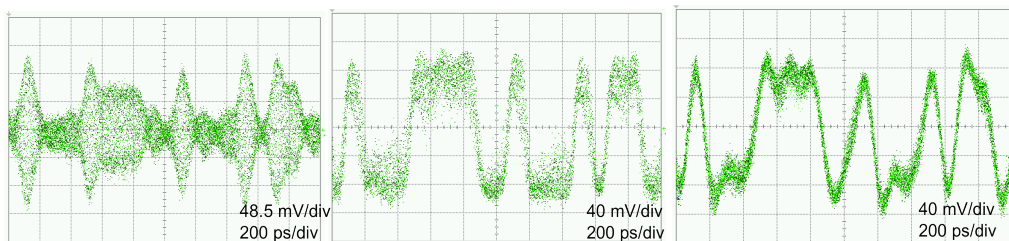

Figure 2. a) Output photodiode, b) output XOR gate, c) output low pass filter

3. Results

The experiment has been performed at 2.5 and 10 Gb/s. The system at 2.5 Gb/s is evaluated with a PIN and a balanced photodiode in order to compare the performance of the two configurations. Figure 3.a shows the bit error ratio (BER) curve after 25 km SSMF. BER below 10^{-9} is measured for received power of -26 dBm with the PIN photodiode and -31 dBm with balanced photodiode. In both cases, no error floor is observed. At the forward error correction (FEC) limit of BER < $2.2*10^{-3}$, the sensitivity is measured at −39 dBm with the balanced photodiode and −37 dBm with the PIN photodiode. In the case of FEC, 7% overhead has to be considered for the effective bit rate. Significant improvement is observed by using balanced photodiode. 5 dB gain in sensitivity at BER < 10^{-9}, and 2 dB sensitivity gain at BER < $2.2*10^{-3}$.

For the 10 Gb/s the performance was assessed with the 20 GHz bandwidth balanced photodiode. Fig. 3.a shows the BER curve. BER below 10^{-9} is measured at −23 dBm. At the FEC limit of BER < $2.2*10^{-3}$, the received power sensitivity is −33 dBm. Fig 3.b shows the optical back-to-back eye diagram at 10 Gb/s. Fig 3.c shows the eye

diagram of the received signal after 25 km SSMF. No pulse broadening due to chromatic dispersion is observed after fiber transmission.

A power budget calculation has been done in order to estimate the maximum splitting ratio allowed by this system with a passive splitter. Considering 9 dB attenuation of the 25 km SSMF at 1.3 μm, the power margin of the received power at the FEC limit sensitivity is 23 dB and 29 dB at 10 Gb/s and 2.5 Gb/s, respectively. These power margins correspond to a passive splitting ratio of 199 and 794 at 10 Gb/s and 2.5 Gb/s, respectively.
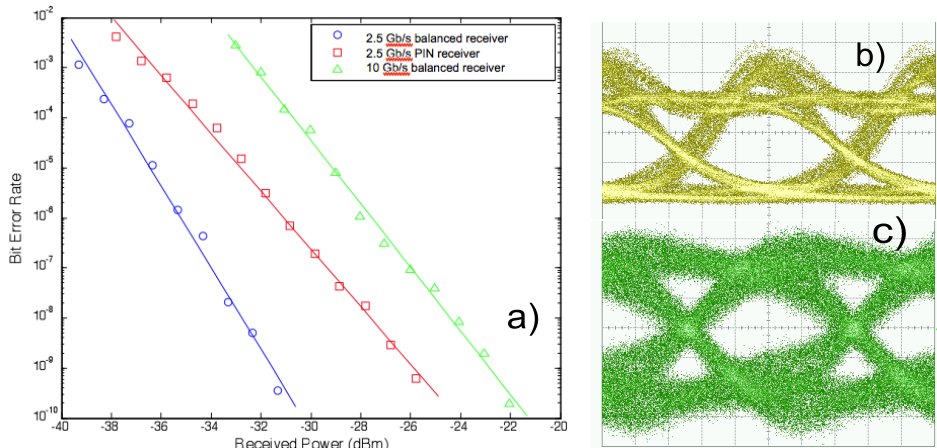
Figure 3. a) BER curves at 2.5 Gb/s and 10 Gb/s after 25 km SSMF, b) eye diagram of the optical back-to-back signal at 10 Gb/s, c) eye diagram of received signal at 10 Gb/s.

4. Conclusion

We have proposed an experimentally demonstrated for the first time an all-VCSEL coherent PON link with realtime demodulation at 10 Gb/s. Transmission after 25 km SSMF was performed with sensitivity of -33 dBm allowing for a passive splitting ratio of 199.

The potential cost reduction and good performance of our proposed approach make VCSEL-based coherent PONs a strong candidate for application in future PONs. Future work on this approach will be done adding more transmitting channels implementing a WDM system.

5. References

[1] Cedric F. Lam, "The road to scalable 1 Gb/s FTTH access networks," ECOC 2011, paper Tu.6.C.2.

[2] Derek Nesset, "Network operator perspective on WDM-PON systems and application," ECOC 2011, paper Th.12.C.6.

[3] Y. C. Chung, "Recent advancement in WDM PON technology," ECOC 2011, paper Th.11.C.4.

[4] E. Kapon et al., "Long-wavelength VCSELs: Power-efficient answer," Nature Photonics 3, 27 – 29 (2009).

[5] R. Rodes et al., "1.3 μm all-VCSEL low complexity coherent detection scheme for high bit rate and high splitting ratio PONs," OFC 2011, paper OThK7.

[6] R. Rodes et al., "All-VCSEL based digital coherent detection link for multi Gbit/s WDM passive optical networks," Optics Express, Vol. 18, Issue 24, pp. 24969-24974 (2010)

Paper 7: 100 Gb/s single VCSEL data transmission link

R. Rodes, J. Estaran, B. Li, M. Mueller, J.B. Jensen, T. Gruendl, M. Ortsiefer, C. Neumeyr, J. Rosskopf, K.J. Larsen, M.-C. Amann, and I.T. Monroy, "100 Gb/s single VCSEL data transmission link," *Optical Fiber Communication Conference and Exposition*, pp. Post Deadline P5D.10, 2012.

100 Gb/s single VCSEL data transmission link

R. Rodes[1], J. Estaran[1], B. Li[1], M. Muller[2], J. B. Jensen[1], T. Gruendl[2], M. Ortsiefer[3], C. Neumeyr[3], J. Rosskopf[3], K. J. Larsen[1], M.-C. Amann[2] and I. T. Monroy[1]

[1].DTU Fotonik, Department of Photonics Engineering, Technical University of Denmark, DK2800 Kgs. Lyngby, Denmark
[2]Walter Schottky Institut, TU München, Am Coulombwall, D-85748 Garching, Germany
[3]VERTILAS GmbH, Lichtenbergstr. 8, D-85748 Garching, Germany
rrlo@fotonik.dtu.dk

Abstract: 100 Gb/s optical fiber transmission link with a single 1.5 um VCSEL has been experimentally demonstrated using 4-level pulse amplitude modulation
OCIS codes: (060.2330) Fiber optics communications; (140.7260) Vertical cavity surface emitting lasers

1. Introduction

The rapid growth of Internet and cloud computing applications drives data centers to upgrade their links from the 10 Gb/s commonly used today to 100 Gb/s and beyond in the near future [1] with little or no increase in carbon and real-estate footprint [2]. These two counteracting demands leads to a quest for higher data capacity on short range optical communication systems employing directly modulated (DM) vertical cavity surface emitting lasers (VCSELs); a laser type that is rapidly becoming the preferable laser source for interconnect applications due to an attractive combination of attributes, including high bit rates [3,4], low drive voltage [5], and the capability of array integration [6].

The existing 100 Gb/s standard for short range interconnects (100GE-SR10) specifies the use of 10 wavelengths each operated at 10 Gb/s while the next generation standard (100GE-SR4) employs 4 lasers each operated at 25 Gb/s [7]. Increasing the data modulation of each laser to 100 Gb/s paves the way for a) an increase the total link capacity to 400 Gb/s or to b) a reduction in footprint and complexity of the 100 Gb/s links since they could be operated with a single laser.

In this paper, we report on research investigation on the capabilities of using a single VCSEL to achieve 100 Gbit/s speed transmission. We have performed directly modulation of a VCSEL by employing a 4-levels pulse amplitude modulation (4-PAM) at 25 Gbaud and polarization multiplexing to achieve a total bitrate of 100 Gb/s link with a single VCSEL. Forward error correction coding has been implemented with an effective bit rate of 86.5 Gb/s. Error free transmission in the experiment with $1.6 \cdot 10^8$ bits of FEC decoding. This is, to the author knowledge, the largest transmission capacity reported for a single VCSEL source.

2. Experimental Setup

Figure 1 shows the setup of the transmission experiment. Two uncorrelated 25 Gb/s subrate channels of an SHF 12103 A pulse pattern generator (PPG) are added to form a 50 Gb/s 4-PAM signal. The link is analyzed with pseudorandom binary sequences (PRBS) and with 2 different forward error correction (FEC) patterns. The PRBS sequence has a pattern length of 2^{11}-1. The FEC codes have a length of 1138489 bits with 7% overhead, and 152881 bits with 20% overhead. We choose the product code with shortened BCH (Bose – Chaudhuri - Hocquenghem) components [8] as FEC codes in our experiments.
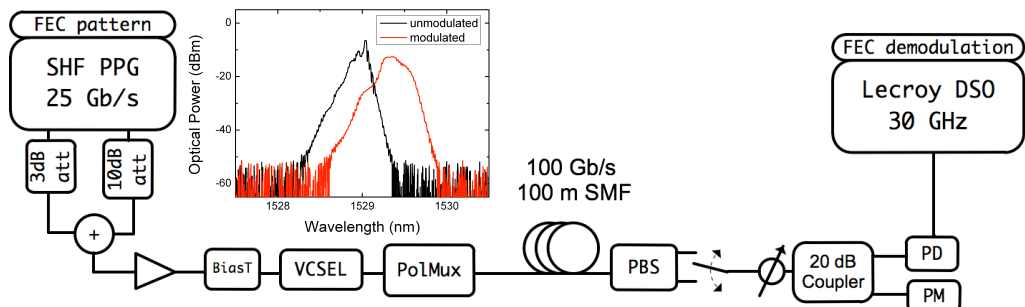

Figure 1. Setup. Pulse pattern generator (PPG), Photodetector (PD), Variable optical attenuator (VOA), Low pass filter (LPF), Power meter (PM), Single mode fiber (SMF), Polarization beam splitter (PBS).

The subchannel addition system is optimized to reduce reflections, and is composed of a 10 dB and a 3 dB electrical attenuator, and a 6 dB electrical combiner. A high-linearity amplifier from SHF is used to amplify the electrical signal up to 1 Vpp in order to utilize the linear region of the VCSEL I-P characteristic curve. L-I-V curve of the VCSEL is shown in Fig. 2.a. The VCSEL used is a high-speed short-cavity VCSEL with 1.55 μm emission wavelength and 3-dB modulation bandwidth of 18 GHz at 20°C. The spectrum of the modulated VCSEL with the 4-PAM signal is shown embedded in Fig. 1. Detailed description of the specific VCSEL characteristics can be found in [9]. The bias of the VCSEL is set to 10 mA for optimum performance. The optical signal from the VCSEL is launched into a polarization multiplexing system with an optical delay between branches to emulate orthogonal polarization transmission uncorrelated at 100 Gb/s. The signal is transmitted over 100 m of standard single mode fiber (SMF). On the receiver side, polarization beam splitter (PBS) separates the two polarizations. Each polarization is detected independently by a 40 GHz photodiode. A Lecroy 30 GHz, 80 Gsa/s digital storage oscilloscope (DSO) is used to store the received signal for offline demodulation. The offline signal demodulation includes bit synchronization and adaptive decision threshold gating.

3. Results

Digital upsampling of the signal to oversampling 10 has been used for better demodulation. Figure 2.b shows the histograms of the optimum sample point of the received signal for different received powers. The histograms show 5000 bits. The minimum points of the histogram for each received power are taken as the symbol decision thresholds. The least significant bit (LSB) and most significant bit (MSB) of each symbol are two uncorrelated patterns. After demodulation, error counting of received LSB and MSB is done independently comparing each bit-stream with the corresponding pattern.

Figure 3.a shows the bit error rate (BER) curve for MSB after 100 m and with back-to-back (B2B) configuration. Figure 3.b shows the BER curves for LSB. We can observe worst performance in LSB as it was expected due to its higher error probability on the symbol. We have used gray mapping to facilitate error correction.
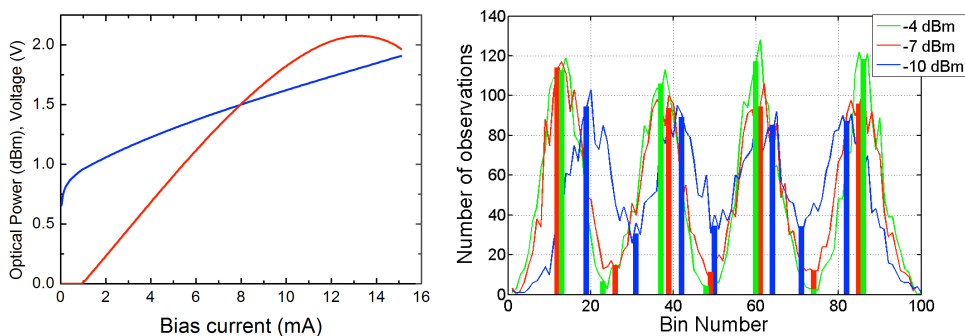

Figure 2. a) LIV curve at 35 °C; b) histogram of optimum sample from received signal

Adaptive FEC:

The theoretical pre-FEC thresholds of 7% overhead and 20% overhead FEC, aiming for after-FEC BER of 10^{-15}, are $4.8 \cdot 10^{-3}$ and $1.3 \cdot 10^{-2}$ [10], while in the FEC performance simulation thresholds are approximately $4.4 \cdot 10^{-3}$ and $1.1 \cdot 10^{-2}$, respectively, due to BCH decoding errors. The 7% overhead FEC is applied to MSB and the 20% overhead FEC is applied to LSB based on the BER results returned from PRBS sequence tests. Figure 3.a and 3.b show with a blue line the FEC limits for 7% and 20%, respectively. Transmissions below the FEC limit can be decoded without errors. By applying different FEC codes to LSB and MSB, the received power sensitivities for error free demodulation coincide. We processed $1.6 \cdot 10^{8}$ bits for the FEC decoding for both channels and got error free after the offline demodulation and FEC decoding at -4 dBm received power sensitivity. The adaptive FEC maximizes the effective bitrate for error free transmission. The 7% and 20% overhead of MSB and LSM, respectively, result in a total effective bitrate of 86.5 Gb/s. Due to the limited number of FEC frames we can save on the DSO, we theoretically calculated the error probability in a longer sequence. Based on the theory in [11], as we had 0 errors in the experiment after several FEC decoding iterations, we have, with 90% confidence, that the BER of less than $2.02 \cdot 10^{-6}$ is expected in repeated experiments. These errors are expected to be corrected after 1 or 2 more iterations

due to the small FEC error floor of less than 10^{-15}. Therefore an error free transmission is still expected in a longer time measurement.
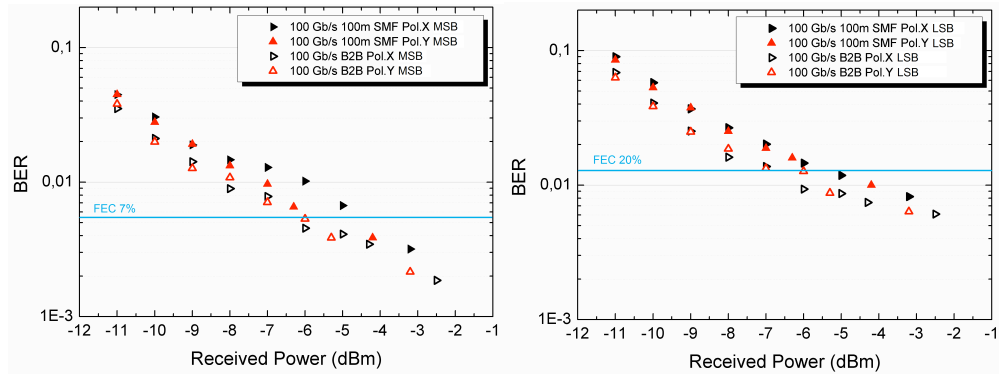

Figure 3. a) BER curves at 100 Gb/s after 100 m SSMF and B2B for MSB, b) BER curves at 100 Gb/s after 100 m SSMF and B2B for LSB

4. Conclusion

Ultimate capacity transmission with a single VCSEL has been investigated by multilevel pulse amplitude modulation and polarization multiplexing over 100 m SMF. We have demonstrated 100 Gb/s transmission with error free transmission after forward error correction with an effective bitrate of 86.5 Gb/s by using adaptive FECs.

5. Acknowledgements

6. References

[1] Hong Liu; Lam, C.F.; Johnson, C.; , "Scaling Optical Interconnects in Datacenter Networks Opportunities and Challenges for WDM," *High Performance Interconnects (HOTI), 2010 IEEE 18th Annual Symposium on* , vol., no., pp.113-116, 18-20 Aug. 2010.

[2] Strategies for Solving the Datacenter Space, Power, and Cooling Crunch: Sun Server and Storage Optimization Techniques. Oracle White paper, March 2010.

[3] Hofmann, W.; Müller, M.; Wolf, P.; Mutig, A.; Gründl, T.; Böhm, G.; Bimberg, D.; Amann, M.-C.; , "40 Gbit/s modulation of 1550 nm VCSEL," *Electronics Letters* , vol.47, no.4, pp.270-271, February 17 2011

[4] Hofmann, W.; Moser, P.; Wolf, P.; Mutig, A.; Kroh, M.; Bimberg, D.; , "44 Gb/s VCSEL for optical interconnects," *Optical Fiber Communication Conference and Exposition (OFC/NFOEC), 2011 and the National Fiber Optic Engineers Conference* , vol., no., pp.1-3, 6-10 March 2011

[5] Moser, P.; Hofmann, W.; Wolf, P.; Fiol, G.; Lott, J.A.; Ledentsov, N.N.; Bimberg, D.; , "83 fJ/bit energy-to-data ratio of 850-nm VCSEL at 17 Gb/s," *Optical Communication (ECOC), 2011 37th European Conference and Exhibition on* , vol., no., pp.1-3, 18-22 Sept. 2011

[6] Hofmann, W.; Gorblich, M.; Bohm, G.; Ortsiefer, M.; Xie, L.; Amann, M.-C.; , "Long-wavelength 2-D VCSEL arrays for optical interconnects," Lasers and Electro-Optics, 2008 and 2008 Conference on Quantum Electronics and Laser Science. CLEO/QELS 2008. Conference on , vol., no., pp.1-2, 4-9 May 2008

[7] Cole Chris, "Next generation 100G client optics," *Optical Communication (ECOC), 2011 37th European Conference and Exhibition on* , workshop 13, 18-22 Sept. 2011

[8] Bomin Li, Knud J. Larsen, Darko Zibar and Idelfonso Tafur Monroy, "Over 10 dB Net Coding Gain Based on 20% Overhead Hard Decision Forward Error Correction in 100G Optical Communication Systems," in Proc. 37th European Conf. and Exhibition on Optical Communication, Geneva, 2011.

[9] M.-C. Amann, E. Wong, M. Mueller, "Energy-efficient High-Speed Short-Cavity VCSELs", Proc. OFC/NFOEC, paper OTh4F, Los Angeles, Ca, USA March 2012.

[10] J. Justesen, "Performance of Product Codes and Related Structures with Iterated Decoding" in IEEE Trans. Commun. 59, 2, 407-415 (2011).

[11] J. L. Massey, "Comparison of Rate One-Half, Equivalent Constraint Length 24, Binary Convolutional Codes for Use with Sequential Decoding on the Deep-Space Channel", Technical Report No. EE-762, University of Notre Dame, Indiana 46556, USA, 1976

Paper 8: High-speed 1550 nm VCSEL data transmission link employing 25 Gbaud 4-PAM modulation and hard decision forward error correction

R. Rodes, M. Mueller, B. Li, J. Estaran, J.B. Jensen, T. Grundl, M. Ortsiefer, C. Neumeyr, J. Rosskopf, K.J. Larsen, M.-C. Amann, and I.T. Monroy, "High-speed 1550 nm VCSEL data transmission link employing 25 Gbaud 4-PAM modulation and hard decision forward error correction," *Journal of Lightwave Technology*, no. 99, 2012.

High-speed 1550 nm VCSEL data transmission link employing 25 Gbaud 4-PAM modulation and Hard Decision Forward Error Correction

Roberto Rodes, Michael Mueller, Bomin Li, Jose Estaran, Jesper Bevensee Jensen, Tobias Gruendl,
Markus Ortsiefer, Christian Neumeyr, Juergen Rosskopf, Knud J. Larsen, M.-C. Amann
and Idelfonso Tafur Monroy

Abstract—**Current short-range optical interconnects capacity is moving from 100 Gb/s to 400 Gb/s and beyond. Directly modulation of several laser sources is used to minimize bandwidth limitations of current optical and electrical components. Either this total capacity is provided by wavelength-division-multiplexing or parallel optics, it is important to investigate on the ultimate transmission capabilities of each laser source to facilitate current capacity standards and allow for future demands.**

High-speed 4-level pulse amplitude modulation at 25 Gbaud of a 1.5 µm VCSEL is presented in this paper. The 20 GHz 3 dB-bandwidth laser is, at the time of submission, the largest bandwidth of a 1.5 µm VCSEL ever reported. Forward error correction (FEC) is implemented to achieve transmission over 100 m virtually error-free after FEC decoding. Linerate of 100 Gb/s is achieved by emulation polarization multiplexing using 50 Gb/s signal obtained from a single VCSEL.

Index Terms—**Fiber optics communication, optical interconnects, vertical cavity surface emitting lasers, forward error correction, 4-PAM.**

I. INTRODUCTION

T HE rapid growth of Internet and cloud computing applications drives data centers to upgrade their links from the 10 Gb/s commonly used today to 100 Gb/s and beyond in the near future [1] with little or no increase in carbon and real-estate footprint [2]. These two counteracting demands lead to a quest for higher data capacity on short-range optical communication systems. Simultaneously, directly modulated (DM) vertical cavity surface emitting

lasers (VCSELs) are rapidly becoming the preferable type of laser source for these short range optical interconnect applications due to an attractive combination of attributes, including high modulation bandwidth, low drive voltage [3], and the capability of array integration [4]. Short wavelength VCSELs have demonstrated modulation speeds up to 40 Gb/s at 850 nm [5], and 44 Gb/s at 980 nm [6]. However, until lately, VCSELs with modulation speed exceeding 10-14 Gb/s have not been available at wavelengths in the O and C bands around 1300 nm and 1550 nm, respectively. Recently, direct modulation of 1550 nm VCSELs at 40 Gb/s has been demonstrated [7].

Currently, high capacity interconnects use the combination of several optical sources to satisfy higher capacity demand. Parallel optics with independent transmission channels, or wavelength-division-multiplexing (WDM) are both considered and under development.

Parallel optics transceiver modules based on VCSELs have been recently demonstrated up to 480 Gb/s [8]. The module is a single chip 90 nm CMOS integrated circuit with 24 lasers. Each of them modulated at 20 Gb/s.

The existing 100 Gb/s standard for short range interconnects (100GE-SR10) specifies the use of 10 wavelengths each operated at 10 Gb/s, while the next generation standard (100GE-SR4) specifies the employment of 4 lasers each operated at 25 Gb/s [9]. Beyond 100 Gb/s, the next OTN rate (OTU5) will most likely 400 Gb/s, where a proposed architecture is to scale the same technology of 100GE-SR4 to 400GE-SR16 for a cost effective solution [10]. This solution does not need higher bandwidth transceivers, reducing the associated cost of investment on R&D to develop new technology. However, scaling the same technology will hardly be feasible for more than 16 channels. Quadrupling the data modulation of each laser or channel to 100 Gb/s, represents a much more drastic step forward, and can potentially pave the way for a) an increase the total link capacity to 400 Gb/s or to b) a reduction in footprint and complexity of the 100 Gb/s links.

In this paper, we report on research investigation on the capabilities of using VCSELs to achieve high-speed transmission for short range optical interconnects. We have performed direct modulation of a VCSEL by employing a 4-

This article has been accepted for publication in a future issue of this journal, but has not been fully edited. Content may change prior to final publication.

> REPLACE THIS LINE WITH YOUR PAPER IDENTIFICATION NUMBER (DOUBLE-CLICK HERE TO EDIT) <   2
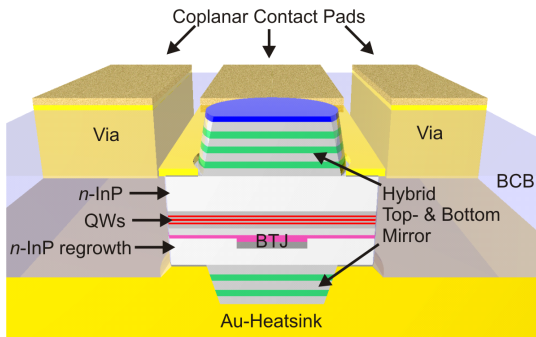
Figure 1. Short-Cavity structure of the Indium Phosphide based buried tunnel junction VCSELs

level pulse amplitude modulation (4-PAM) at 25 Gbaud. This is not a single VCSEL link, as 2 different polarizations are required. However, in the experiment we have used a single VCSEL source. The optical signal from the VCSEL was split, delayed and combined in orthogonal polarizations to emulate polarization multiplexing with a total linerate of 100 Gb/s. Forward error-correction coding has been implemented resulting in an effective bit rate of 86.5 Gb/s. Error free demodulation was demonstrated in the experiment with $1.6 \cdot 10^8$ bits of FEC decoding.

II. HIGH-SPEED VCSEL

Vertical Cavity surface emitting lasers (VCSEL) are currently attracting a lot of attention for short-range optical links due to their potential cost-effective fabrication, low power consumption, easy fiber-coupling and high-bandwidth modulation. For the 1550 nm wavelength range, Indium Phosphide based buried tunnel junction (BTJ) VCSELs implementing a novel short cavity concept have recently shown the most promising results with respect to energy-efficient high data-rate transmission [11]. The following two paragraphs shortly discuss the device concept and provide the static and dynamic features of these short-cavity (SC) VCSELs.

A. Device Structure

In order to achieve high modulation bandwidth, it is beneficial to reduce the effective cavity length and, consequentially, the photon lifetime in the VCSEL cavity [12]. Therefore, the SC-VCSEL concept implements two dielectric distributed Bragg reflectors (DBRs) featuring a short penetration depth of the optical field of only 410 nm compared to typical values of 1500 nm for commonly used epitaxial DBRs based on the AlGaInAs material system. Fig. 1 depicts an isometric view of the SC-VCSEL structure. Highly compressively strained AlGaInAs/InGaAs quantum wells yield high (differential) gain and guarantee high relaxation-resonance frequencies being essential to achieve high modulation bandwidths. Small diameter (< 30 μm) of the semiconductor mesa, reduced contact-pad areas and benzo-cyclobuthene spacer-layers allow for the reduction of parasitic
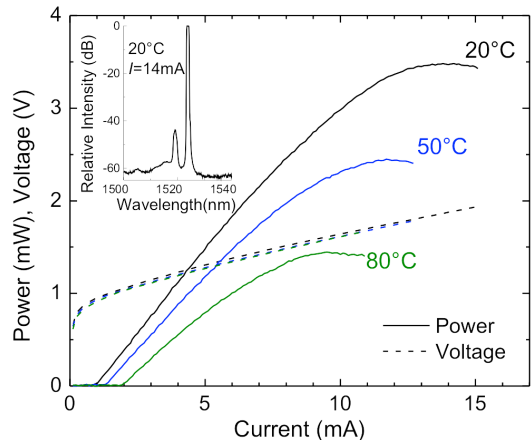

Figure 2. L-I-V curves of a 5 μm SC-VCSEL for 20, 50 and 80 degrees Celsius heat-sink temperatures

effects compromising high speed modulation. For an in detail account on the active region design and the BTJ concept, the reader is referred to [11].

B. Device Performance

Presented results correspond to a typical SC-device with a current aperture of 5 μm and an effective cavity-length of 2.5 μm. Figure 2 plots the voltage and output-power versus current for different heat-sink temperatures. Threshold currents range from 1.0 mA at 20 °C to 1.9 mA at 80 °C. Maximum output powers are above 3.5 mW and 1.4 mW at the respective temperatures. At 20 °C, the threshold-voltage is only 0.95 V, indicating a voltage drop of less than 150 mV at the hetero-barriers for photon energy of 0.8 eV. The inset of Figure 2 shows the single-mode spectrum of the same device operated at room-temperature and roll-over current. The side-mode suppression ratio (SMSR) exceeds 40 dB over the entire current and temperature range.
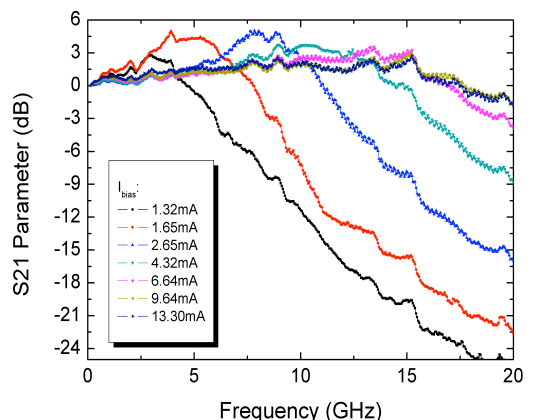

Figure 3. S21-response for a 5 μm device biased at various currents at 20°C
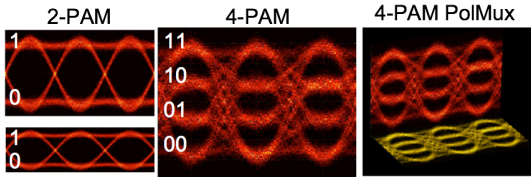
Figure 4. Eyediagrams for 2-PAM, 4-PAM and 4-PAM PolMux modulation formats

Figure 3 plots the small signal modulation response of the same 5 μm device for different bias-levels at 20 °C. Maximum modulation bandwidths exceed 20 GHz. For typical biases applied under large-signal modulation the relaxation-resonance peak is strongly damped, yielding a flat response as favored by most applications.

Rise and fall times at 20%-80% of the devices are 16 ps and 21 ps, respectively. Measured relative intensity noise is -142 dB/Hz.

III.   4-PAM PolMux

In order to investigate the ultimate capacity of a VCSEL-based link, multilevel pulse amplitude modulation (PAM) is proposed because of the combination of higher spectral efficiency compared to on-off keying (OOK), suitability for direct modulation of VCSELs with full bandwidth exploitation, and simple demodulation. 4-PAM has advantages over OOK of less sensitivity to time jitter and high-frequency noise [13]. Furthermore, two times faster frequency required on OOK usually requires more than double power consumption [13].

CMOS integrated circuits of 4-PAM drivers have been previously demonstrated. Modulation of VCSELs has been demonstrated at 10 Gb/s [14] including 2-taps feedforward equalizer with CMOS 4-PAM drivers. However, CMOS 4-PAM electrical transmitters have reached up to 32 Gb/s with an output swing of 1250 mV [15]. With research equipment, 4-PAM VCSEL modulation up to 30 Gb/s has been presented [16].

Figure 4 shows a representation of the eyediagram of a 4-PAM PolMux modulation signal used in this work. The 4-PAM signal is the result of adding up two 2-PAM signals, with double amplitude of one respect to the other. In the optical domain, two optical 4-PAM signals are combined with orthogonal polarizations in order to minimize interference on the optical transmission and allowing for independent detection.

IV.   FORWARD ERROR-CORRECTION

To compensate for transmission impairments, forward error-correction (FEC) is an efficient solution. Unfortunately this solution is also rather complex so various schemes of concatenating simple component codes have been suggested. Further the performance may be improved by iterative decoding methods. In this paper we propose two different product codes with shortened BCH (Bose-Chaudhuri-
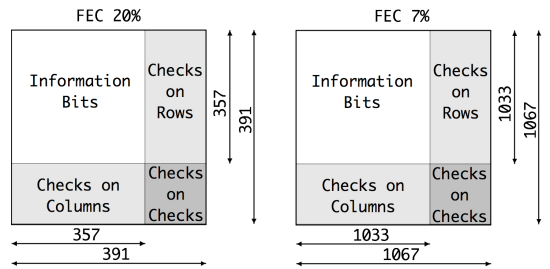

Figure 5. Product code structures. a) 20% overhead FEC. b) 7% overhead FEC

Hocqenghem) component codes and iterative decoding [17]. The resulting product codes have lengths of 1138489 bits and 152881 bits with 7% and 20% overhead, respectively. We choose hard-decision FEC since it has already proved 10 dB net coding gain, and requires less effort than soft-decision FEC for real-time implementation. Figure 5 shows the code structure for both codes used in the forward error correction. Both codes are able to correct three errors and detect error patterns of even weight, e.g. patterns with four errors. This detection is included to reduce the risk of making wrong decodings. This risk is further reduced by using BCH codes of original length $2^{11} - 1$ shortened to lengths of 391 and 1067 for the two different overhead values.

As described above, iterative decoding provides a good performance. The performance as a function of the input bit error rate may roughly be described as a section where the coding does not improve the performance and then a rather steep section – as a threshold – where the performance improves drastically down to the so-called error-floor where the performance only improves slightly. The overall performance goal for the presented system is an output bit error rate of 10^{-15} and the codes are chosen such that the error-floor may be calculated to be below this number. For a product code the threshold may be estimated by a method shown in [18] to be $4.8 \cdot 10^{-3}$ and $1.3 \cdot 10^{-2}$ (aiming at 10^{-15}) for the 7% overhead and 20% overhead codes, respectively.

The codes proposed here are much stronger than the code suggested for IEEE 802.3bj [19] with overhead 2.7%. The suggested code obtains output bit error rate of 10^{-15} at an input error rate at $4.7 \cdot 10^{-6}$.

V.   EXPERIMENTAL DEMONSTRATION

In the section we describe the setup of our experiment to assess the performance of a 100 Gb/s transmission by modulating the VCSEL described in Section II, with the modulation format of Section III and applying the terror correction explain in Section IV. Figure 6 shows the setup of the transmission experiment. The link is analyzed with pseudorandom binary sequences (PRBS) and with both forward error correction (FEC) patterns described in Section IV. The PRBS sequence has a pattern length of $2^{11} - 1$. Two uncorrelated 25 Gb/s subrate channels of an SHF 12103 A
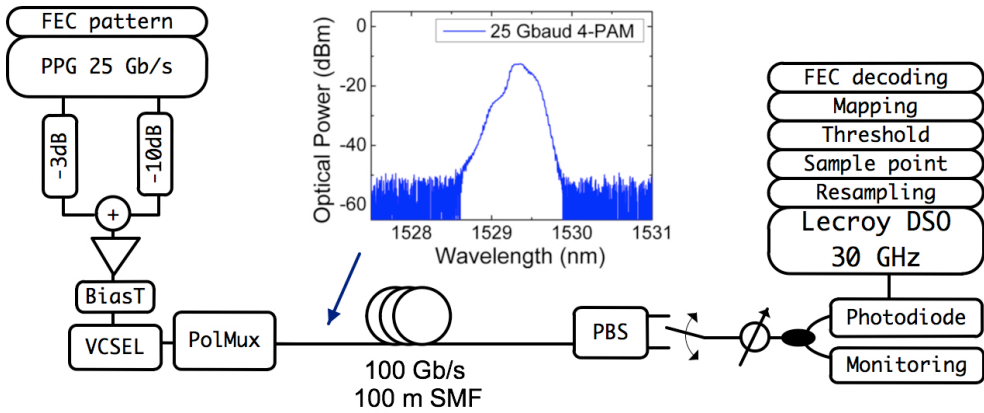
Figure 6. Experimental setup. Forward error correction (FEC), pulse pattern generator (PPG), single mode fiber (SMF), polarization beam splitter (PBS), digital storage oscilloscope (DSO)

pulse pattern generator (PPG) are added to form a 50 Gb/s 4-PAM signal. The subchannel addition system is optimized to reduce reflections and improve quality of the electrical signal into the VCSEL. It is composed of a 10 dB and a 3 dB electrical attenuator, and a 6 dB electrical combiner. A high-linearity amplifier from SHF is used to amplify the electrical signal to utilize the linear region of the VCSEL I-P characteristic curve shown in Figure 2. Time jitter of the electrical signal at the input of the VCSEL is 19 ps. The optimum bias point of the VCSEL was found to be 10 mA, with a driving voltage of 1 V peak-to-peak. No optical isolator is used on the VCSEL. The optical signal from the VCSEL is launched into a polarization multiplexing (PolMux) system with an optical delay between branches to emulate orthogonal polarization transmission uncorrelated at 100 Gb/s. Polarizations are controlled on the PolMux system to match polarizations of the receiver. The insertion loss of the PolMux system is 5 dB.

The signal is transmitted over 100 m of standard single mode fiber (SMF-28). On the receiver side, a polarization

beam splitter (PBS) separates the two polarizations. The transmission path loss and receiver PBS is 1 dB. Each polarization is detected independently by a 40 GHz
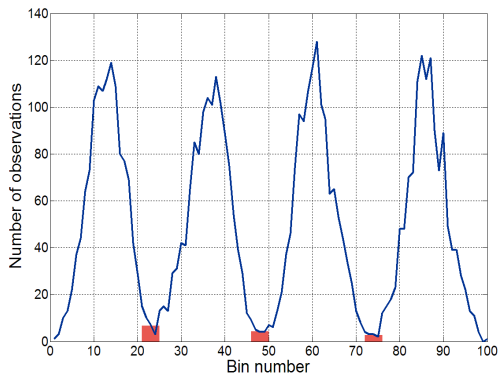

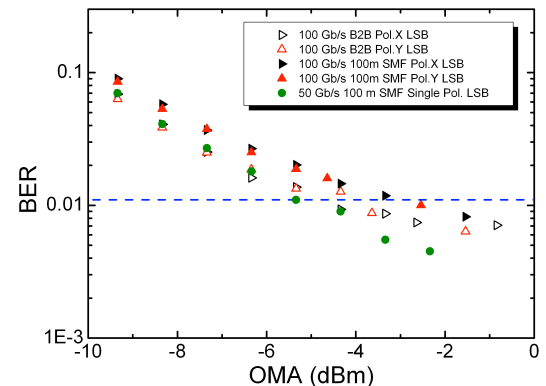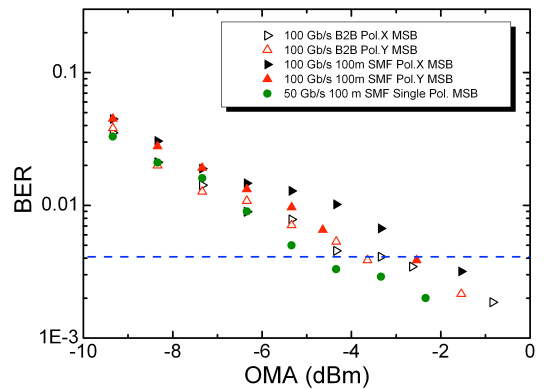Figure 7. Histogram in demodulation

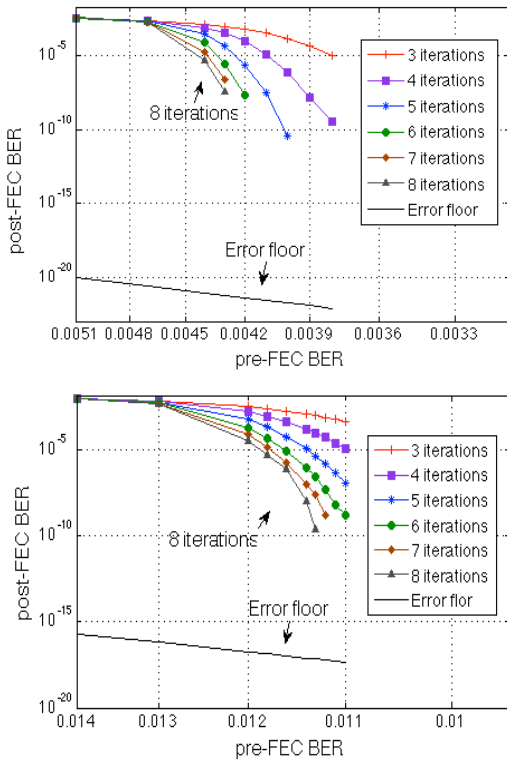Figure 8. a) BER curves for MSB, b) BER curves for LSB

Figure 9. BER curve simulation. a) 7% overhead FEC, b) 20% overhead FEC

photodiode. A Lecroy 30 GHz, 80 Gsa/s digital storage oscilloscope (DSO) is used to store the received signal for offline demodulation. The offline signal demodulation includes bit synchronization and adaptive decision threshold gating. Afterwards, the offline forward error correction decoding is performed. The implementation of the decoder is discussed in [17].

VI. RESULTS

Digital upsampling of the signal to an oversampling factor of 10 has been used for better demodulation. Demodulation is done in blocks of 5000 bits, with clock recovery and decision thresholds update every block. Figure 7 shows the histogram of one block at the optimum sample point of the received signal. The minimums of the histogram are taken as the symbol decision thresholds. The least significant bit (LSB) and most significant bit (MSB) of each symbol are two uncorrelated patterns. After demodulation, error counting of the received LSB and MSB is done independently comparing each bit-stream with the corresponding pattern.

Figure 8.a shows the bit error rate (BER) curve for the MSB after 100 m and with back-to-back (B2B) configuration respect to the received optical modulation amplitude (OMA). Figure 8.b shows the BER curves for the LSB. We can observe worst performance in the LSB as it was expected due

to its higher error probability on the symbol. We have used Gray mapping to facilitate error correction. BER curves for the single polarization transmission are also included in Figure 8.a and 8.b. Penalty of 1 dB on received OMA sensitivity is appreciated compared to dual polarization transmission.

Section IV presents $4.8 \cdot 10^{-3}$ and $1.3 \cdot 10^{-2}$ as theoretical pre-FEC limit for the 7% overhead and 20% overhead codes, respectively. However, since the decoding of a BCH code sometimes results in a wrong codeword, the theoretical pre-FEC thresholds increase in real implementations. In order to estimate the real pre-FEC error, a simulation of the actual decoding is shown in Figure 9. Simulating down to 10^{-15} is impossible due to time reasons, but the curves seem to indicate that thresholds of approximately $4.1 \cdot 10^{-3}$ and $1.1 \cdot 10^{-2}$, respectively, are achievable. Figure 8.a and 8.b are plotted with the estimated real pre-FEC limit. The 7% overhead FEC is applied to the MSB and the 20% overhead FEC is applied to the LSB based on the BER results returned from PRBS sequence tests. Figure 8.a and 8.b show with a blue line the FEC thresholds for 7% and 20%, respectively. Transmissions below the threshold can be decoded to an output bit error rate of less than 10^{-15}. By applying different FEC codes to the LSB and the MSB, the received OMA sensitivities for error free demodulation coincide. We processed $1.6 \cdot 10^8$ bits for the FEC decoding for both channels and got an error free sequence after the offline demodulation and FEC decoding at −2 dBm received OMA sensitivity. The FEC adapted in this way maximizes the effective bitrate for error free demodulation. The 7% and 20% overhead of the MSB and the LSM, respectively, result in a total effective bitrate of 86.5 Gb/s. Due to the limited number of FEC frames we can save on the DSO, we theoretically calculated the error probability in a longer sequence. Based on the theory in [20], as we had zero errors in the experiment after several FEC decoding iterations, we have, with 95% confidence, that the BER of less than $3 \cdot 10^{-7}$ is expected in repeated experiments. Since the error floor is less than 10^{-15} the possible error rate is expected to be smaller especially if more iterations are used and thus a virtually error free demodulation is still expected in a longer time measurement.

VII. CONCLUSIONS

High capacity VCSEL transmission has been investigated with multilevel pulse amplitude modulation at 50 Gbps with a total linerate of 100 Gb/s by emulating polarization multiplexing over 100 m SMF.

Error free demodulation of $1.6 \cdot 10^8$ bits was achieved after forward error-correction with an effective bitrate of 86.5 Gb/s.

The system reduces to number of channels needed to reach an aggregated capacity by increasing bandwidth efficiency and including error correction capability. Scaling by 4 the proposed system, by either spatial or wavelength multiplexing, could be a candidate solution to provide future standards capacity of 400 Gb/s.

Future work will experimentally scale the system with independent sources for orthogonal polarization and channel multiplexing; extend the fiber transmission length and

evaluate dispersion effect; perform reliability test of the VCSEL. Moreover, different combinations of FEC codes could be investigated in order to determine an optimum balance between effective bitrate, computation processing, overhead and latency.

REFERENCES

[1] H. Liu, C.F. Lam, C. Johnson, "Scaling Optical Interconnects in Datacenter Networks Opportunities and Challenges for WDM," *High Performance Interconnects (HOTI), 2010 IEEE 18th Annual Symposium on* , vol., no., pp.113-116, 18-20 Aug. 2010.

[2] "Strategies for Solving the Datacenter Space, Power, and Cooling Crunch: Sun Server and Storage Optimization Techniques". Oracle White paper, March 2010.

[3] P. Moser, W. Hofmann, P. Wolf, G. Fiol, J.A. Lott, N.N. Ledentsov, D. Bimberg, "83 fJ/bit energy-to-data ratio of 850-nm VCSEL at 17 Gb/s," *Optical Communication (ECOC), 2011 37th European Conference and Exhibition on* , vol., no., pp.1-3, 18-22 Sept. 2011

[4] W. Hofmann, M. Gorblich, G. Bohm, M. Ortsiefer, L. Xie, M.-C. Amann, "Long-wavelength 2-D VCSEL arrays for optical interconnects," Lasers and Electro-Optics, 2008 and 2008 Conference on Quantum Electronics and Laser Science. CLEO/QELS 2008. Conference on , vol., no., pp.1-2, 4-9 May 2008

[5] P. Westbergh, J.S. Gustavsson, B. Kögel, A. Haglund, A. Larsson, A. Mutig, A. Nadtochiy, D. Bimberg, A. Joel, "40 Gbit/s error-free operation of oxide-confined 850 nm VCSEL," *Electronics Letters* , vol.46, no.14, pp.1014-1016, July 2010

[6] W. Hofmann, P. Moser, P. Wolf, A. Mutig, M. Kroh, D. Bimberg, "44 Gb/s VCSEL for optical interconnects," *Optical Fiber Communication Conference and Exposition (OFC/NFOEC), 2011 and the National Fiber Optic Engineers Conference*, vol., no., pp.1-3, 6-10 March 2011

[7] W. Hofmann, M. Müller, P. Wolf, A. Mutig, T Gründl, G Böhm, D. Bimberg, M.-C. Amann, , "40 Gbit/s modulation of 1550 nm VCSEL," *Electronics Letters* , vol.47, no.4, pp.270-271, February 17 2011

[8] F.E. Doany, B.G. Lee, A.V. Rylyakov, D.M. Kuchta, C. Baks, C. Jahnes, F. Libsch, C.L. Schow, "Terabit/sec VCSEL-based parallel optical module based on holey CMOS transceiver IC," Optical Fiber Communication Conference and Exposition (OFC/NFOEC), 2012 and the National Fiber Optic Engineers Conference , vol., no., pp.1-3, 4-8 March 2012.

[9] C. Cole "Next generation 100G client optics," Optical Communication (ECOC), 2011 37th European Conference and Exhibition on , workshop 13, 18-22 Sept. 2011.

[10] C, Cole, "Beyond 100G client optics," Communications Magazine, IEEE , vol.50, no.2, pp. 58- 66, February 2012.

[11] M. Mueller, W. Hofmann, T. Grundl, M. Horn, P. Wolf, R.D. Nagel, E. Ronneberg, G. Bohm, D. Bimberg, M.-C. Amann, "1550nm High-Speed Short-Cavity VCSELs," IEEE Journal of Selected Topics in Quantum Electronics, vol. 17, no. 5, pp. 1158-1166, Sept./Oct. 2011.

[12] P. Westbergh, J.S. Gustavsson, B. Kogel, A. Haglund, A. Larsson, "Impact of photon lifetime on High-Speed VCSEL performance", IEEE Journal of Selected Topics in Quantum Electronics, vol. 17, no. 6, pp. 1603-1613, Sept./Oct. 2011.

[13] A. Ran, IEEE P802.3bj 100 Gb/s Backplane and Copper Cable Task Force 14 January 2012.

[14] D. Watanabe, A. Ono, T. Okayasu, "CMOS optical 4-PAM VCSEL driver with modal-dispersion equalizer for 10Gb/s 500m MMF transmission," Solid-State Circuits Conference - Digest of Technical Papers, 2009. ISSCC 2009. IEEE International , vol., no., pp.106-107,107a, 8-12 Feb. 2009.

[15] H. Cheng, A.C. Carusone, "A 32/16 Gb/s 4/2-PAM transmitter with PWM pre-Emphasis and 1.2 Vpp per side output swing in 0.13-μm CMOS," *Custom Integrated Circuits Conference, 2008. CICC 2008. IEEE* , vol., no., pp.635-638, 21-24 Sept. 2008.

[16] K. Szczerba, P. Westbergh, J. Gustavsson, A. Haglund, J. Karout, M. Karlsson, P. Andrekson, E. Agrell, A. Larsson, "30 Gbps 4-PAM transmission over 200m of MMF using an 850 nm VCSEL," *Optical Communication* (ECOC), 2011 37th European Conference and Exhibition on , vol., no., pp.1-3, 18-22 Sept. 2011.

[17] B. Li, K. J. Larsen, D. Zibar and I. Tafur Monroy, "Over 10 dB Net Coding Gain Based on 20% Overhead Hard Decision Forward Error Correction in 100G Optical Communication Systems," in Proc. 37th European Conf. and Exhibition on Optical Communication, Geneva, 2011.

[18] J. Justesen, "Performance of Product Codes and Related Structures with Iterated Decoding", IEEE Trans. Commun. 59, 2, 407-415 (2011).

[19] S. Bates, M. Brown, R. Cideciyan, M. Gustlin, A. Healey, M. Langhammer, J. Slavick, and Z. Wang, "Backplne NRZ FEC Baseline Proposal", http://www.ieee802.org/3/bj/public/mar12/gustlin_01_0312, March 2012.

[20] J. L. Massey, "Comparison of Rate One-Half, Equivalent Constraint Length 24, Binary Convolutional Codes for Use with Sequential Decoding on the Deep-Space Channel", Technical Report No. EE-762, University of Notre Dame, Indiana 46556, USA, 1976.

Roberto Rodes was born in Zaragoza, Spain, in 1984. He received his Electrical Engineering MSc in 2010 from the Technical University of Denmark. Since March 2010, he is working on his PhD at the Fotonik department of the Technical University of Denmark, within the metro-access and short range communication systems group. He has been a visitor researcher at U.C Berkeley in the Optoelectronics Research group of Prof. Chang-Hasnain. His research includes advanced modulation of VCSELs and coherent detection using VCSELs. He is currently also involved in the European FP7 GigaWaM project.

Michael Müller was born in Donauwörth, Germany, in 1981. He received his Dipl. Phys. degree in semiconductor physics and nanotechnology from the Ludwig Maximilians Universität München, Germany in 2007. Since then, he is working on his PhD at the Walter Schottky Insitut at the Technische Universität München, where he is engaged in the research on InP-based high-speed vertical-cavity surface-emitting lasers (VCSELs) including their design, manufacturing and characterization. Recently, he received a DAAD-scholarship for his work on "VCSELs for future IPTV services". Currently, he is engaged in the development of high-speed VCSEL arrays for next generation optical interconnects within the realm of European FP7 MIRAGE project. He has authored and co-authored some 40 articles in leading scientific journals and conference proceedings including 7 invited papers and talks. Michael Müller is a member of the Deutsche Physikalische Gesellschaft and the IEEE Photonics Society.

Bomin Li received the M.Sc. degree in Telecommunications from the Department of Photonics Engineering of Technical University of Denmark, Lyngby, Denmark, in 2009, where she is currently working toward the Ph.D. degree. Her research interests include code investigation and performance evaluation of forward error correction for high speed optical communications.

Jose Estaran was born in Zaragoza, Spain, in 1987. He completed his MSc in Telecommunications from Universidad de Zaragoza, Zaragoza, Spain in 2012 and the Electrical Engineering MSc from the Technical University of Denmark, Kongens Lyngby, Denmark in 2012, where he has recently been accepted for a Ph.D. position in the Photonics Department within The Villum Foundation´s Young Investigator Programme. His research interests are near-capacity modulation formats, advanced modulation of VCSELs and multi-channel transmission systems.

Jesper Bevensee Jensen is Assistant Professor in the Metro-access and Short Range Communications Group Department of Photonics Engineering at the Technical University of Denmark, from which he received his PhD in 2008. He has worked as a Postdoc on photonic wireless convergence in home and access networks within the European project ICT-Alpha. He is the coauthor of more than 70 journal and conference papers on optical communication technologies. His research interests include advanced modulation formats, access and in-home network technologies, multicore fiber transmission,

This article has been accepted for publication in a future issue of this journal, but has not been fully edited. Content may change prior to final publication.

> REPLACE THIS LINE WITH YOUR PAPER IDENTIFICATION NUMBER (DOUBLE-CLICK HERE TO EDIT) <   7

advanced modulation of VCSELs, coherent detection using VCSELs, and photonic wireless integration.

Tobias Gruendl. Not available at the time of submission

Dr. Markus Ortsiefer received the university degree in physics in 1997 and the doctoral degree in 2001, both from the Technical University of Munich. During his PhD work he was working on InP-based lasers and related materials. He is co-founder of VERTILAS where he was managing director from 2001 to 2003. Since 2003, he holds the position of the CTO and is responsible for the company's production and research activities. Markus Ortsiefer is member of the German Physical Society and has authored or co-authored more than 130 publications in scientific journals, conference proceedings and books and filed several patents on optoelectronic devices.

Christian Neumeyr has over 20 years experience in the semiconductor and optoelectronics industry with over 14 years focusing on communications applications. He holds a university degree in electrical engineering and an M.B.A. He had held executive positions at a number of leading and innovative technology companies incl. Marketing Director at Infineon, Vice President at Multilink Technology, Director Business Line at Broadcom. In 2006 Mr. Neumeyr has been appointed CEO at VERTILAS. He took on several international assignments where he developed a network of contacts in various business fields. His professional accomplishments include establishing and managing fast-growing and profitable business lines and expanding businesses into new markets.

Juergen Rosskopf. Not available at the time of submission.

Knud J. Larsen received his M.S.E.E. and Ph.D. degrees from the Technical University of Denmark, Kgs. Lyngby. He was at Ericsson Signal Systems as a senior engineer and project manager involved in design and implementation of communication systems and traffic control systems. Since 1986 he has been a professor at the Technical University of Denmark (previously the Institute of Telecommunication, now the Department of Photonics), teaching and doing research in communication theory and coding. He has worked extensively on studies of error correction for the European Space Agency and is now involved in projects related to optical transmission. Together with four colleagues he received the 1991 Information Theory Society Paper Award for a paper on algebraic geometry codes.

M.-C. Amann. Not available at the time of submission

Idelfonso Tafur Monroy is currently Professor and head of the metro-access and short range communications group of the Department of Photonics Engineering at the Technical University of Denmark. He graduated from the Bonch-Bruevitch Institute of Communications, St. Petersburg, Russia, in 1992, where he received a M.Sc. degree in multichannel telecommunications. In 1996 he received a Technology Licenciate degree in telecommunications theory from the Royal Institute of Technology, Stockholm, Sweden. The same year he joined the Electrical Engineering Department of the Eindhoven University of Technology, The Netherlands, where he earned a Ph.D. degree in 1999 and worked as an assistant professor until 2006. He has participated in several European research framework projects in photonic technologies and their applications to communication systems and networks. At the moment he is involved in the ICT European projects GigaWaM and EURO-FOS and is the technical coordinator of the ICT-CHRON project. His research interests are in hybrid optical-wireless communication systems, high-capacity optical fiber communications, digital signal processing for optical transceivers for baseband and radio-over-fiber links, application of nanophotonic technologies in the metropolitan and access segments of optical networks as well as in short range optical-wireless communication links.

Paper 9: Quad 14Gbps L-Band VCSEL-based system for WDM migration of 4-lanes 56 Gbps optical data links

J. Estaran, **R. Rodes**, T.-T. Pham, M. Ortsiefer, C. Neumeyr, J. Rosskopf, and I.T. Monroy, "Quad 14Gbps L-Band VCSEL-based system for WDM migration of 4-lanes 56 Gbps optical data links," *Optics Express*, 2012.

Quad 14 Gbps L-band VCSEL-based system for WDM migration of 4-lanes 56 Gbps optical data links

Jose Estaran,[1,*] Roberto Rodes,[1] Tien Thang Pham,[1] Markus Ortsiefer,[2] Christian Neumeyr,[2] Jürgen Rosskopf,[2] and Idelfonso Tafur Monroy[1]

[1]*DTU Fotonik, Department of Photonics Engineering, Technical University of Denmark, DK2800 Kgs. Lyngby, Denmark*
[2]*VERTILAS GmbH, Lichtenbergstr. 8, D-85748 Garching, Germany*
*jome@fotonik.dtu.dk

Abstract: We report on migrating multiple-lane link into an L-band VCSEL-based WDM system. Experimental validation achieves successful transmission over 10 km of SMF at 4x14Gbps. Inter-channel crosstalk penalty is observed to be less than 0.5 dB and a transmission penalty around 1 dB. The power budget margin ranges within 6 dB and 7 dB.

OCIS codes: (060.0060) Fiber optics and optical communications. (200.4650) Optical interconnects.

References and links

1. H. Liu, C. F. Lam, and C. Johnson, "Scaling optical interconnects in datacenter networks opportunities and challenges for WDM," in *Proceedings of the 18th Annual Symposium on High Performance Interconnects*, 2010, 113 – 116.
2. A. Vahdat, H. Liu, X. Zhao, and C. Johnson, "The emerging optical data center" in *Proceedings of OFC/NOEFC '11*, Los Angeles Convention Center, Los Angeles, CA, 2011, OTuH2.
3. C. Kachris, and I. Tomkos, "Power consumption evaluation of hybrid WDM PON networks for data centers," in *Proceedings of the 16th European Conference on Networks and Optical Communication (NOC)*, 2011, 118 – 121.
4. DatacenterDynamics (DCD) white paper, "The 2011 census," (DCD Industry CENSUS, 2011).
5. InfiniBand™ Trade Association 2012. http://www.infinibandta.org/index.php.
6. Fiber Channel Industry Association 2012.http://www.fibrechannel.org/roadmaps.
7. H. S. Hamza, and J. S. Deogun, "WDM optical interconnects: a balanced design approach," IEEE/ACM Trans. Netw. **15**(6), 1565 – 1578 (2007)
8. J. Cheng, "Topics in VCSEL-based high-speed WDM optical interconnects," in *IEEE Avionics, Fiber-Optics and Photonics Technology Conference*, 2008, 65-66.
9. M. Haurylau, G. Chen, H. Chen, J. Zhang, N. A. Nelson, D. H. Albonesi, E.G. Friedman, and P. M. Fauchet, "On-chip optical interconnect roadmap: challenges and critical directions," IEEE J. Sel. Topics Quantum Electron. **12**(6), 1699-1705 (2006).
10. R. Rodes, J. Estaran, B. Li, M. Mueller, J. B. Jensen, T. Gründl, M. Ortsiefer, C. Neumeyr, J. Rosskopf, K. J. Larsen, M. Amann, and I. Tafur Monroy, "100 Gb/s single VCSEL data transmission link," in *OFC/NOEFC'12*, OSA Technical Digest (Optical Society of America, 2012), paper PDP5D.10.
11. L. Chrostowski, C.-H. Chang, R. Stone, and C. J. Chang-Hasnain, "Demonstration of long-wavelength directly modulated VCSEL transmission using SOAs," IEEE Photon. Technol. Lett. **14**(9), 1369-1371 (2002).
12. R. J. Stone, R. F. Nabiev, J. Boucart, W. Yuen, P. Kner, G. S. Li, R. Carico, L. Scheffel, M. Jansen, D. P. Worland, and C. J. Chang-Hasnain, "50 km error-free 10 Gbit/s WDM transmission using directly modulated long-wavelength VCSELs," Electron. Lett. **36**(21), 1793-1794 (2000).
13. FP7 European project GigaWam, "Next-generation WDM-PON enabling gigabit per-user data bandwidth". http://www.gigawam.org/.
14. J. C. Charlier, and S. Krüger, "Long-wavelength VCSELs ready to benefit 40/100-GbE modules," Lightwave®, 2012.http://www.lightwaveonline.com/articles/print/volume-28/issue-6/technology/long-wavelength-vcsel-technology-improves.html.
15. A. Ran, IEEE P802.3bj 100 Gb/s Backplane and Copper Cable TaskForce 14 January 2012.

16. F. Chang, K. Onohara, and T. Mizuochi, "Forward error correction for 100 G transport networks," IEEE Commun. Mag. **48**(3), S48-S55 (2010).

1. Introduction

Over the past few years, the quick proliferation of Internet use and cloud computing applications has substantially increased the bandwidth needs not only in backbones but prominently in data processing centers (DPCs) [1]. Albeit great part of the traffic will continue to flow between end-users and such computer centers, an increasing fraction is flowing within the DPCs themselves [2, 3]. This situation has triggered a worldwide investment to upgrade the existing facilities or building new ones in order to cope with the growing bandwidth demand that has been estimated to reach $35BN in 2012 [4]. Accordingly, the major networking technologies for the interconnection of peripherals and data storage keep on releasing roadmaps and future milestones that clearly exceed the 10Gbps barrier, and therefore recently solutions such as fourteen data rate (FDR) of InfiniBand technology [5] or 16GFC of Fiber Channel [6] have been proposed. However, the need to scale to higher and bidirectional transmission capacities (bandwidth milestones reaching 300Gbps by 2013) [5] is also accompanied by the demand to secure high density, low cost, efficiency and reliability.
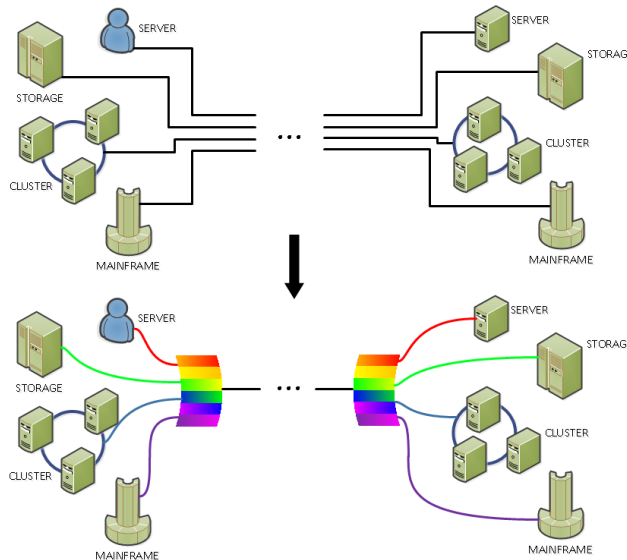

Fig. 1. Datacenter & Storage network topology migration. Multilane/multilink physical point-to-point (P2P) connections (top). L-band VCSEL-based WDM system (bottom).

In this context, wavelength division multiplexing (WDM) techniques in combination with compact integration of light sources and detectors, is an interesting technology candidate for delivering scalable and flexible optical data links with low power consumption, high data throughput, longer transmission distance, and the cost effectiveness needed to efficiently cope with present and future stringent bandwidth requirements in data centers [1, 7-9].

In concordance, regarding light sources, VCSELs offer an attractive combination of high bit rates, low power consumption and array integration that along with their tuning capabilities make them perfectly suitable for compact and wideband optical interconnects [8,10].

Long-wavelength technology is relatively new in vertical-cavity surface-emitting lasers (VCSELs). Some investigations [11, 12] have demonstrated the feasibility of long-reach WDM transmissions at 2.5 Gbps, where L-band is especially suitable due to the lower impact of four-wave mixing (FWM) and the possibility of seizing upon distributed Raman amplification. Some other ongoing investigations are using L-band VCSELs as downstream (OLT to ONU) in a WDM-PON system as the new future proof FTTH technology [13].

In this paper we look into high-speed, cost-efficient and power-efficient VCSEL-based WDM system oriented towards short-range optical fiber connectivity. Four L-band VCSELs are directly modulated with quaternary pulse amplitude modulation (4-PAM) signal at 7 Gbauds to generate a total data nominal rate of 56 Gbps. The multilevel signal has been chosen because of its spectral efficiency,. The 4 lanes are launched into a 50 GHz spaced WDM system. Bit-error rate (BER), crosstalk penalty, transmission penalty and power margin are measured for one of the middle carriers.

The paper is organized as follows. In section 2, a description of the VCSEL used for signal modulation is presented. In section 3, the experimental setup is shown and described. In section 4, details about the digital signal processing (DSP) are provided. Finally, in section 5 the main results and findings are presented .

2. Long-wavelength VCSELs

Historically, VCSELs for longer wavelengths of 1300 to 1700 nm have been difficult to produce because of the refractive index of InGaAsP. But in the early 2000s, development of different combinations of III-V elements led to more practical long-wavelength VCSELs [14]. In general, VCSELs are rapidly becoming the preferable light source for interconnect applications owed to an interesting combination of high modulation bandwidth, low power consumption and reduced manufacturing cost [10]. Besides, their 2-D array integrability, their tuning capabilities and the light coupling ease due to its circular beam, make them perfectly suitable for WDM systems. The following section provides the reader with relevant data about the main characteristics of the device focusing on tunability and temperature considerations.
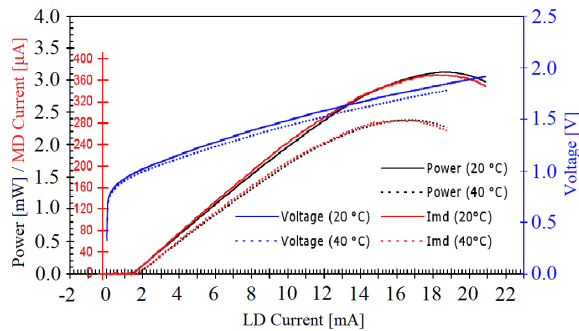

Fig. 2. L-I-V curve of VCSEL#3 and monitor diode (MD) current.

The L-band VCSELs used for the experiments performed in this paper range between 1577 nm and 1583 nm. Such devices exhibit the following measured characteristics: maximum output power around 3 mW and a 3-dB modulation bandwidth of 10 GHz at 20°C. The lasers show fast rise and fall times, low threshold voltage (1.5 mA – 2 mA) with a maximum

operating rating around 19 mA, excellent side mode suppression ratio (SMSR) performance and extremely low power dissipation. Figure 2 depicts the L-I-V curve of the VCSEL#3. For its part, VCSELs' tunability depends mainly on bias current and temperature. Table 1. presents concrete measured values about the lasers' tuning ranges at 20°C and 40°C. Figure 3 shows the graphical trend of the emitted wavelength variation with respect to the bias current and temperature for VCSEL#2 (1580.66 nm).
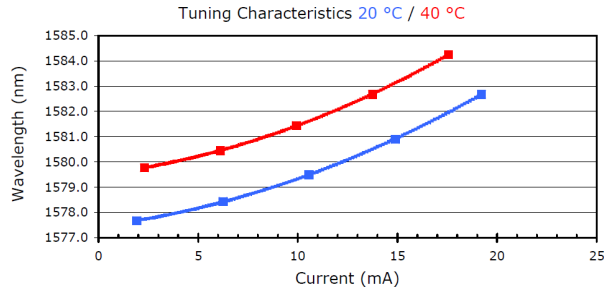

Fig. 3. Tuning characteristics with respect to bias current and temperature of VCSEL#2.

VCSELs are much more sensitive to bias currents concerning wavelength tunability than to temperature. Besides, changing temperature is a slow process, more complicated to control and considerably more power consuming. Thereby, the experiment was conducted inside an isolated room at ambience temperature and the measurements were taken after some stabilization minutes. The impact of the little temperature drifts were corrected through slight variations of the bias currents that never exceeded ±0.5 mA max. An example of eye diagram correction through bias current is shown in Fig. 4.

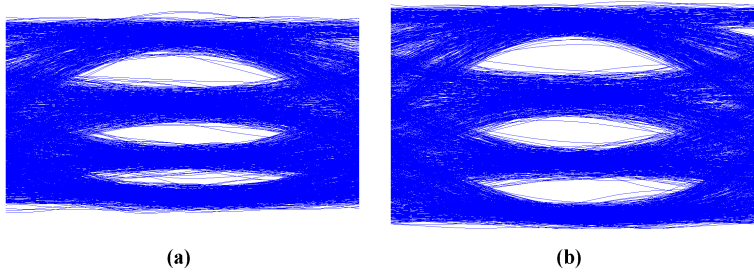**(a)**   **(b)**

Fig. 4 Illustration of a normalized digital eye diagram before bias current correction (a) and after bias current correction (b).

Table 1. Bias current and their corresponding wavelength interval delimiters for each VCSEL.

	20°C		40°C	
	Bias Current (mA)	Wavelength (nm)	Bias Current (mA)	Wavelength (nm)
VCSEL#1	6.82 / 15.51	1577.87 / 1580.37	6.75 / 14.32	1579.91 / 1582.13
VCSEL#2	6.25 / 14.89	1578.44 / 1580.90	6.12 / 13.75	1580.45 / 1581.44
VCSEL#3	6.23 / 14.48	1579.24 / 1581.90	6.08 / 13.10	1581.24 / 1583.50
VCSEL#4	6.86 / 14.53	1579.97 / 1582.57	6.98 / 13.40	1582.09 / 1584.31

3. Experimental setup

The experimental set-up is presented in Fig. 5. The pulse pattern generator (PPG) is used to generate two pseudorandom binary sequences (PRBS) NRZ streams of length 2^{15}-1 at 7 Gbps. The 4-PAM electrical signal is generated in the following way: Firstly, the two NRZ streams are passed through 10 dB and 3 dB attenuators respectively in order to reduce reflections and allow us to track the amplitudes while still keeping the convenient proportion for creating the multilevel signal. Time decorrelation matching is adjusted with a mechanical delay-line inserted into the higher power branch. Subsequently, the binary sequences are added up through a 6dB power combiner to make the 14 Gbps 4-PAM signal shown in Fig. 6. The 4-PAM signal is replicated by four with a 10 GHz active RF splitter. The peak-to-peak voltage after amplification is set to 0.6 V for all the outputs and the time decorrelation between each of them is perform with internal and pre-configured delay lines. The offset of the input signal is tuned to locate the dynamic range well within the most linear range of the internal amplifier.
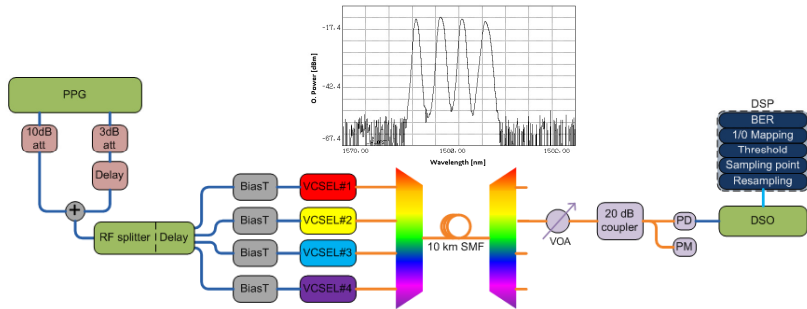
Fig. 5. Experimental setup. Pulse pattern generator (PPG), array waveguide grating (AWG), single mode fiber (SMF), digital storage oscilloscope (DSO), digital signal processing (DSP).

The four outputs of the splitter are driven into the L-band VCSELs. Bias-Ts and evaluation boards are used with an initial bias current of 10.5 mA. The cathode, anode and reference pin of the VCSELs were trimmed off to avoid interferences. Later on, they were appropriately welded to flexible flaps that were connected to the evaluation boards. In order to improve light coupling, four high-precision alignment stations were utilized to approach four independent cleaved fibers to the lasers' aperture. Backwards reflections were drastically reduced by adding index-matching oil to the fibers' end tips. The approaching process was controlled with one microscope and one optical power meter.
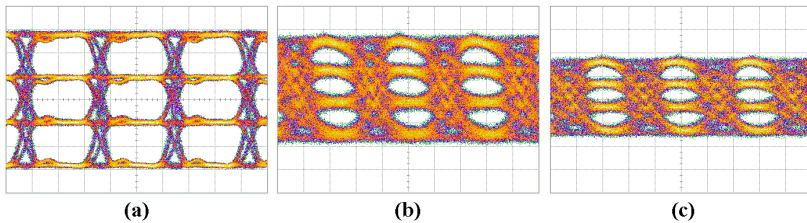

(a)   (b)   (c)

Fig. 6. Electrical 4-PAM signal (a). Optical 4-PAM signal after the VCSEL (b). Electrical 4-PAM after the photodiode (c).

At the optimum light coupling, the lasers showed ~2.5dBm output power for the initial bias current. In this stage the 4-PAM signals were injected (see Fig. 6.). The combined optical spectrum after the first AWG was analyzed. The pre-established 10.5 mA bias currents were tuned independently for each laser to make their output wavelengths match the 50 GHz-spaced AWG's channels. The center wavelengths are 1580.24 nm, 1580.66 nm, 1581.03 nm and 1581.43 nm. Z-axis alignment was modified to create the flat optical spectrum shown in Fig. 5. Minor changes in the bias currents and modulation amplitudes are performed at this stage in order to optimize the individual eye diagrams.

The WDM signal is propagated over a 10 km-long pool of SSMF and demultiplexed with another AWG. At the receiver side, the channel 1580.66 nm is measured. A variable attenuator, a 20dB coupler and an optical power meter are used to control and monitor the incoming optical power. One high-sensitivity PIN photodiode with integrated GaAs preamplifier and 10GHz of 3-dB bandwidth is used to detect the signal. Finally, a 13 GHz digital storage oscilloscope (DSO) at 40 GS/s is used to store the signal for offline processing.

4. Digital signal processing (DSP)

Quaternary pulse amplitude modulation (4-PAM) is used to achieve 14 Gbps (7 Gbauds) due to the spectral efficiency of 2 bit/s/Hz.. Besides, doubling the modulation frequency in OOK requires more than double power consumption [15]. This section shortly develops on the offline demodulation stages of the 4-PAM signal and the enhancement features of the code to attain improved BER results.

4.1 General BER calculation
For each power level, 10 frames in chunks of 2^{15}-1 symbols (327670 symbols) are evaluated. Two samples were stored for each power level so that the final BER results are averaged. After storing the signal with the DSO, a ~3-fold up-sampling is performed. This makes around 20 samples per symbol hence allowing the correction of the eye diagram's tilt and facilitating the optimum sampling point calculation. After resampling, reshaping is performed for each of the chunks in order to create a matrix of dimensions 20x327670. This allows us to overlap all the symbols (see Fig. 4.) to calculate the 2-D variance and thereby the optimum sampling point of the combined shapeform.

The histograms for all of the chunks are calculated at the optimum sampling point with 60 bins each. By detecting the bin numbers with the lowest number of observations between peaks, the amplitude thresholds are located. The noise distribution is not taken into account. Once the optimum sampling points are determined, the 1/0 mapping is performed, giving 2 bits for every symbol analyzed (4-PAM). Finally, the BER is calculated by comparing the binary sequences obtained for the least significant bit (LSB) and most significant bit (MSB) with the circularly shifted PRBS used in the signal generation. The exact offset for each bit is calculated by performing x-correlation. When error counting yielded error free transmission, Gaussian fitting and estimated BER was applied. However, its utilization was exclusively necessary to confirm the absence of error floors when the 4 channels were transmitting.

4.2 Enhanced features
Some further advanced signal processing was implemented to improve the BER results. Here we briefly describe three of them. Desynchronization between DSO and our signal, eye diagram tilt correction and Gray coding emulation.

The effect of the desynchronization between the DSO and the signal is a relative displacement of the optimum sampling point with respect to the observation window. If this effect was not taken into consideration, a symbol was counted twice every certain amount of samples. This changes the PRBS offset and consequently increases the BER given that the displacement is only calculated in the very first iteration to reduce the computation time. In order to correct for this, the chunks were in turn subdivided into smaller pieces of around

5000 symbols and the displacement of the sampling point could be tracked with enough precision. When the error occurred, the repeated symbol was automatically deleted and the process continued.

The correction of the eye diagram's tilt literally straightens the eye diagram so that those points with higher variance in every level are put in a common sampling point for the four levels instead of calculating the optimum compromise. An example of this can be observed in Fig. 6. by comparing signal out of the VCSEL and the digitalized one.

Gray coding emulation can be performed when the PRBS is known as well as the relative sequence offset of the LSB with respect to the MSB. In such case, by performing a logical XOR between the original PRBS and itself displaced, a new PRBS is created for the LSB. This reduces the number of errors in the LSB since the mapping for the MSB remains the same.
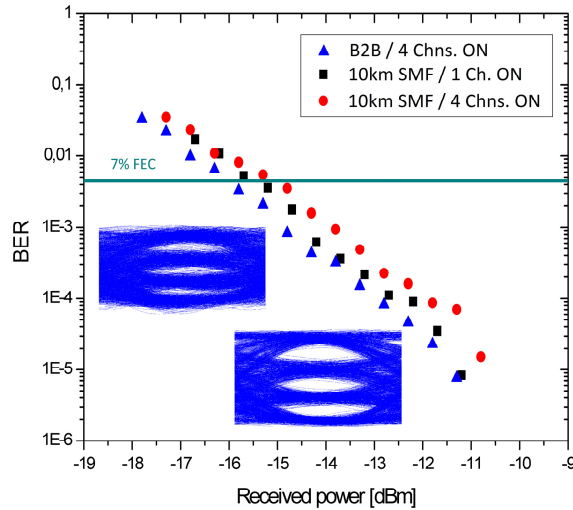
Fig. 7. Averaged BER versus received optical power.

5. Results

The experimental results for each of the three measurements conducted are shown in Fig. 7. Bit error rates are obtained for one of the center channels (1580.66 nm) in back-to-back configuration (blue triangles), after 10 km SMF when only that specific channel is transmitted (black squares) and after 10 km SMF when the four lanes are transmitted in parallel (red circles). Targeting post-FEC bit error rate of 10^{-15}, the green line in Fig. 7. indicates the threshold (4.5·10-3) [16] of a 7% overhead FEC code.

The BER performance difference between single-channel and four-channel transmission is negligible below ~16dBm received power. For higher power levels, an average crosstalk penalty of less than 0.5dB is observed. The comparison with back-to-back performance shows a transmission penalty of ~0.5dB with respect to single-lane configuration. Around 1dB penalty is observed as compared to the four-lane case with a local maximum of 1.3dB.
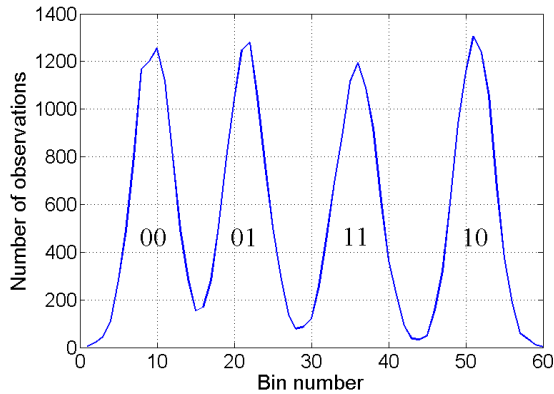
Fig. 8. Histogram of four-channel transmission frame (32767 bits) at -15dBm.

No error floors are observed within the tested received power interval and the WDM signal clearly exceeds the 7%-FEC threshold for received power levels higher than -15dBm. This grants error free transmission (BER~10^{-15}) under considerably relaxed power budget conditions allowing hence the allocation of ~6-7 dB extra loss along the link.

Figure 8. shows the received histogram at the optimum sampling point for a frame of BER~$2.5 \cdot 10^{-3}$ under full WDM operation at the 7%-FEC threshold, which corresponds to -15dBm. Gray mapping is superimposed. The slightly higher accumulation of observations between the 00-01 dip is due to slight instabilities that displace the optimum working point (effect illustrated in Fig. 4.)

6. Conclusions

4x14Gbps L-band VCSEL-based WDM transmission over 10 km of SSMF was investigated. Successful transmission of four channels with quaternary pulse amplitude modulation at 7Gbauds with post-FEC (7% overhead) error free operation has been proven. The crosstalk power penalty was measured to be ~0.5 dB and the power budget margin ranges between 6dB and 7dB. Our results show the potential of the reported system to migrate 4-lanes 56Gbps data links into a compact WDM link.

Paper 10: VCSEL-based DWDM PON with 4 bit/s/Hz spectral efficiency using carrierless amplitude phase modulation

R. Rodes, M. Wieckowski, T.-T. Pham, J.B. Jensen, and I.T. Monroy, "VCSEL-based DWDM PON with 4 bit/s/Hz spectral efficiency using carrierless amplitude phase modulation," *European Conference and Exhibition on Optical Communication*, pp. 1-3, 2011.

VCSEL-based DWDM PON with 4 bit/s/Hz Spectral Efficiency using Carrierless Amplitude Phase Modulation

Roberto Rodes, Marcin Wieckowski, Thang Tien Pham, Jesper Bevensee Jensen and Idelfonso Tafur Monroy

DTU Fotonik, Department of Photonics Engineering, Technical University of Denmark, Dk-2800 Kgs. Lyngby, Denmark.
rrlo@fotonik.dtu.dk

Abstract: We experimental demonstrate successful performance of VCSEL-based WDM link supporting advanced 16-level carrierless amplitude/phase modulation up to 1.25 Gbps, over 26 km SSMF with spectral efficiency of 4 bit/s/Hz for application in high capacity PONs.
OCIS codes: (060.2330) Fiber optics communications; (060.4080) Modulation.

1. Introduction

The increasing bit-rate per user demand in access networks requires systems that can support higher capacity. In order to satisfy the capacity needs, access networks are moving from classic spectral inefficient non-return to zero time-division multiplexing (NRZ-TDM), to wavelength-division multiplexing (WDM) and more advanced modulation formats. Moreover, the complexity raise has to be kept to the minimum in order make the system feasible for access networks. Different techniques have been used for advanced modulation, such as discrete multi-tone (DMT) [1], and carrierless amplitude/phase CAP [2]. For high-speed transmission, the overall CAP architecture has been demonstrated to be less complex and with better performance than DMT architecture [3]. Moreover, high-speed multilevel CAP implementation has been demonstrated by using analog filters [4].

Vertical cavity surface emitting lasers (VCSELs) are especially attractive for access networks, due to their low manufacturing cost and low power consumption. Compared to edge-emitting lasers, VCSELs have inferior performance in terms of linewidth, chirp, stability or linearity. Therefore it is very important to understand and evaluate the feasibility of employing VCSELs for applications requiring higher laser performance.

Our paper proposes and experimentally demonstrates a VCSEL-based WDM system with CAP modulation for access networks. The experiment successfully demodulates 4 channels 100 GHz spacing after 26 km of SSMF. Each VCSEL is directly modulated at 1.25 Gbps in a 312.5 MHz bandwidth, corresponding to a spectral efficiency of 4 bit/s/Hz. To our knowledge, this is the first demonstration of a VCSEL based WDM CAP system. This shows the potential for using VCSELs as light sources in DWDM PON, supporting spectral efficient modulation formats and operating over a modest baseband bandwidth favoring low complexity electronics.

2. CAP Modulation for Access Networks and short-range links

Carrierless amplitude/phase modulation (CAP) is a multilevel and multidimensional modulation technique proposed by Bell Labs [5]. In contrast with quadrature amplitude modulation (QAM), CAP does not use a sinusoidal carrier to generate two orthogonal components. CAP uses two orthogonal signature waveforms to modulate the data in two dimensions. At the receiver, two filters reconstruct the signal from each component. CAP is especially attractive for access networks and short-range links as it uses low complexity electronics, and more channels allocation due to the high spectral efficiency.

In this experiment, we have used four levels encoding for each dimension generating the so-called CAP-16. Previous publication demonstrated 8 levels encoding CAP-64 [6], 3 orthogonal components 3D-CAP[7] and working with bit-rate up to 40 Gbps [4].

3. Experimental Setup

Figure 1 shows the setup used in the proof of principle experiment. A 500 MHz-bandwidth, 1.25 Gsa/s Arbitrary Waveform Generator (ArbWG) is used to generate the CAP-16 signal at 1.25 Gbps. ArbWG features limits our CAP-16 signal up to 1.25 Gbps with an upsampling 4 to ensure no aliasing products. The 2 outputs of the ArbWG are split in 2 and delayed to emulate 4 x 1.25 Gbps uncorrelated CAP signals. Each uncorrelated CAP signal directly modulates a 1550 nm VCSEL. The output power of each VCSEL is approximately -1 dBm. At the transmitter side, the four wavelengths or channels, are multiplexed with a passive optical power combiner; while at the receiver side, wavelength demultiplexing is done with an arrayed waveguide grating (AWG). The power combiner has conversion loss of 7.5 dB. The AWG has an insertion loss of 1.5 dB. The VCSELs are wavelength-tuned by tuning the bias current in order to fit the 100 GHz-spacing grid of the AWG. Optionally, 2 AWGs with the same grid can be used for multiplexing and demultiplexing wavelengths, resulting in 6 dB additional power margin. The system was

evaluated after 26 km transmission of standard single mode fiber (SSMF), with total fiber attenuation of 7.8 dB. A variable optical attenuator is placed after the fiber for bit error rate (BER) measurements. Each channel is detected by a PIN photodiode and stored in a digital storage scope (DSO) for offline demodulation. The demodulation is done in Matlab by filtering the signal with 2 receiving CAP filters to reconstruct each orthogonal component.
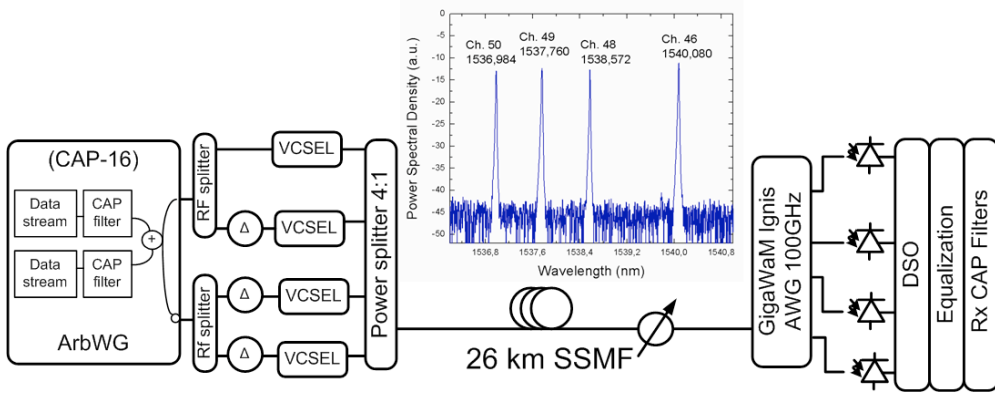

Fig. 1. Experimental Setup. Arbitrary waveform generator (ArbWG), array waveguide grating (AWG), digital storage scope (DSO).

4. Results

The VCSELs were tuned to fit the ITU channels number 50, 49, 48, and 46. The embedded graph in Fig.1 shows the optical spectrum of the WDM-CAP signal with the corresponding wavelengths of each channel.

Figure 2 shows the CAP filters in time and frequency domain, and the electrical spectrum of the CAP signal directly from the ArbWG. The 3dB-bandwidth of each 1.25 Gbps CAP-16 is 312.5 MHz that corresponds to 4 bit/s/Hz spectral efficiency.
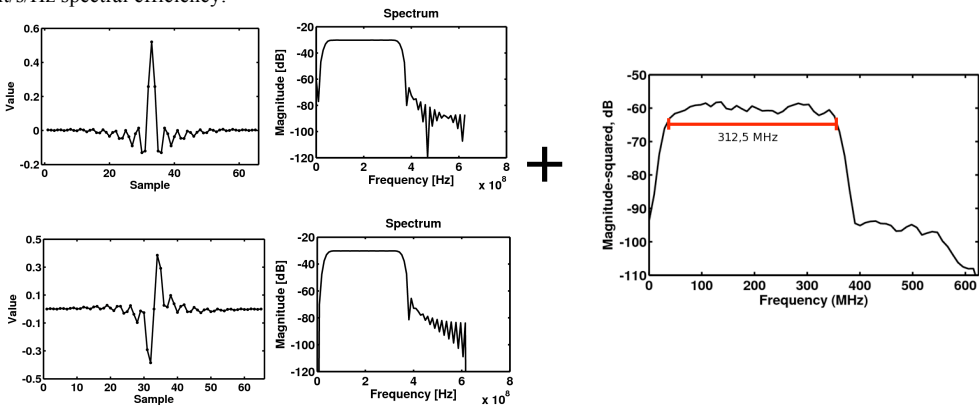
Fig. 2. CAP filters in time and frequency domain, and frequency spectrum of 1.25 Gbps CAP-16 after ArbWG

The received signal filtered with the receiver CAP filters is decomposed in both orthogonal components. Both components can be represented in an I/Q constellation diagram like QAM signals. Fig. 3.a shows the clear constellation diagram of the demodulated electrical B2B signal. Fig. 3.b shows the demodulated optical B2B with −19 dBm received optical power; constellation after electrical-to-optical conversion is still very clear. Fig. 3.c and d show the signals at −22 dBm received optical power, for B2B and after 26 km configurations, respectively. No constellation degradation is appreciated after transmission compared to B2B, as it is shown also later in the BER curves.
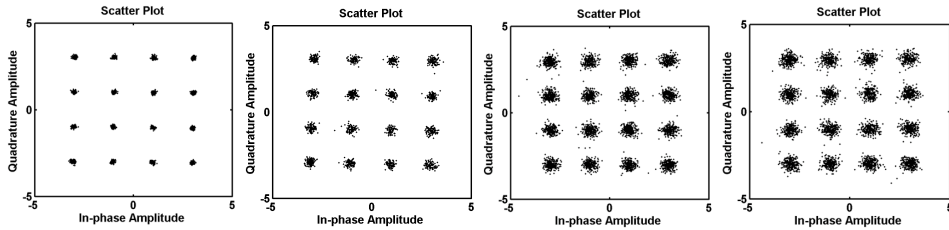
Fig. 3. Constellation CAP-16 for a) electrical B2B, b) optical B2B at -19 dBm, c) optical B2B at -22 dBm. d) after 26 km SSMF at -22 dBm.

Figure 4.a shows the BER curves of the demodulated channel 49 to evaluate the transmission effects and cross talk between channels. The figure compares the performance when only channel 49 is transmitting and when the 4 channels are transmitting simultaneously. No receiver sensitivity power penalty is measured from multiplexing or transmission. Figure 4.b shows all 4 channels after 26 km transmission. The forward error correction (FEC) limit of BER = $2,2 \cdot 10^{-3}$ is considered as a reference. We achieved received power sensitivity below -24 dBm for all the channels.
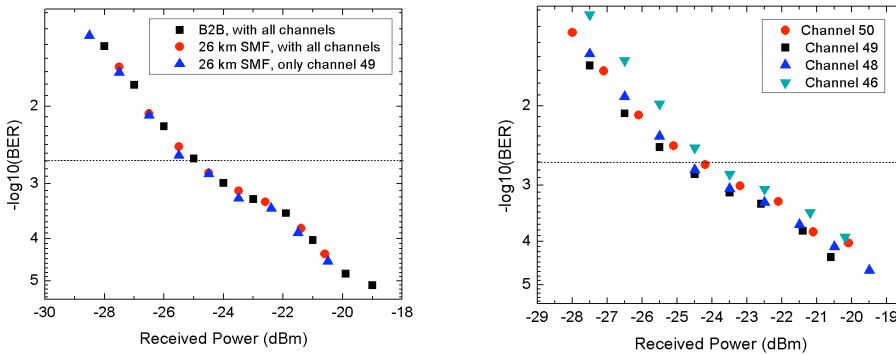
Fig. 4. BER curves CAP-16. a) Channel 49 b) all channels after 26 km SSMF.

5. Summary

We have experimentally demonstrated directly modulation of CAP-16 in commercially available VCSELs, with a spectral efficiency of 4 bit/s/Hz. The system has been evaluated with 4 close spaced channels at 1.25 Gbps each, for a total bitrate of 5 Gbps over 26 km fiber transmission. All the channels achieved received power sensitivity below -24 dBm. Future work will evaluate the system for higher bitrates overcoming the transmitter limitations by using analog CAP filters.

We believe direct CAP modulation of VCSELs is a candidate for next generation PONs and short range systems due to the high spectral efficiency, scalability to higher order modulation, potentially low cost implementation and simplicity compare to modulation formats with carrier.

6. References

[1] I. Kalet, "The multitone channel," IEEE Trans. Commun., vol. 37, (Feb. 1989), pp.119–124.
[2] G.-H. Im, D. D. Harman, G. Huang, A. V. Mandzik, M.-H. Nguyen, and J.-J. Werner, "51.84 Mb/s 16-CAP ATM LAN standard," IEEE J. Select. Areas Commun., vol. 13 (1995), pp. 620–632.
[3] A. Shalash, K.K. Parhi, "Comparison of discrete multitone and carrierless AM/PM techniques for line equalization," IEEE International Symposium on Circuits and Systems, vol.2 (1996). pp. 560–563.
[4] J. D. Ingham, R. Penty, I. White, D. Cunningham. "40 Gb/s Carrierless Amplitude and Phase Modulation for Low-Cost Optical Datacommunication Links," Conference on Optical Fiber Communications, OFC (2011).
[5] Chen, W. Y.; Im, G. H.; Werner, J. J.; , "Design of Digital Carrierless AM/PM Transceivers", AT&T and Bellcore contribution to ANSI T1E1.4/92-149, (1992)
[6] M. Wieckowski, J. B. Jensen, I. Tafur Monroy, J. Siuzdak, J. P. Turkiewicz. " 300 Mbps Transmission with 4.6 bit/s/Hz Spectral Efficiency over 50 m PMMA POF Link Using RC-LED and Multi-Level Carrierless Amplitude Phase Modulation," Conference on Optical Fiber Communications, OFC (2011).
[7] A. Shalash, K.K. Parhi, " Multidimensional Carrierless AM/PM Systems for Digital Subscriber Loops," IEEE Transactions on Communications, vol. 47, no. 11, November (1999).

Paper 11: Carrierless amplitude phase modulation of VCSEL with 4 bit/s/Hz spectral efficiency for use in WDM-PON

Carrierless amplitude phase modulation of VCSEL with 4 bit/s/Hz spectral efficiency for use in WDM-PON

Roberto Rodes,[1,*] Marcin Wieckowski,[1,2] Thang Tien Pham,[1] Jesper Bevensee Jensen,[1] Jarek Turkiewicz,[2] Jerzy Siuzdak,[2] and Idelfonso Tafur Monroy[1]

[1]DTU Fotonik, Technical University of Denmark, Denmark
[2]Warsaw University of Technology, Poland
[*]rrlo@fotonik.dtu.dk

Abstract: We experimentally demonstrate successful performance of VCSEL-based WDM link supporting advanced 16-level carrierless amplitude/phase modulation up to 1.25 Gbps, over 26 km SSMF with spectral efficiency of 4 bit/s/Hz for application in high capacity PONs.

OCIS codes: (060.2330) Fiber optics communications; (060.4080) Modulation.

References and links

1. I. Kalet, "The multitone channel," IEEE Trans. Commun. **37**(2), 119–124 (1989).
2. G.-H. Im, D. D. Harman, G. Huang, A. V. Mandzik, M.-H. Nguyen, and J.-J. Werner, "51.84 Mb/s 16-CAP ATM LAN standard," IEEE J. Sel. Areas Comm. **13**(4), 620–632 (1995).
3. A. Shalash and K. K. Parhi, "Comparison of discrete multitone and carrierless AM/PM techniques for line equalization," *IEEE International Symposium on Circuits and Systems*, **2**, 560–563, (1996).
4. J. D. Ingham, R. Penty, I. White, and D. Cunningham, "40 Gb/s carrierless amplitude and phase modulation for low-cost optical datacommunication links," *Optical Fiber Communication Conference and Exposition* (OFC/NFOEC) (2011).
5. W. Y. Chen, G. H. Im, and J. J. Werner, "Design of digital carrierless AM/PM transceivers," AT&T and Bellcore contribution to ANSI T1E1.4/92-149, (1992).
6. M. Wieckowski, J. B. Jensen, I. Tafur Monroy, J. Siuzdak, and J. P. Turkiewicz, "300 Mbps transmission with 4.6 bit/s/Hz spectral efficiency over 50 m PMMA POF link using RC-LED and multi-level carrierless amplitude phase modulation," *National Fiber Optic Engineers Conference*, OSA Technical Digest (CD) (Optical Society of America 2011) paper NTuB8.
7. A. Shalash and K. K. Parhi, "Multidimensional carrierless AM/PM systems for digital subscriber loops," IEEE Trans. Commun. **47**(11), 1655–1667 (1999).
8. D. Hillerkuss, R. Schmogrow, T. Schellinger, M. Jordan, M. Winter, G. Huber, T. Vallaitis, R. Bonk, P. Kleinow, F. Frey, M. Roeger, S. Koenig, A. Ludwig, A. Marculescu, J. Li, M. Hoh, M. Dreschmann, J. Meyer, S. Ben Ezra, N. Narkiss, B. Nebendahl, F. Parmigiani, P. Petropoulos, B. Resan, A. Oehler, K. Weingarten, T. Ellermeyer, J. Lutz, M. Moeller, M. Huebner, J. Becker, C. Koos, W. Freude, and J. Leuthold, "26 Tbit s−1 line-rate super-channel transmission utilizing all-optical fast Fourier transform processing," Nat. Photonics **5**(6), 364–371 (2011).
9. R. Shafik, S. Rahman, and A. R. Islam, "On the extended relationships among EVM, BER and SNR as performance metrics," in Proc. *4th International Conference on Electrical and Computer Engineering* (ICECE), 408–411 (2006).

1. Introduction

 The increasing bit-rate per user demand in access networks requires systems that can support higher capacity. In order to satisfy the capacity needs, access networks are moving from classic spectral inefficient non-return to zero time-division multiplexing (NRZ-TDM), to wavelength-division multiplexing (WDM) and more advanced modulation formats. Moreover, the complexity raise has to be kept to the minimum in order make the system feasible for access networks. Different techniques have been used for advanced modulation, such as discrete multitone (DMT) [1], and carrierless amplitude/phase CAP [2]. For high-speed transmission, the overall CAP architecture has been demonstrated to be less complex and with better performance than DMT architecture [3]. Moreover, high-speed multilevel CAP

implementation has been demonstrated by using transversal filters developed for equalization of NRZ data [4].

Vertical cavity surface emitting lasers (VCSELs) are especially attractive for access networks, due to their low manufacturing cost and low power consumption. Compared to edge-emitting lasers, VCSELs have inferior performance in terms of linewidth, chirp, stability and linearity. Therefore, it is important to understand and evaluate the feasibility of employing VCSELs for applications requiring higher laser performance.

Our paper proposes and experimentally demonstrates a VCSEL-based WDM system with CAP modulation for access networks. The experiment successfully demodulates 4 channels 100 GHz spacing after 26 km of SSMF. Each VCSEL is directly modulated at 1.25 Gbps in a 312.5 MHz bandwidth, corresponding to a spectral efficiency of 4 bit/s/Hz. To our knowledge, this is the first demonstration of a VCSEL based WDM CAP system. Our experiment shows the potential for using VCSELs as light sources in WDM PON, supporting spectral efficient modulation formats and operating over a modest baseband bandwidth favoring low complexity electronics.

2. CAP modulation for access networks and short-range links

Carrierless amplitude/phase modulation (CAP) is a multilevel and multidimensional modulation technique proposed by Bell Labs [5]. In contrast to quadrature amplitude modulation (QAM), CAP does not use a sinusoidal carrier to generate two orthogonal components. CAP uses two orthogonal signature waveforms to modulate the data in two dimensions. At the receiver, two filters are used to reconstruct the signal from each component. CAP is especially attractive for access networks and short-range links, as it employs low complexity electronics, and allows for narrow channel spacing due to the high spectral efficiency.

In this experiment, we have used four-level encoding for each dimension generating the so-called CAP-16. Previous publication demonstrated 8 levels encoding CAP-64 [6], 3 orthogonal components 3D-CAP [7] and working with bit-rate up to 40 Gbps [4].
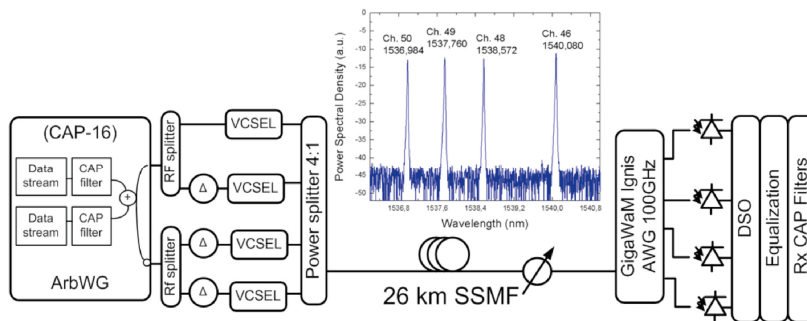
3. Experimental setup

Fig. 1. Experimental Setup. Arbitrary waveform generator (ArbWG), array waveguide grating (AWG), digital storage scope (DSO).

Figure 1 shows the setup used in the proof of principle experiment. A 500 MHz-bandwidth, 1.25 Gsa/s Arbitrary Waveform Generator (ArbWG) is used to generate the CAP-16 signal at 1.25 Gbps. ArbWG features limits our CAP-16 signal up to 1.25 Gbps with an upsampling 4 to ensure no aliasing products. The ArbWG has 10-bits vertical resolution. The 2 outputs of the ArbWG are split in 2 and delayed to emulate 4 x 1.25 Gbps uncorrelated CAP signals. The minimum decorrelation between channels is 7 ns or approximately 2 bauds. Each uncorrelated

CAP signal directly modulates a commercially available 1550 nm-wavelength, 4.5 GHz-bandwidth VCSEL from RayCan. The output power of each VCSEL is approximately -1 dBm. At the transmitter side, the four wavelengths or channels, are multiplexed with a passive optical power combiner; while at the receiver side, wavelength demultiplexing is done with an arrayed waveguide grating (AWG). The power combiner has conversion loss of 7.5 dB. The AWG has an insertion loss of 1.5 dB. The VCSELs are uncooled. The VCSELs are wavelength-tuned by tuning the bias current in order to keep wavelength spacing and fit the 100 GHz-spacing grid of the AWG. Optionally, 2 AWGs with the same grid can be used for multiplexing and demultiplexing wavelengths, resulting in 6 dB additional power margin. The system was evaluated after 26 km transmission of standard single mode fiber (SSMF), with total fiber attenuation of 7.8 dB. A variable optical attenuator is placed after the fiber for bit error rate (BER) measurements. Each channel is detected by a 10 GHz PIN photodiode and stored in a digital storage scope (DSO) for offline demodulation. The demodulation is done in Matlab by filtering the signal with 2 receiving CAP filters to reconstruct each orthogonal component.

4. Results

The VCSELs were tuned to fit the ITU channels number 50, 49, 48, and 46. The embedded graph in Fig. 1 shows the optical spectrum of the WDM-CAP signal with the corresponding wavelengths of each channel. Figure 2 shows the 65-taps CAP filters in time and frequency domain, and the electrical spectrum of the CAP signal directly from the ArbWG. The 3dB-bandwidth of each 1.25 Gbps CAP-16 is 312.5 MHz that corresponds to 4 bit/s/Hz spectral efficiency.
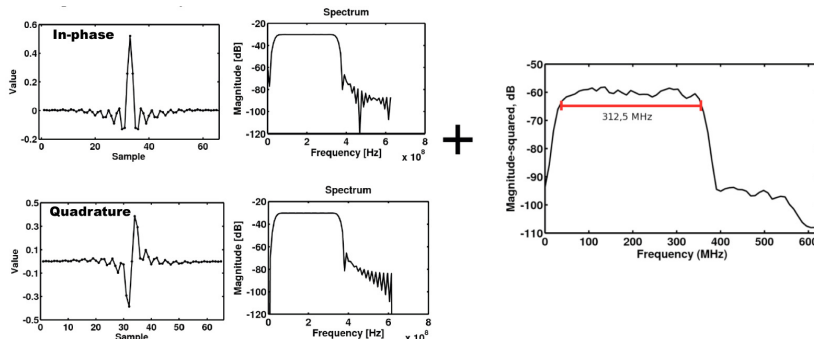

Fig. 2. CAP filters in time and frequency domain, and frequency spectrum of 1.25 Gbps CAP-16 after ArbWG

The received signal filtered with the receiver CAP filters is decomposed in both orthogonal components. Both components can be represented in an I/Q constellation diagram like QAM signals. Figure 3(a) shows the clear constellation diagram of the demodulated electrical B2B signal. Figure 3(b) shows the demodulated optical B2B with −19 dBm received optical power; constellation after electrical-to-optical conversion is still very clear. Figure 3(c) and d show the signals at − 22 dBm received optical power, for B2B and after 26 km configurations, respectively. No constellation degradation is appreciated after transmission compared to B2B, as it is shown also later in the BER curves.
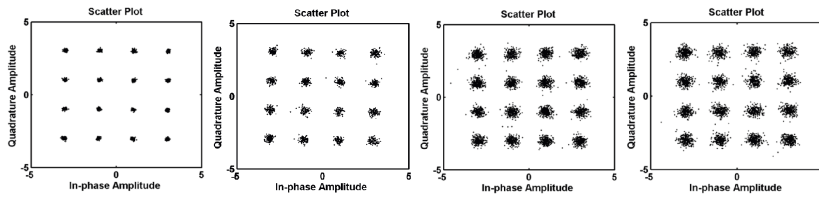
Fig. 3. Constellation CAP-16 for a) electrical B2B, b) optical B2B at -19 dBm, c) optical B2B at -22 dBm. d) after 26 km SSMF at -22 dBm.

Figure 4(a) shows the measured BER curves of the demodulated channel 49 to evaluate the transmission effects and cross talk between channels. The figure compares the performance when only channel 49 is transmitting and when the 4 channels are transmitting simultaneously. No receiver sensitivity power penalty is measured from multiplexing or transmission. Figure 4(b) shows all 4 channels after 26 km transmission. The forward error correction (FEC) limit of BER = $2.2 \cdot 10^{-3}$ is considered as a reference. We achieved receiver power sensitivity below -24 dBm for all the channels.
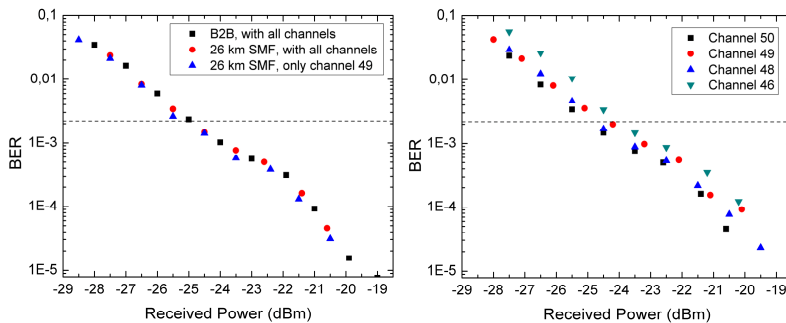

Fig. 4. BER curves CAP-16. a) Channel 49 b) all channels after 26 km SSMF.

5. Simulation of CAP requirements

In this section, simulations have been performed in order to determine the minimum requirements for ADCs and digital filters in a CAP system.

5.1. Resolutions and sample rates:

The price of high performance Analog to Digital Converters (ADC) will not be suitable for PON applications where cost reduction is the main challenge. It is desirable to reduce the requirements in terms of sample rate and vertical resolution of ADCs. Simulations have been performed to analyze what are the requirements for CAP-16 signals with respect to ADC resolution, number of tabs in filters, and degree of oversampling in order to obtain good performance with the minimum complexity. Figure 5 shows the demodulated constellation of the simulated signal when different precision of the filter coefficients is used. The number of filter taps on the simulation was set to the experimental value used of 65.
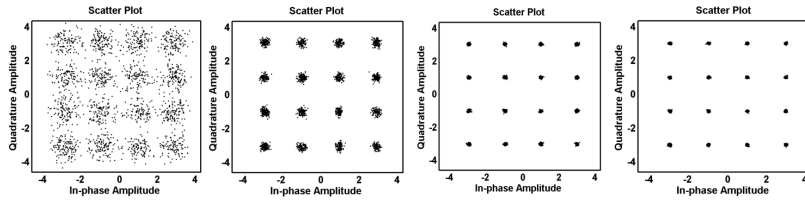
Fig. 5. Constellation CAP-16 for a) 4-bit precision, b) 6-bit precision, c) 8-bit precision, d) 10-bit precision.

Figure 6(a) shows the error vector magnitude (EVM) respect to the coefficient precision. EVM of 12% corresponds to a BER at the FEC limit for a 16 QAM constellation [8] [9], which is the same constellation than CAP-16. Bit precision of 6 or more are needed for electrical signal with EVM below 12%.

The second parameter to consider is the sample rate. The maximum baud rate of our ADC allows will depend on the sample rate of the ADC and the required oversampling of the CAP signal. The optimum upsampling factor for a CAP system is 4, as described in [5].
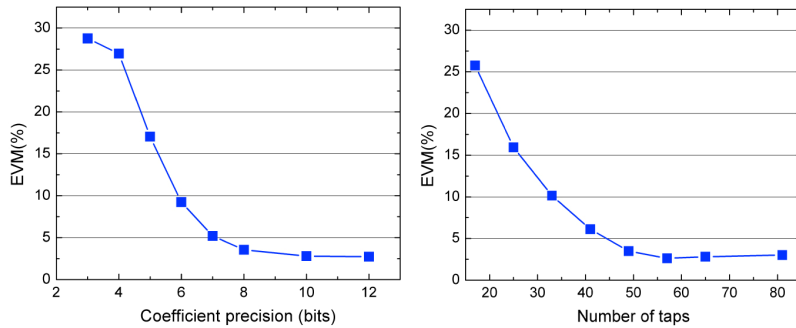

Fig. 6. EVM for CAP 16 respect to a) Coefficient precision, b) number of filter taps

5.2. Filter taps:

CAP modulation has been demonstrated to be simpler than DMT [3]. In contrast with DMT, CAP does not require of IFFT and FFT to generate and demodulate multiple subcarriers. Instead, CAP uses a filter or digital convolution with less computational complexity. This simplicity makes CAP suitable for next generation access networks where cost is the main challenge. The computational complexity to generate and demodulate CAP signals is directly related with the number of taps of the CAP filter. Therefore, it is important to investigate the requirements of the CAP filter in order to decrease the computational complexity maintaining a good performance. Figure 7 shows the demodulated constellation of the simulated signal using different number of filter taps. The number of bit precision on the simulation was set to the experimental value used of 10. Figure 6(b) shows the EVM respect to the number of filter taps. For an EVM below 12%, the number of taps has to be 33 or more.
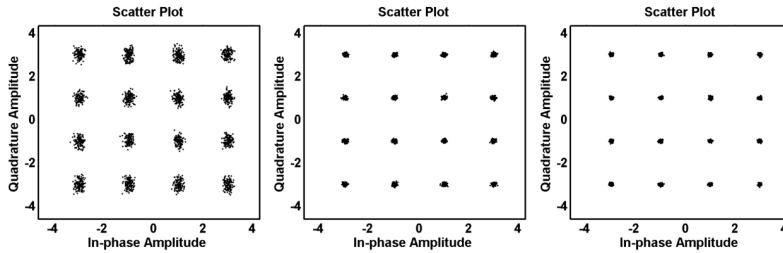
Fig. 7. Constellation CAP-16 for CAP filters with a) 33 taps, b) 49 taps, c) 65 taps

6. Summary

We have experimentally demonstrated directly modulation of CAP-16 in commercially available VCSELs, with a spectral efficiency of 4 bit/s/Hz. The system has been evaluated with 4 close spaced channels at 1.25 Gbps each, for a total bitrate of 5 Gbps over 26 km fiber transmission. All the channels achieved receiver power sensitivity below -24 dBm. Moreover, we have presented simulation on the requirements of CAP signals. Future work will evaluate the system for higher bitrates overcoming the transmitter limitations by using analog CAP filters.

We believe direct CAP modulation of VCSELs is a candidate for next generation PONs and short range systems. CAP allows for scalability in multilevel and multidimension. Therefore, CAP has a potentially very high spectral efficiency attractive for bitrates beyond 15 Gb/s where NRZ-OOK becomes challenging. Due to the high spectral efficiency, it has a low bandwidth occupation and very close channel spacing without crosstalk can be achieved. Therefore is also very attractive solution for dense. WDM-PONs. It has a potentially low cost implementation and simplicity compare to modulation formats with carrier.

Paper 12: Half-cycle QAM modulation for VCSEL-based optical links

Sub-cycle QAM modulation for VCSEL-based optical fiber links

Tien-Thang Pham,[1,*] Roberto Rodes,[1] Jesper Bevensee Jensen,[1] Connie J. Chang-Hasnain,[2] and Idelfonso Tafur Monroy[1]

[1]*DTU Fotonik, Department of Photonics Engineering, Technical University of Denmark, DK2800 Kgs. Lyngby, Denmark.*
[2]*Dept. of Electrical Engineering and Computer Science, University of California, Berkeley, CA 94720, USA*
*[*ptit@fotonik.dtu.dk](mailto:ptit@fotonik.dtu.dk)*

Abstract: QAM modulation utilizing subcarrier frequency lower than the symbol rate is both theoretically and experimentally investigated. High spectral efficiency and concentration of power in low frequencies make sub-cycle QAM signals attractive for IM-DD optical fiber links with direct modulated light sources. Real-time generated 10-Gbps 4-level QAM signal in a 7.5-GHz bandwidth utilizing subcarrier frequency at a half symbol rate was successfully transmitted over 20-km SMF using an un-cooled 1.5-µm VCSEL. Only 2.5-dB fiber transmission power penalty was observed with no equalization applied.

©2012 Optical Society of America

OCIS codes: (060.2330) Fiber optics communications; (060.4080) Modulation.

References and links

1. W. Hofmann, " 40 Gbit/s modulation of 1550 nm VCSEL," Electron. Lett., **47**, 270-271 (2011).
2. P. Moser, W. Hofmann, P. Wolf, G. Fiol, J. A. Lott, N. N. Ledentsov, and D. Bimberg, "83 fJ/bit energy-to-data ratio of 850-nm VCSEL at 17 Gb/s," in *Proceedings of 37th European Conference on Optical Communication* (2011) , pp. 1-3.
3. W. Hofmann, M. Görblich, G. Böhm, M. Ortsiefer, L. Xie, and M.-C. Amann, " Long-wavelength 2-D VCSEL arrays for optical interconnects," in *Proceedings of Lasers and Electro-Optics (CLEO) and Quantum Electronics and Laser Science Conference* (2008), pp.1- 2.
4. M. C. Y. Huang, K. B. Cheng, Y. Zhou, A. Pisano, and C. Chang-Hasnain, "Monolithic integrated piezoelectric MEMS-tunable VCSEL," IEEE IEEE J. Sel. Topics Quantum Electron. **13**, 374-380 (2007).
5. B. Zhang, X. Zhao, L. Christen, D. Parekh, W. Hofmann, M. C. Wu, M. C. Amann, C. J. Chang-Hasnain, and A. E. Willner, "Adjustable chirp injection-locked 1.55-µm VCSELs for enhanced chromatic dispersion compensation at 10-Gbit/s," in *Optical Fiber Communication Conference* (Optical Society of America, 2008) paper OWT7.
6. L. Xu, H. K. Tsang, W. Hofmann, and M.-C. Amann, "10-Gb/s colorless re-modulation of signal from 1550nm vertical cavity surface emitting laser array in WDM PON," in *Proceedings of Lasers and Electro-Optics (CLEO) and Quantum Electronics and Laser Science Conference* (2009), paper CI3_4.
7. T. B. Gibbon, K. Prince, T. T. Pham, A. Tatarczak, C. Neumeyr, E. Rönneberg, M. Ortsiefer, and I. Tafur Monroy, " VCSEL transmission at 10Gb/s for 20km single mode fiber WDM-PON without dispersion compensation or injection locking," Optical Fiber Tech. **17**, 41-45 (2011).
8. K. Prince, M. Ma, T. B. Gibbon, C. Neumeyr, E. Rönneberg, M. Ortsiefer, and I. Tafur Monroy, "Free-running 1550 nm VCSEL for 10.7 Gb/s transmission in 99.7 km PON," IEEE/OSA JOCN. **3**, 399-403 (2011)
9. R. Rodes, J. Estaran, B. Li, M. Muller, J. B. Jensen, T. Gruendl, M. Ortsiefer, C. Neumeyr, J. Rosskopf, K. J. Larsen, M.-C. Amann, and I. T. Monroy, "100 Gb/s single VCSEL data transmission link," in *Optical Fiber Communication Conference* (Optical Society of America, 2012), paper PDP5D.
10. E. Hugues-Salas, R. P. Giddings, X. Q. Jin, J. L. Wei, X. Zheng,Y. Hong, C. Shu, and J. M. Tang," Real-time experimental demonstration of low-cost VCSEL intensity-modulated 11.25Gb/s optical OFDM signal transmission over 25km PON systems," Opt. Express **19**, 2979-2988 (2011). http://www.opticsinfobase.org/oe/abstract.cfm?URI=oe-19-4-2979
11. S. C. J. Lee, F. Breyer, S. Randel, J. Zeng, F. Huijskens, H. P. van den Boom, A. M. Koonen, and N. Hanik, "24-Gb/s transmission over 730 m of multimode fiber by direct modulation of an 850-nm VCSEL using discrete multi-tone modulation," in *Optical Fiber Communication Conference* (Optical Society of America, 2009), paper PDP5.

12. K. Szczerba, P. Westberg, J. Gustavsson, A. Haglund, J. Karout, M. Karlsson, P. Andrekson, E. Agrell, and A. Larsson, "30 Gbps 4-PAM transmission over 200m of MMF using an 850 nm VCSEL," in *Proceedings of 37th European Conference on Optical Communication* (2011) , paper We.7.B.2.
13. J. Proakis and M. Salehi, *Digital Communications* (McGraw-Hill, 2007).
14. J. Justesen, "Performance of product codes and related structures with iterated decoding," IEEE Trans. Commun. **59**, 407-415 (2011).

1. Introduction

Vertical cavity surface emitting lasers (VCSELs) have several attractive properties such as large modulation bandwidth, low driving voltage, wavelength tunability, wafer-scale testing, easy packaging, and low carbon footprint [1-4]. These advantages make VCSELs attractive light sources for high-speed optical communication links in data centers and optical access networks using intensity modulation/ direct detection (IM/DD) technique. Optical links that use long-wavelength VCSELs and on-off keying (OOK) modulation are limited in transmission reach by chromatic dispersion of optical fibers due to frequency chirping caused by direct modulation of the VCSEL and large occupied bandwidth of signals [5-8]. For 10-Gbps data transmission using 1.5-µm VCSELs, a 3-dB power penalty after 10-km single mode fiber (SMF) transmission was experimentally observed [6] and a 11-dB power penalty after 20-km SMF was observed after numerical simulations [7]. To deal with the effect of chromatic dispersion for OOK systems, dispersion management and dispersion mitigation methods have been proposed [5-8]. Advanced modulation formats also have been proposed to reduce the bandwidth of the signals. High-speed pulse amplitude modulation (PAM) for VCSELs has been demonstrated [9]. Its scalability is limited because it is single dimension modulation. Multi-tone modulation (DMT), a sub-class of orthogonal frequency division multiplexing (OFDM), is a promising technology for both increasing spectral efficiency and dispersion tolerance. High speed data transmission of DMT signal using VCSELs has been demonstrated recently [10-11]. However, to support high-speed data transmission, DMT requires fast analogue to digital (ADC) and digital to analogue (DAC) converters. Additionally, DMT transceivers consume high power for signal processing compared to conventional OOK transceivers. A simpler method, single-cycle subcarrier quadrature amplitude modulation (QAM) was proposed in which the subcarrier frequency is equal to the symbol rate. Transmission of 10-Gbaud 16-QAM data in a 20-GHz bandwidth over 200-m MMF using 850-nm VCSELs has been reported [12].

In this paper, we analyze and demonstrate sub-cycle QAM modulation for spectrally efficient VCSEL-based optical links. We point out that the subcarrier frequency can be reduced to a quarter or a half of the symbol rate to improve spectral efficiency while the simplicity of the transceiver is maintained. For instance, by using a subcarrier frequency at half the symbol rate, the spectral width, defined as the frequency of the first null in the spectrum, of the QAM signal is reduced by 25% compared to conventional QAM modulation. We demonstrate the generation and detection of 10-Gpbs and 16-Gbps 4-QAM signals transmitted over 20-km and 3-km SMFs respectively using an un-cooled commercially available 10-GHz, 1.5-µm VCSEL. Bit error ratio (BER) below $4.8x10^{-3}$, the limit of forward error correction (FEC) with 7% payload overhead, was achieved for both cases. 2.5-dB power penalty was observed for 10-Gbps 4-QAM signal after 20-km fiber transmission.

2. Sub-cycle QAM modulation and demodulation

QAM is a two-dimensional signaling method which uses the in-phase and quadrature (cosine and sine waves, respectively). Two basis functions of QAM [13]:

$$\phi_1(t) = \sqrt{\frac{2}{E_g}} g(t) \cos 2\pi f_c t \tag{1}$$

$$\phi_2(t) = -\sqrt{\frac{2}{E_g}} g(t) \sin 2\pi f_c t \tag{2}$$

The corresponding signal waveform of M-QAM signals:

$$s_m(t) = A_{mI}\sqrt{\frac{E_g}{2}}\phi_1(t) + A_{mQ}\sqrt{\frac{E_g}{2}}\phi_2(t), \qquad m=1, 2,..., M \tag{3}$$

$$= A_{mI} g(t)\cos 2\pi f_c t - A_{mQ} g(t)\sin 2\pi f_c t$$

where E_g is the energy of the signal with the lowest amplitude and $g(t)$ is a pulse shape. A_{mI} and A_{mQ} denote the set of M possible amplitudes for I and Q channels. The norms of two basis functions in a symbol duration [0, T]:

$$\langle \phi_1(t), \phi_1(t) \rangle = \int_0^T \left(\sqrt{\frac{2}{E_g}} g(t)\cos(2\pi f_c t + \varphi) \right)^2$$
$$= \int_0^T \frac{2}{E_g} g^2(t)\cos^2(2\pi f_c t + \varphi) \tag{4}$$

$$\langle \phi_2(t), \phi_2(t) \rangle = \int_0^T \left(\sqrt{\frac{2}{E_g}} g(t)\sin(2\pi f_c t + \varphi) \right)^2$$
$$= \int_0^T \frac{2}{E_g} g^2(t)\sin^2(2\pi f_c t + \varphi) \tag{5}$$

The inner product of two basis functions in a symbol duration [0, T]:

$$\langle \phi_1(t), \phi_2(t) \rangle = \int_0^T \sqrt{\frac{2}{E_g}} g(t)\cos(2\pi f_c t + \varphi)\sqrt{\frac{2}{E_g}} g(t)\sin(2\pi f_c t + \varphi)$$
$$= \int_0^T \frac{2}{E_g} g^2(t)\sin 2(2\pi f_c t + \varphi) \tag{6}$$

The two basis functions are orthogonal if integral of $\sin 4\pi f_c t$ is equal to zero in a symbol duration. We consider the cases subcarrier frequencies are lower than the symbol rate. There are two basic options to achieve that.

2.1. Subcarrier frequency is at half symbol rate.

If the carrier frequency is a half the symbol rate, $fc = \dfrac{1}{2T}$ (half-cycle modulation), the integral in equation (6) is taken in one cycle of $\sin(4\pi f_c t)$. It is equal to zero regardless the phase of basis functions. The two basis functions for half-cycle QAM modulation:

$$\phi_1(t) = \pm\sqrt{\frac{2}{E_g}}g(t)\cos\left(2\pi\frac{1}{2T}t+\varphi\right) \qquad t=[0, T] \qquad (7)$$

$$\phi_2(t) = \mp\sqrt{\frac{2}{E_g}}g(t)\sin\left(2\pi\frac{1}{2T}t+\varphi\right) \qquad t=[0, T] \qquad (8)$$

As in Eq. (7) and (8), there are two available values for each basis function: positive and negative ones. When full cycle sine/cosine signals are used for data modulation. Those two values of each basis functions are alternately used for two consecutive bits. Nevertheless the two basis functions have unit norm regardless the sign. Therefore, they are an orthonomal set.
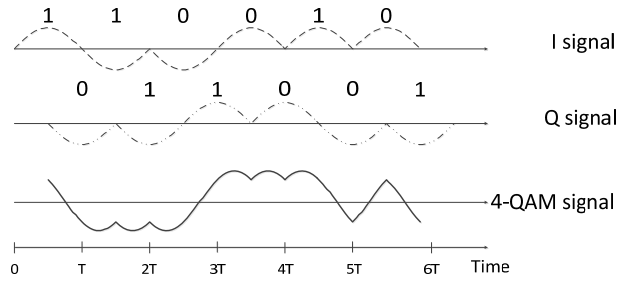
Fig. 1. Simulated waveforms of BPSK signals from I and Q channels and 4-QAM half-cycle signal. There is a half-period offset between the two signal components.
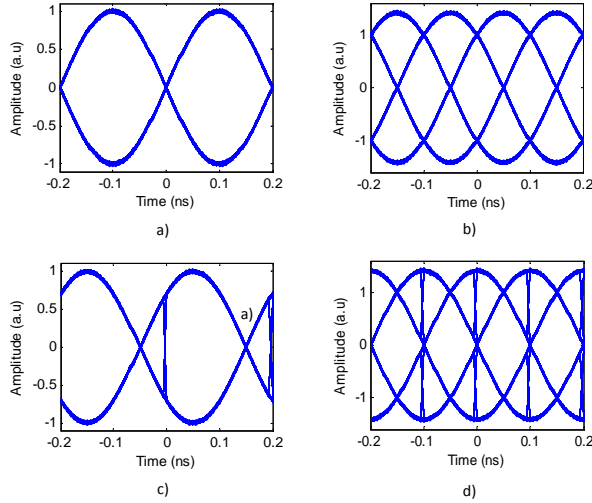

Fig. 2. Simulated eye diagram of 5-Gbaud BPSK signal from I channel and 4-QAM signal in two-baud duration (a,b): data bits start at ±kπ phase of subcarrier, (c,d): data bits start at a different phase.
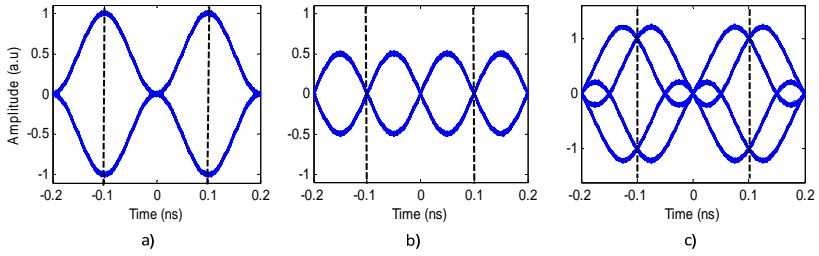
Fig. 3. Simulated eye diagrams of BPSK signal from a) I channel, b) Q channel and c) 4-QAM signal after multiplication with sine signal for detection. Dash lines indicate center of bits - the optimal sampling instant.
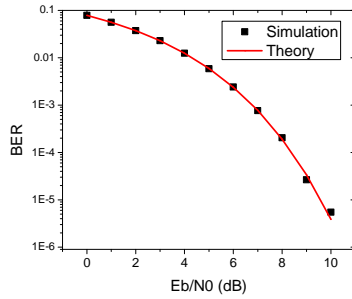

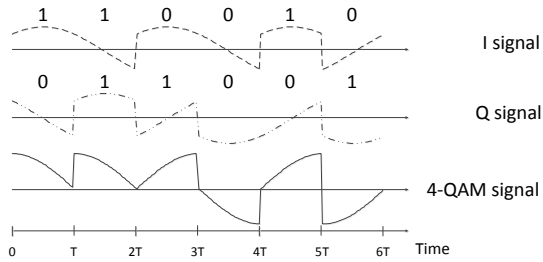Fig.4. Theoritical and simulated BER of half-cycle 4-QAM signal in AWGN channel.

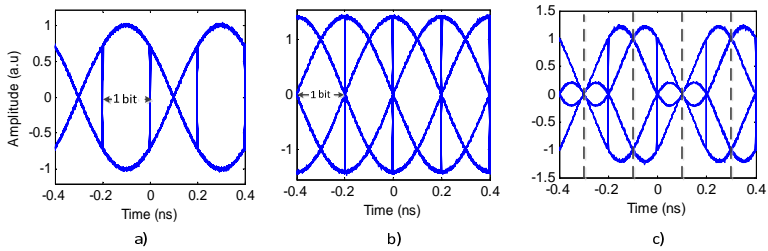Fig.5. Simulated waveforms of BPSK signals from I and Q channels and 4-QAM quarter-cycle signal.

Fig. 6. Simulated eye diagram of 5-Gbaud quarter-cycle modulation signal in 4-baud duration. (a) BPSK signal, (b) 4-QAM signal, (c) 4-QAM signal after multiplication with sine signal. Dash lines indicate center of bits.

Examples of simulated waveforms of the BPSK signals from I and Q channels and 4-QAM half-cycle signal are depicted in Fig.1. Simulated eye-diagrams of the BPSK signals and the 4-QAM signal are illustrated in Fig. 2. In Fig. 2(a) and 2(b), data bits start when the phase of subcarrier is $\pm k\pi$ (k=0, 1, 2...) while in Fig. 1(c) and 2(d) data bits start at $\pm\pi/4+k\pi$ of the subcarrier phase. Data in Q channel is half a bit delayed to make the half-cycle QAM signal consistent with the signal generated in the experiment which is presented in section 3.

The half-cycle QAM signal can be demodulated using a correlation receiver [13]. When multiplied with sine/cosine signals, two values of each basis function are again alternately used. It removes the effect of the sign of the basis functions on the demodulated data. Figure 3 shows the eye-diagrams for two symbols of the BPSK signals from I and Q channels and the 4-QAM signal after multiplication with a sine signal for detection. It shows clearly that the optimal sampling point for threshold gating is at the center of bits when the interference is zero. Therefore, the integration step can be eliminated. The theoretical BER for half-cycle QAM modulation is similar other subcarrier frequencies which is expressed in [13]. The theoretical and simulated BER of the half-cycle 4-QAM signal versus energy-per-bit-to-noise ratio (Eb/N0) in additive white Gaussian noise (AWGN) channel is presented in Fig. 4.

2.2. Subcarrier frequency is at a quarter of the symbol rate.

In this case, the integral in equation (6) is taken in one half cycle of $\sin\left(4\pi f_c t\right)$ starting at $\pm\pi/2$ and ending at $\mp\pi/2$, precisely. It means that data bits must start at $\pm l\pi/2+\pi/4$ (l=1,2, ...). The two basis functions for quarter-cycle QAM modulation:

$$\phi_1(t) = \pm\sqrt{\frac{2}{E_g}} g(t)\cos\left(2\pi\frac{1}{4T}t+\frac{k}{4}\pi\right) \quad \text{t=[0, T], k=1,3} \tag{9}$$

$$\phi_2(t) = \mp\sqrt{\frac{2}{E_g}} g(t)\sin\left(2\pi\frac{1}{4T}t+\frac{k}{4}\pi\right) \quad \text{t=[0, T], k=1,3} \tag{10}$$

There are four possible values for each basis functions as expressed in Eq. (9) and (10). However, these four values gives only two different norms. Different norms from different basis functions make the same symbols have different energy levels. Similarly to half-cycle modulation, when full cycle of sine/cosine signal is used for data modulation, all four values are alternately used. Example waveforms of BPSK signals from I and Q channels and 4-QAM quarter-cycle signal are depicted in Fig. 5. Eye-diagrams of the I channel output and 4-QAM signal are illustrated in Fig. 6(a) and Fig. 6(b). Figure 6(c) represents the eye-diagram of 4-QAM signal after multiplication with the sine signal. As shown in the figure, the interference from the Q channel is zero at the center of the bits. However, the waveforms and average levels of two consecutive bits are totally different. It means that quarter-cycle modulation not only requires strict phase condition alignment but also a more complicated method for detection.

3. Experimental setup

Due to the strict phase requirement for signal generation and complication of signal detection of quarter-cycle modulation, we chose only half-cycle modulation for the experiment. The experimental setup is illustrated in Fig. 4. There are two important parts in the setup: real time generation and transmission of a half-cycle 4-QAM signal.
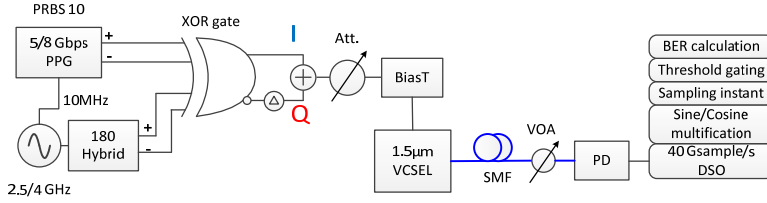
Fig. 7. Experimental setup: Pulse pattern generator (PPG), photodetector (PD), variable optical attenuator (VOA), single mode fiber (SMF), digital storage oscilloscope (DSO).

3.1. Half-cycle 4-QAM signal generation

To generate the electrical half-cycle 4-QAM signal, we used the method proposed in [12]. However, in our case, the subcarrier frequency was equal to half the symbol rate. 2.5/4-GHz subcarrier and synchronized 5/8-Gbps data with PRBS length of 2^{10}-1 were fed to a 13-GHz bandwidth XOR gate (Inphi 13610XR) to create two BPSK signals in the two outputs of the XOR gate. Due to the slow response of the XOR gate, the data bit stream was delayed approximately $\pi/4$ to force the XOR outputs always cross the zero level regardless the input bits. One output of the XOR gate was delayed and then combined with the other one using a power combiner to form a 4-QAM signal. The delay time was optimized in order to secure that the two signals from the XOR outputs are uncorrelated and 90 degrees out of phase. Utilizing a XOR gate to generate half-cycle QAM signals means transmitters of half-cycle QAM signals can be integrated using existing semiconductor process technologies. Compact, low-power transmitters can be produced.

The half-cycle QAM signal has some special features. Firstly, the first null in the spectrum of the signal is at 1.5 times the symbol rate while the first null point of single cycle QAM modulation is at twice the symbol rate. This means that the spectral efficiency of half-cycle QAM modulation is improved by 25% compared to single cycle modulation. The spectra of the generated half-cycle and single-cycle 5-Gbaud 4-QAM signals are illustrated in Fig. 5. It is observed that the width of the first lobe of the half-cycle modulation and the single-cycle modulation is 7.5 and 10 GHz, respectively. In comparison with a OOK signal at the same bit rate, the spectrum of half-cycle signal has similar shape to that of the OOK signal but width of slopes is smaller. For instance, in the case of a 4-QAM signal, the first lobe is 25% less and higher order lobes are 50% less than that of the OOK signal. Secondly, unlike the single-cycle QAM signal, most of the power of the half-cycle QAM signal is concentrated in the low frequency region. This makes the signal more tolerant towards high-frequency roll-off of VCSELs and photodiodes.

3.2. Half-cycle QAM signal transmission

The generated 4-QAM signal was fed to an un-cooled 1.5-μm VCSEL using a BiasT. The threshold current of the VCSEL was 17 mA and it was biased at 22.5 mA for the best performance. With 5-Gbaud data, the optical signal from the VCSEL was transmitted over 20-km standard SMF. The 8-Gbaud signal was transmitted through 3-km SMF. A variable optical attenuator (VOA) was utilized to vary the optical power level into the photodetector (PD). The 3-dB bandwidth of the VCSEL, evaluation board and PD was approximately 10 GHz. The photodetected signal was digitized using a 40-GSamples/s digital storage oscilloscope (DSO) for offline digital signal processing (DSP). The DSP algorithm was kept simple without any equalization technique. It includes I/Q detection, optimal sampling, threshold gating and bit error rate (BER) calculation. It indicates that receivers for half-cycle

QAM signals can be developed by using the current technologies for receivers of OOK and PAM signals without employing a high-speed ADC.
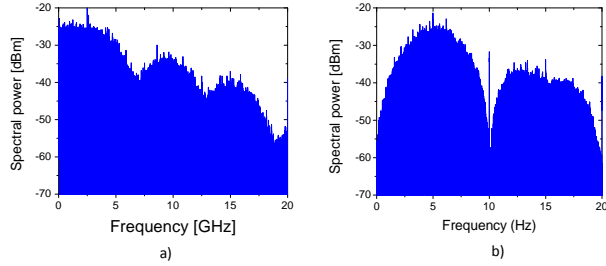

Fig.8. Spectrum of (a) 5-Gbaud half-cycle 4-QAM signal and (b) 5-Gbaud single-cycle 4-QAM signal
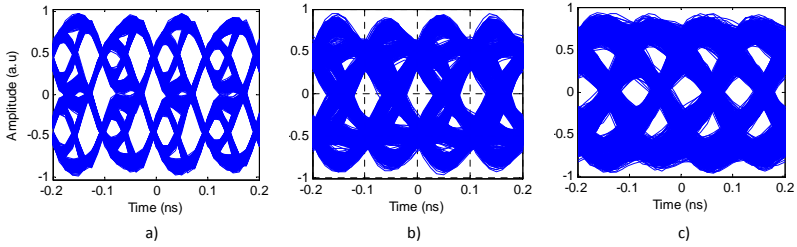

Fig 9. Eye-diagram of electrical 10-Gbps 4-QAM signal: (a) after XOR gate and after photodetection (b) at B2B and (c) after 20-km SSMF transmission.

4. Experimental results

4.1. Performance of half-cycle QAM signals

The eye-diagrams of the 10-Gbps 4-QAM signals driving the VCSEL, detected signals B2B and after fiber transmission is illustrated in Fig. 6. To assess the performance of the system, approximately 150k symbols (300k bits) were used to calculate the BER of the signals at both data rates. This number of symbols is limited by BER measurement using offline processing. The lowest detectable BER when there is error is approximately 10^{-5}. Figure 3 shows the BER of the signals B2B and after fiber transmission. For the 5-Gbaud signal, the optical power to achieve BER of 10^{-5} was about -12 dBm and -10 dBm for B2B and fiber transmission cases, respectively. Assuming that product code with shortened BCH (1023,992) (Bose-Chaudhuri-Hocqenghem) component codes is used and 7% payload is utilized for FEC header, the limit of pre-FEC BER aiming for after- FEC BER of 10^{-15} is 4.8×10^{-3} [14]. At this FEC limit, the receiver sensitivity B2B was approximately -15 dBm and the power penalty after 20-km SSMF transmission was only 2.5 dB.

For the 8-Gbaud signal B2B, as shown in Fig. 3(b), the receiver sensitivity at BER of 10^{-5} was about -6.7 dBm and at the FEC limit was -11.0 dBm. Due to the increased signal bandwidth and the strong effect of jitter after fiber transmission, the 8-Gbaud signal has higher transmission power penalty than the 5-Gbaud signal. After 3-km SMF, the power penalty was approximately 1.5 dB. In general, the receiver sensitivity was approximately 5 dB worse than for the 5-Gbaud signal. This performance limitation are attributed the imperfection of the generated QAM signal before modulation and limited bandwidth of the transceivers. The generated 8-Gbaud signal had lower signal-to-noise ratio (SNR) than the 5-Gbaud signal and the bandwidth of the 8-Gbaud signal was 12 GHz. Examples of the constellations of both 5-

Gbaud and 8-Gbaud signals before modulating the VCSEL and at B2B are presented in Fig. 8 and Fig. 9.
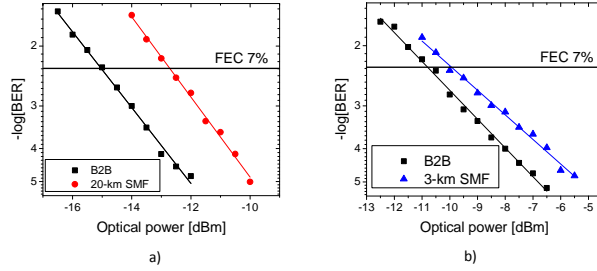

Fig.10. Performance of 4-QAM signals at B2B and after fiber transmission: (a) 5 Gbaud (10Gbps) and (b) 8 Gbaud (16 Gbps).
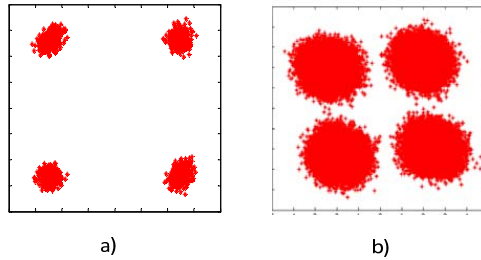

Fig.11. Constellation of 5-Gbaud 4-QAM signal: (a) generated electrical signal and (b) at -12.0 dBm B2B
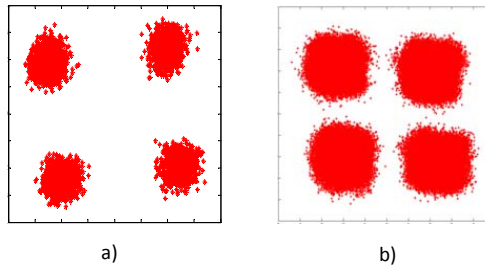

Fig. 12. Constellation of 8-Gbaud 4-QAM signal: (a) generated electrical signal and (b) at -6.5 dBm B2B

4.2. Comparison with OOK signal

In this section, we compare the performance of our proposed half-cycle QAM signal with the conventional OOK signals. Two data rates of 5 Gbps and 10 Gbps with direct current (DC) removed were chosen for the comparison with 5-Gbaud 4-QAM signal. The 5-Gbps OOK signal has the same baudrate while the 10-Gbps signal has the same data rate to the half-cycle QAM signal. The peak-to-peak voltage (V_{p-p}) of OOK signal driving the VCSEL was chosen to be equal to the V_{p-p} of the half-cycle QAM signals at the optimal sampling points as shown in Fig. 2(a). No other conditions of the experiment were changed. The performance of OOK signals at B2B and after 20-km fiber transmission is illustrated in Fig. 4.

At the FEC limit, the sensitivity of the QAM signal was approximately 2 dB and 1.5 dB lower than that of 5-Gbps and 10-Gbps OOK signal because the QAM signal has lower signal-to-

noise ratio (SNR). Power penalty after 20-km fiber transmission of 5-Gbps OOK signal was only 1 dB but power penalty of 10-Gbps signal was about 3-dB at FEC limit and increased up to 5-dB at BER of 10^{-5}. It means that the half-cycle QAM signal has improved the dispersion tolerance by only 0.5 dB at FEC limit but it increases dramatically at lower BER. At BER of 10^{-5}, 2.5-dB improvement has been observed.
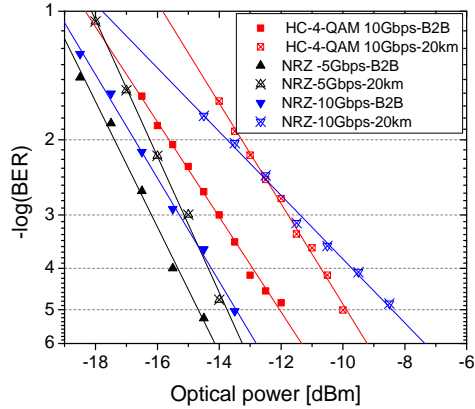

Fig. 10. Performance of 5-Gpbs and 10-Gbps NRZ signals at B2B and after fiber transmission in comparison with 10-Gbps half-cycle 4-QAM signal.

6. Conclusions

We have investigated QAM modulation utilizing sub-cycle subcarrier for VCSEL-based optical links to improve spectral efficiency. The transmission of 10-Gbps 4-QAM data in 7.5-GHz electrical bandwidth over 20-km single mode fiber was demonstrated with BER below the FEC limit and only 2.5-dB power penalty. Half-cycle signals have superior dispersion tolerance compared to OOK signals at the same data rate. Spectral efficiency can be improved by increasing the levels of the QAM signal. Both the transmitter and the receiver can be implemented using available electronics. Half-cycle subcarrier QAM modulation has potential for applications in high-speed PON networks as well as high-performance data centers.

Paper 13: Energy-efficient VCSEL-based multigigabit IR-UWB over fiber with airlink transmission system

Energy-efficient VCSEL-based multiGigabit IR-UWB over Fiber with Airlink Transmission System

Roberto Rodes, Tien-Thang Pham, Jesper Bevensee Jensen, Timothy Braidwood Gibbon, and
Idelfonso Tafur Monroy, *Member, IEEE*

Abstract—We propose VCSEL based impulse-radio ultra-wideband technology for energy efficient high-speed wireless networks; with full passive signal distribution, from the central office to the home with high-speed wireless connection to the final user.

Index Terms—Energy efficiency, passive optical network, ultra-wide band, vertical cavity surface emitting laser.

I. INTRODUCTION

Recently, energy consumption has become a key environmental issue for all industrial sectors including information and communication technologies (ICT) [1]. Impulse radio (IR) ultra-wideband (UWB) is acquiring attention for high-speed short-range wireless communication because of advantages such as high bandwidth and coexistence with other technologies. The extremely low radiated power allowed for this technology [2] ensures non-p

roblematic coexistence with other narrow-band technologies sharing the same spectrum, and makes UWB a good candidate for energy-efficient short-range communication systems. In order to harvest the potential energy efficiency provided by IR-UWB technology, it is important that the backhaul fiber-optic link is passive and based on low-power consuming photonic technologies.Vertical cavity surface emitting lasers (VCSELs) have long been promoted as a promising technology because of their low cost of high-volume production and low drive current compared to distributed feedback (DFB) lasers.

In this paper, we propose and demonstrate the application of directly modulated VCSELs for transmission of impulse radio IR-UWB over a 25 km un-amplified standard single mode fiber (SSMF) without dispersion compensation. The signal is transmitted through the fiber, photodetected, and fed directly to the transmitting antenna without electrical amplification. Due to the efficient use of the UWB spectrum, bit-error-ratio (BER) of less than 10^{-3} is achieved for 2 and 3 Gbps signals after up to 4 and 2 m wireless transmission , respectively.

II. EXPERIMENTAL SETUP

Fig. 1 shows the experimental setup. A fifth order derivative Gaussian pulse shape was chosen due to its good compliance with the FCC mask [2]. The signal is electrically generated by an arbitrary waveform generator (AWG), with 9 GHz

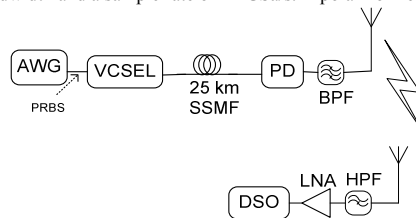bandwidth and a sample rate of 24 GSa/s. Bipolar non return

Fig. 1. Experimental setup

to zero coding of the UWB pulse is employed in order to reduce spectral lines at the pulse repetition frequency. The signal pattern is a pseudorandom bit sequence (PRBS) of word length 2^{11}-1. The output of the AWG directly modulates a VCSEL at a wavelength of 1550 nm, with a peak-to-peak voltage signal of 0.5 V. The bias point of the VCSEL is set at 15 mA. The measured optical power launched to the fiber is 0.26 dBm. The signal is transmitted over 25 km of SSMF, with total fiber attenuation of 5.1 dB and dispersion of 435 ps/nm. No optical amplification or dispersion compensation is used. The input power to the photodetector (PD) is -4.9 dBm. The optical UWB signal is recovered by a PIN photodiode and fed to the transmitter antenna through a band pass filter to ensure compliance with the FCC mask. Transmitter and receiver antennas are both bowtie phased-array antennas with a gain varying from 4.65 to 12.5 dBi within the 3.1- to 10.6-GHz spectrum, and a gain value of 10 dBi at the signal peak frequency of 6 GHz. On the receiver side, the signal from the antenna is high-pass filtered with a 3.1 GHz cut-off frequency, and electrically amplified before being digitized by a digital sampling scope (DSO). Data demodulation is performed using an off-line algorithm which performs synchronization and calculates the correlation between the received signal and a fifth-order derivative Gaussian pulse before performing single-threshold decision gating.

III. EXPERIMENTAL RESULTS

Fig. 2 shows the eye diagram of the signal detected by the photodiode after fiber transmission. The eye diagram is clearly open and no error is detected after demodulation. The 5-peak shape of the eye diagram is a consequence of the 5th derivative Gaussian pulse used in the experiment. The experiment was performed with 2 Gbps and 3 Gbps UWB signals. 10^{5} bits were recorded for each wireless distance at 1, 2, 3 and 4 meters. Table 2 shows the BER obtained after demodulation.

| Component	High energy consumption	Low energy consumption approach
Laser Source	DFB: T.C.≈ 20 mA; W.C.≈ 30-40 mA	VCSEL: W.C.= 7-15 mA
Optical Amplification	EDFA: W.C. ≈ 150 mA SOA: T.C. ≈ 10 mA; W.C.≈ 100 mA RSOA: T.C.≈ 10 mA; W.C. ≈ 20-50 mA	No optical amplification
Electrical amplifier	Broadband electrical amplifier: W.C. ≈ 300 mA	No electrical amplification
Transmitter antenna	Omni directional antenna. Radiatted power in all directions. No gain.	Directive antenna. Focus emitted power. High gain.

Table 1. Comparison of energy saving key factors
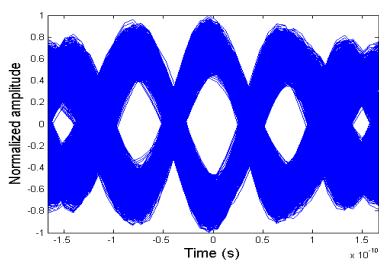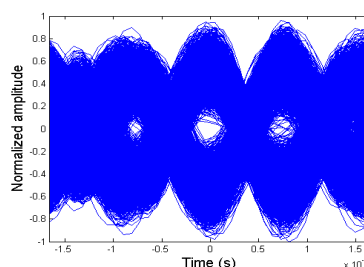

Fig. 3. Eye diagram: 3 Gbps after photodetection.

Fig. 4. Eye diagram: 3 Gbps over 2 meter airlink

After 1 and 2 meters wireless transmission at 2 Gbps, and after 1 meter at 3 Gbps, no errors were detected in the 10^5 recorded bits. At 2 Gbps, the BER remained below the FEC limit of 10-3 even after 4 meters wireless transmission. It should, however, be emphasized the FEC was not employed in the experiment, and that the effective data-rate in the case of 7% FEC overhead would be 1.86 Gbps. Fig. 4 and 5 show the eye diagrams of the received and demodulated signals. A clear and open eye diagram is observed after 2 meters at 3 Gbps; for 2 Gbps after 4 meters, the eye is slightly more closed.

Bit-rate / Distance	2 Gbps	3 Gbps
1 m	$< 10^{-5}$	$< 10^{-5}$
2 m	$< 10^{-5}$	7.08×10^{-5}
3 m	1.04×10^{-5}	4.49×10^{-3}
4 m	4.99×10^{-4}	7.21×10^{-3}

Table 2. BER after fiber and wireless transmission

Our achieved experimental results demonstrate the viability of the proposed system from a performance point of view. In order to address the increment in energy efficiency obtained by the proposed system (VCSEL, passive optical link, directive antennas), a comparison with a more conventional system based on DFB lasers, optical amplification and omnidirectional antennas has been made on Table 1.

IV. CONCLUSION

This paper presents a system approach based on VCSEL for distributing high-speed IR-UWB signals in an energy efficient communication system. By eliminating all amplifiers for the optical transmission part as well as for the wireless transmission part (apart from a single amplifier after the receiving antenna), system complexity and power consumption have been considerably reduced. With our proposed scheme, a 2 Gbps IR-UWB signal was transmitted over 25 km SSMF and a 2 meter in-home wireless link with no errors detected, and a BER of 4.99×10^{-4} after 4 meters wireless transmission.

REFERENCES

[1] M. Gupta and S. Singh, "Greening of the Internet", *Proc. SIGCOMM'03: Applications, Technologies, Architectures, and Protocols for Computer Communications*, 2003.
[2] Revision of Part 15 of the Commission's Rules Regarding Ultra-Wideband Transmission Systems Federal Communications Commission, Feb. 2002.
[3] H. Sheng, P. Orlik, A. M. Haimovich, L. J. Cimini Jr., and J. Zhang, "On the spectral and power requirements for ultra wideband transmission," in *Proc. IEEE Int. Conf. Communications*, 2003, pp. 738–742.

List of acronyms

WAN wide area network

LAN local area network

EIRP equivalent isotropically radiated power

FCC Federal Communications Commission

ONU optical network unit

OLT optical line termination

ICI inter-carrier interference

ISI inter-symbol interference

SRRC square-root raised cosine filter

PAPR peak-to-average power ratio

FFT fast fourier transform

PSD power spectral density

PolMux polarization multiplexing

CW continuous wave

DMT discrete multitone

PAM-M M-ary pulse amplitude modulation

FEC forward error correction

HC-QAM half-cycle quadrature amplitude modulation

SC-QAM single-cycle quadrature amplitude modulation

LO local oscillator

NRZ-OOK non return-to-zero on-off keying

QPSK quadrature phase shift keying

SMF single-mode fibre

MMF multi-mode fibre

WDM-PON wavelength division multiplexing passive optical network

WDM wavelength division multiplexing

BER bit error rate

AWG arrayed waveguide grating

DSP digital signal processing

QAM quadrature amplitude modulation

OFDMA orthogonal frequency-division multiplexing access

MB-OFDM multi-band orthogonal frequency-division multiplexing

ECL external cavity laser

DARPA Defense Advanced Research Projects Agency

DBR distributed Bragg reflector

DFB distributed feedback

CAP carrierless amplitude phase

PON passive optical network

VCSEL vertical-cavity surface-emitting laser

PAM-4 4-level pulse amplitude modulation

IFT inverse fourier transform

SNR signal-to-noise ratio

LIV light-current-voltage

IR-UWB impulse-radio ultra-wide band

UWB ultra-wide band

RSOA reflective semiconductor optical amplifier

Bibliography

[1] R. Michalzik, Ed., *VCSELs Fundamentals, Technology and Applications of Vertical-Cavity Surface-Emitting Lasers.* Springer, 2012.

[2] H. Li and K. Iga, *Vertical-Cavity Surface-Emitting Laser Devices.* Springer, 2002.

[3] L. A. C. S. W. Corzine, *Diode Laser and Photonic Integrated Circuits.* Wiley, 1995.

[4] M. Ortsiefer, R. Shau, R. Mederer, R. Michalzik, J. Rosskopf, G. Bohm, F. Kohler, C. Lauer, M. Maute, and M.-C. Amann, "High-speed data transmission with 1.55 pm vertical-cavity surface-emitting lasers," in *Optical Communication, 2002. ECOC 2002. 28th European Conference on*, vol. 5, sept. 2002, pp. 1 –2.

[5] M.-C. Amann and W. Hofmann, "Inp-based long-wavelength vcsels and vcsel arrays," *Selected Topics in Quantum Electronics, IEEE Journal of*, vol. 15, no. 3, pp. 861 –868, may-june 2009.

[6] P. Westbergh, J. Gustavsson, A. Haglund, M. Skold, A. Joel, and A. Larsson, "High-speed, low-current-density 850 nm vcsels," *Selected Topics in Quantum Electronics, IEEE Journal of*, vol. 15, no. 3, pp. 694 –703, may-june 2009.

[7] *Modulating VCSELs, Application sheet*, Honeywell.

[8] F. KOYAMA, Susumu, KINOSHITA, and K. IGA, "Room temperature cw operation of gaas vertical cavity surface emitting laser," *IEICE TRANSACTIONS*, vol. 71, pp. 1089–1090, 1988.

[9] E. Towe, R. Leheny, and A. Yang, "A historical perspective of the development of the vertical-cavity surface-emitting laser," *Selected Topics*

in *Quantum Electronics, IEEE Journal of*, vol. 6, no. 6, pp. 1458 –1464, nov.-dec. 2000.

[10] *http://www.fibrechannel.org/fibre-channel-roadmaps.html.*

[11] A. Vahdat, H. Liu, X. Zhao, and C. Johnson, "The emerging optical data center," in *Optical Fiber Communication Conference.* Optical Society of America, 2011, p. OTuH2. [Online]. Available: `http://www.opticsinfobase.org/abstract.cfm?URI=OFC-2011-OTuH2`

[12] B. J. Offrein, "Silicon photonics packaging requirements," in *Silicon Photonics Workshop*, 2011.

[13] *http://www.ieee802.org/3/.*

[14] *http://www.infinibandta.org.*

[15] E. Kapon and A. Sirbu, "Long-wavelength vcsels: Power-efficient answer," *Nature Photonics*, vol. 3, pp. 27–29, 2009.

[16] *http://www.gigawam.org/.*

[17] K. Prince, T. Gibbon, R. Rodes, E. Hviid, C. Mikkelsen, C. Neumeyr, M. Ortsiefer, E. Ronneberg, J. Rosskopf, P. Ohlen, E. De Betou, B. Stoltz, E. Goobar, J. Olsson, R. Fletcher, C. Abbott, M. Rask, N. Plappert, G. Vollrath, and I. Monroy, "Gigawam. next-generation wdm-pon enabling gigabit per-user data bandwidth," *Lightwave Technology, Journal of*, vol. 30, no. 10, pp. 1444 –1454, may15, 2012.

[18] G. P. Agrawal, *Fiber-Optic Communication Systems.* Third edition, chapter 10. Wiley, 2010.

[19] T. Gibbon, K. Prince, T. Pham, A. Tatarczak, C. Neumeyr, E. Ronneberg, M. Ortsiefer, and I. T. Monroy, "Vcsel transmission at 10 gb/s for 20 km single mode fiber wdm-pon without dispersion compensation or injection locking," *Optical Fiber Technology*, vol. 17, no. 1, pp. 41 – 45, 2011. [Online]. Available: `http://www.sciencedirect.com/science/article/pii/S1068520010001021`

[20] D. Nesset, "Network operator perspective on wdm-pon systems and applications," in *Optical Communication (ECOC), 2011 37th European Conference and Exhibition on*, sept. 2011, pp. 1 –3.

[21] K. Szczerba, B. Olsson, P. Westbergh, A. Rhodin, J. Gustavsson, A. Haglund, M. Karlsson, A. Larsson, and P. Andrekson, "37 gbps transmission over 200 m of mmf using single cycle subcarrier modulation and a vcsel with 20 ghz modulation bandwidth," in *Optical Communication (ECOC), 2010 36th European Conference and Exhibition on*, sept. 2010, pp. 1 –3.

[22] S. Lee, F. Breyer, S. Randel, D. Cardenas, H. van den Boom, and A. Koonen, "Discrete multitone modulation for high-speed data transmission over multimode fibers using 850-nm vcsel," in *Optical Fiber Communication - incudes post deadline papers, 2009. OFC 2009. Conference on*, march 2009, pp. 1 –3.

[23] S. H. Han and J. H. Lee, "An overview of peak-to-average power ratio reduction techniques for multicarrier transmission," *Wireless Communications, IEEE*, vol. 12, no. 2, pp. 56 – 65, april 2005.

[24] S. Randel, F. Breyer, S. Lee, and J. Walewski, "Advanced modulation schemes for short-range optical communications," *Selected Topics in Quantum Electronics, IEEE Journal of*, vol. 16, no. 5, pp. 1280 –1289, sept.-oct. 2010.

[25] D. D. Falconer, "Carrierless am/pm," in *Bell Laboratories Technical Memorandum*, 1975.

[26] A. Shalash and K. Parhi, "Multidimensional carrierless am/pm systems for digital subscriber loops," *Communications, IEEE Transactions on*, vol. 47, no. 11, pp. 1655 –1667, nov 1999.

[27] "Revision of part 15 of the commissions rules regarding ultra-wideband transmission systems," in *Federal Communications Commision*, 2002.

[28] H. Sheng, P. Orlik, A. Haimovich, J. Cimini, L.J., and J. Zhang, "On the spectral and power requirements for ultra-wideband transmission," in *Communications, 2003. ICC '03. IEEE International Conference on*, vol. 1, may 2003, pp. 738 – 742 vol.1.

[29] P. Westbergh, R. Safaisini, E. Haglund, B. Kš andgel, J. Gustavsson, A. Larsson, M. Geen, R. Lawrence, and A. Joel, "High-speed 850 nm vcsels with 28 ghz modulation bandwidth operating error-free up to 44 gbit/s," *Electronics Letters*, vol. 48, no. 18, pp. 1145 –1147, 30 2012.

[30] D. M. Kuchta, A. V. Rylyakov, C. L. Schow, J. E. Proesel, C. Baks, C. Kocot, L. Graham, R. Johnson, G. Landry, E. Shaw, A. MacInnes, and J. Tatum, "A 55gb/s directly modulated 850nm vcsel-based optical link," in *Photonics Conference (IPC), 2012 IEEE*, sept. 2012, pp. 1 –2.

[31] Y.-C. Chang and L. Coldren, "Efficient, high-data-rate, tapered oxide-aperture vertical-cavity surface-emitting lasers," *Selected Topics in Quantum Electronics, IEEE Journal of*, vol. 15, no. 3, pp. 704 –715, may-june 2009.

[32] W. Hofmann, P. Moser, P. Wolf, A. Mutig, M. Kroh, and D. Bimberg, "44 gb/s vcsel for optical interconnects," in *Optical Fiber Communication Conference and Exposition (OFC/NFOEC), 2011 and the National Fiber Optic Engineers Conference*, march 2011, pp. 1 –3.

[33] P. Moser, P. Wolf, A. Mutig, G. Larisch, W. Unrau, W. Hofmann, and D. Bimberg, "85 c error-free operation at 38 gb/s of oxide-confined 980-nm vertical-cavity surface-emitting lasers," *Applied Physics Letters*, vol. 100, no. 8, pp. 081 103 –081 103–3, feb 2012.

[34] T. Anan, N. Suzuki, K. Yashiki, K. Fukatsu, H. Hatakeyama, T. Akagawa, K. Tokutome, and M. Tsuji, "High-speed 1.1-um-range ingaas vcsels," in *Optical Fiber communication/National Fiber Optic Engineers Conference, 2008. OFC/NFOEC 2008. Conference on*, feb. 2008, pp. 1 –3.

[35] M. Muller, P. Wolf, T. Grundl, C. Grasse, J. Rosskopf, W. Hofmann, D. Bimberg, and M.-C. Amann, "Energy-efficient 1.3 um short-cavity vcsels for 30 gb/s error-free optical links," in *Semiconductor Laser Conference (ISLC), 2012 23rd IEEE International*, oct. 2012, pp. 1 –2.

[36] W. Hofmann, M. Müller, A. Nadtochiy, C. Meltzer, A. Mutig, G. Böhm, J. Rosskopf, D. Bimberg, M.-C. Amann, and C. Chang-Hasnain, "22-gb/s long wavelength vcsels," *Opt. Express*, vol. 17, no. 20, pp. 17 547–17 554, Sep 2009. [Online]. Available: http://www.opticsexpress.org/abstract.cfm?URI=oe-17-20-17547

[37] M. Muller, W. Hofmann, T. Grundl, M. Horn, P. Wolf, R. Nagel, E. Ronneberg, G. Bohm, D. Bimberg, and M. Amann, "1550-nm high-speed short-cavity vcsels," *Selected Topics in Quantum Electronics, IEEE Journal of*, vol. 17, no. 5, pp. 1158 –1166, sept.-oct. 2011.

[38] W. Hofmann, M. MŸ andller, P. Wolf, A. Mutig, T. GrŸ andndl, G. Bš andhm, D. Bimberg, and M.-C. Amann, "40 gbit/s modulation of 1550 nm vcsel," *Electronics Letters*, vol. 47, no. 4, pp. 270 –271, 17 2011.

[39] D. Qian, N. Cvijetic, Y.-K. Huang, J. Hu, and T. Wang, "Single-wavelength 108 gb/s upstream ofdma-pon transmission," in *Optical Communication, 2009. ECOC '09. 35th European Conference on*, vol. 2009-Supplement, sept. 2009, pp. 1 –2.

[40] D. Qian, N. Cvijetic, Y.-K. Huang, J. Yu, and T. Wang, "100km long reach upstream 36gb/s-ofdma-pon over a single wavelength with source-free onus," in *Optical Communication, 2009. ECOC '09. 35th European Conference on*, sept. 2009, pp. 1 –2.

[41] N. Cvijetic, M.-F. Huang, E. Ip, Y.-K. Huang, D. Qian, and T. Wang, "1.2 tb/s symmetric wdm-ofdma-pon over 90km straight ssmf and 1:32 passive split with digitally-selective onus and coherent receiver olt," in *Optical Fiber Communication Conference and Exposition (OFC/NFOEC), 2011 and the National Fiber Optic Engineers Conference*, march 2011, pp. 1 –3.

[42] S.-Y. Kim, N. Sakurai, H. Kimura, and H. Hadama, "Vcsel-based coherent detection of 10-gbit/s qpsk signals using digital phase noise cancellation for future optical access systems," in *Optical Fiber Communication (OFC), collocated National Fiber Optic Engineers Conference, 2010 Conference on (OFC/NFOEC)*, march 2010, pp. 1 –3.

[43] S. Smolorz, E. Gottwald, H. Rohde, D. Smith, and A. Poustie, "Demonstration of a coherent udwdm-pon with real-time processing," in *Optical Fiber Communication Conference and Exposition (OFC/NFOEC), 2011 and the National Fiber Optic Engineers Conference*, march 2011, pp. 1 –3.

[44] K. Cho, U. Hong, A. Agata, T. Sano, Y. Horiuchi, H. Tanaka, M. Suzuki, and Y. Chung, "10-gb/s, 80-km reach rsoa-based wdm pon employing qpsk signal and self-homodyne receiver," in *Optical Fiber Communication Conference and Exposition (OFC/NFOEC), 2012 and the National Fiber Optic Engineers Conference*, march 2012, pp. 1 –3.

[45] K. Cho, K. Tanaka, T. Sano, S. Jung, J. Chang, Y. Takushima, A. Agata, Y. Horiuchi, M. Suzuki, and Y. Chung, "Long-reach coherent wdm pon employing self-polarization-stabilization technique,"

Lightwave Technology, Journal of, vol. 29, no. 4, pp. 456 –462, feb.15, 2011.

[46] D. Lavery, R. Maher, D. Millar, B. Thomsen, P. Bayvel, and S. Savory, "Demonstration of 10 gbit/s colorless coherent pon incorporating tunable ds-dbr lasers and low-complexity parallel dsp," in *Optical Fiber Communication Conference and Exposition (OFC/NFOEC), 2012 and the National Fiber Optic Engineers Conference*, march 2012, pp. 1 –3.

[47] K. Szczerba, P. Westbergh, J. Gustavsson, A. Haglund, J. Karout, M. Karlsson, P. Andrekson, E. Agrell, and A. Larsson, "30 gbps 4-pam transmission over 200m of mmf using an 850 nm vcsel," in *Optical Communication (ECOC), 2011 37th European Conference and Exhibition on*, sept. 2011, pp. 1 –3.

[48] J. Ingham, R. Penty, I. White, P. Westbergh, J. Gustavsson, A. Haglund, and A. Larsson, "32 gb/s multilevel modulation of an 850 nm vcsel for next-generation datacommunication standards," in *Lasers and Electro-Optics (CLEO), 2011 Conference on*, may 2011, pp. 1 –2.

[49] J. Ingham, R. Penty, I. White, and D. Cunningham, "40 gb/s carrierless amplitude and phase modulation for low-cost optical datacommunication links," in *Optical Fiber Communication Conference and Exposition (OFC/NFOEC), 2011 and the National Fiber Optic Engineers Conference*, march 2011, pp. 1 –3.

[50] M. Othman, X. Zhang, L. Deng, M. Wieckowski, J. Jensen, and I. Monroy, "Experimental investigations of 3-d-/4-d-cap modulation with directly modulated vcsels," *Photonics Technology Letters, IEEE*, vol. 24, no. 22, pp. 2009 –2012, nov.15, 2012.

[51] X. Yu, T. Gibbon, R. Rodes, T. Pham, and I. Tafur Monroy, "System wide implementation of photonically generated impulse radio ultra-wideband for gigabit fiber-wireless access," *Lightwave Technology, Journal of*, vol. PP, no. 99, p. 1, 2012.

[52] M. Thakur, T. Quinlan, C. Bock, S. Walker, M. Toycan, S. Dudley, D. Smith, A. Borghesani, D. Moodie, M. Ran, and Y. Ben-Ezra, "480-mbps, bi-directional, ultra-wideband radio-over-fiber transmission using a 1308/1564-nm reflective electro-absorption transducer and commercially available vcsels," *Lightwave Technology, Journal of*, vol. 27, no. 3, pp. 266 –272, feb.1, 2009.

[53] G. Feher, C. Fuzy, A. Zolomy, and T. Berceli, "Multi-band impulse filtered uwb signal transmission by wideband optical vcsel transmitter," in *Microwaves, Radar and Remote Sensing Symposium (MRRS), 2011*, aug. 2011, pp. 114 –117.

[54] M. Beltran, J. Jensen, X. Yu, R. Llorente, R. Rodes, M. Ortsiefer, C. Neumeyr, and I. Monroy, "Performance of a 60-ghz dcm-ofdm and bpsk-impulse ultra-wideband system with radio-over-fiber and wireless transmission employing a directly-modulated vcsel," *Selected Areas in Communications, IEEE Journal on*, vol. 29, no. 6, pp. 1295 –1303, june 2011.

[55] S. Smolorz, H. Rohde, P. Ossieur, C. Antony, P. Townsend, T. De Ridder, B. Baekelandt, X. Qiu, S. Appathurai, H.-G. Krimmel, D. Smith, and A. Poustie, "Next generation access networks: Pieman and beyond," in *Photonics in Switching, 2009. PS '09. International Conference on*, sept. 2009, pp. 1 –4.

[56] J. Wei, J. Ingham, D. Cunningham, R. Penty, and I. White, "Performance and power dissipation comparisons between 28 gb/s nrz, pam, cap and optical ofdm systems for data communication applications," *Lightwave Technology, Journal of*, vol. 30, no. 20, pp. 3273 –3280, oct.15, 2012.